Improvements for the prediction of the fatigue life of the deck plate in orthotropic steel decks

A design optimization study

P. Beld

TU Delft

Iv-Infra

Improvements for the prediction of the fatigue life of the deck plate in orthotropic steel decks

A design optimization study

by

P. Beld

to obtain the degree of Master of Science
in Structural Engineering
at the Delft University of Technology,
to be defended publicly on 17 June, 2019 at 15:00 PM.

Student number:	4232364	
Project duration:	September 10, 2018 – June, 2019	
Thesis committee:	Prof. dr. ir. M. Veljkovic,	TU Delft
	Dr. H. Xin,	TU Delft
	Dr. ir. P.C.J. Hoogenboom,	TU Delft
	Ir. W. Langedijk,	Iv-Infra

An electronic version of this thesis is available at `http://repository.tudelft.nl/`.

Cover image: The Erasmus Bridge in Rotterdam. Made by Arthur van Rhijn.

TU Delft

Iv-Infra

Preface

This report presents the graduation research to finish my study Structural Engineering at the TU Delft, which I followed with a great pleasure. Fatigue in bridges is an actual topic for a lot of bridges in The Netherlands and therefore, this topic sought my interest. This report consists a research to the fatigue behaviour of one of the important details of the orthotropic steel deck, which is the trough web to deck plate joint.

This thesis if fulfilled at Iv-Infra. I would like to thank the people from Iv-Infra who gave me the opportunity to graduate at their company and for their hospitality. Especially, I want to thanks ir. Walter Langedijk, my daily supervisor. He was always available for discussions about my thesis and to share his experiences.

I would like to thank the members of the thesis committe. Professor Veljkovic and dr. ir. P. Hoogenboom, because without their judgements during the meetings, this report was not finished. Thanks to dr. H. Xin, my supervisor form the university, for his knowledge about fatigue and particularly his knowledge about the Abaqus software and for the help for learning me.

Further, I want to thank my family for the mental support to finish this report and thanks to my friend who cares for the relaxed moments, activities and bringing my mind to something else than studying.

At least, a special thanks to Arthur who was always there to listen to me and to give me new energy when I did not saw light at the end of the tunnel.

I have written this report with a lot of enthusiasm. Enjoy reading.

P. Beld
Haarlem, May 2019

Abstract

Fatigue is an important issue for orthotropic steel deck (OSD) bridges and therefore a design criterium. Cracks will initiate at several locations of the bridge deck. It is likely that a crack at the trough web to deck plate joint at the crossbeam will initiate first. This crack initiates at the weld root and propagates through the deck plate. A crack at this location is harmful because it is not optically visible and therefore hard to detect.

The first part of the report focuses on the fatigue assessment of the trough web to deck plate joint at the crossbeam. Fatigue assessment of this joint is possible with different assessment methods which are the nominal stress method and the hot spot stress method as given in the Eurocode, and the effective notch stress method, described by the IIW. A hand calculation using a simple 2D model is made and a finite element (FE) model is used for the assessment. Both a shell and solid element model are build. The fatigue life of the joint for a deck segment is made. Experimental results for the same deck segment are available and used for validation of the FE models. The fatigue life of each method is compared to the determined load cycles to failure from the experiment. There is concluded that the hot spot stress method results in the most accurate fatigue life prediction and a solid element model gives a slightly longer fatigue life than using shell elements. The effective notch stress method results in a conservative fatigue life for this specific joint.

Stresses in the zone near the weld root of the rib-to-deck plate joint at the crossbeam are in compression, while fatigue cracks will initiate due to tensile stresses. During welding, residual stresses appear in the joint. Therefore, a fatigue life prediction is made which includes these residual stresses. An approximation of the residual stresses is included in the initial state of the finite element model. Using the Smith Watson, Topper parameter, which is a local critical plane based fatigue assessment, the amount of load cycles to failure is determined. The result is comparable to the experimental result.

The second part of the report is focused on the geometry of the deck segment. A shell element model and the hot spot stress method are used to analyse different parameters. When the width between the trough webs is larger, a thicker deck plate thickness is required.

Four alternatives for a bridge deck are made. The alternatives have a different amount of troughs over the width, which means that the width between the trough webs differs per alternative. The deck plate thickness is chosen so that each alternative results in a damage value just below 1 for traffic category 2 and a design life of 50 years. Fatigue load model 4 is considered. The weight of the alternatives is determined. There can be concluded that reducing the amount of troughs over the width results in a heavier deck. This is because the weight of the deck plate is a large part of the total weight of the OSD and if more troughs are used, a thicker deck plate is applied.

There was assumed that the stress in the joint only is affected by deformation of the deck plate. However, the in-plane deformation of the crossbeam has a negative effect on the stress range in the trough web-to-deck plate joint.

Besides the geometry, the effect of some assumptions for modeling are investigated. Including a load dispersal through the surface layer by applying a larger wheel contact area results in a reduced fatigue damage value of about 50% and is therefore beneficial to take into account in the design calculations. The stress range in the joint is highest if a wheel load is placed in the center of the trough. A transverse shift of the wheel results in a large decrease in stress. Therefore it is important to take into account the design load cycles per transverse wheel position.

Contents

1 Introduction

1.1. Background information

An orthotropic steel deck (OSD) is a popular structure for a bridge deck. It is an integral deck, consisting of the deck plate, longitudinal stiffeners and crossbeams. The deck is generally supported by two main girders. The stiffeners can be open or closed. The decks are often applied because of the light weight, its slenderness and a high load bearing capacity. It is used both in fixed and movable bridges.

Because of cyclic loading due to traffic and a large amount of welding, the decks are sensitive to fatigue. Fatigue cracks are detected in several bridges with an OSD. In The Netherlands, cracks are only found in highway bridges [8]. An example is the Van Brienenoord bridge in Rotterdam [17].

The fatigue life depends on the intensity of load cycles and the stress range. Highways are more sensitive to fatigue because the heavy traffic intensity, and thus the amount of load cycles, is much higher than for secondary- and local roads.

Fatigue cracks are detected at different locations of the OSD. These locations are in the trough web to deck plate joint between two crossbeams or at the crossbeam, see figure 1.1. Other locations are in the joint between the trough and crossbeam and in the trough splice joint.

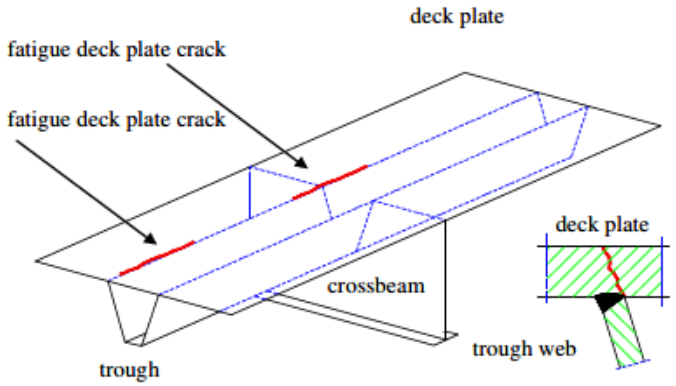

Figure 1.1: Locations of fatigue cracks in the deck plate [9]

Cracks in deck plate at the rib-to-deck plate and crossbeam joint can be seen as most harmful. The crack is not visually observable because it generally initiates at the weld root, which is at the inside of the trough. Therefore, this crack type should be prevented or limited. The deck plate acts as the top flange of the crossbeam. If there is a crack in the deck plate, the bearing capacity of the crossbeam may is not sufficient anymore.

Therefore, de Jong [8] states that a crack at this location can be a treat for traffic safety. This will be the case if the crack is over the full thickness and has a length of approximately 50 cm in longitudinal direction. Except from this joint, fatigue cracks will not lead to a safety risk for traffic, because if the dimension of the crack is limited, redistribution of loads is possible [8].

1.1.1. Deck plate thickness

The fatigue resistance of OSDs is influenced by the geometry of the deck structure. For older bridges, the resistance of the decks was not determined by fatigue resistance but by static capacity under maximum wheel loads. For this reason, most of the bridges in The Netherlands have a deck plate thickness of 10 mm (fixed bridges) to 12 mm (movable bridges) [9]. However, in different studies it is proven that a thicker deck plate results in an increased fatigue life [24], [11], [6]. Therefore, the deck plate thickness of new bridges is 18 to 22 mm.

Eurocode 3 part 2 [30] and the Dutch National Annex [31] give information about the minimum deck plate thickness. The heavy traffic intensity of different road types differs, which results in a difference of the amount of load cycles per year. Therefore, the minimum required deck plate thickness depends on the traffic category.

The deck plate thickness is the only parameter which is determined for all traffic categories separately. According to the Eurocode, the width between the troughs should always be less than 300 mm. This value is independent of the traffic categories. Information about the trough shape is not given in the code, but this will may have an influence on the fatigue life as well.

1.1.2. Fatigue assessment methods

Different methods to predict the fatigue life are developed. The methods described in Eurocode 3 part 1-9 [29] are the (modified) nominal stress method and the hot spot stress method. Both methods have some limitations and therefore, a third method, the effective notch stress method, is developed. This method is described by the International Institute of Welding (IIW) [12] but is not yet included in the Eurocode.

The nominal stress method is generally seen as a conservative way of calculating and it is difficult to apply for details with a complex geometry. The hot spot stress and effective notch stress method are less conservative methods. However, the accuracy is dependent on the finite element model, because the type and size of the elements have an influence on the resulting stress range. How more detailed the model is, how more accurate the fatigue strength calculation will be. However, a more detailed model is more labor intensive and more computation time is required.

The fatigue assessment according to the Eurocode is based on the S-N curves. These S-N curves are determined by laboratory tests. Over the years, the weld methods and steel quality are improved, which results in an improved quality of OSDs. Because the detail categories are based on the available tests, this improvement is not taken into account yet and can lead to a conservative prediction of the fatigue life [5]. A local critical plane model can be used as alternative for the S-N curve. This method does not consider a detail category for each detail.

1.2. Problem definition and objectives

1.2.1. Research question

This report is divided in two objectives. As mentioned in the introduction, fatigue cracks are generally found in highway bridges. But if focusing on movable bridges in urban area, does fatigue still be a big problem for smaller heavy traffic flow? Nevertheless, except for requirement of the deck plate thickness, the requirement of the design of the orthotropic steel bridge decks is the same for all traffic categories. An optimization of the decks per traffic category may result in less material use. Especially for movable bridges, this is beneficial, because of the reduction of the weight of the bridge deck. Therefore, the first objective of this report focuses on the possibility to optimize the design to reduce the amount of weight of the bridge deck.

This leads to the following research question:

Can there be found a combination of parameters for the OSD which results in a reduced weight of the structure compared to general dimensions with respect to the rib-to-deck plate and crossbeam joint.

To give an answer on this question, the following sub question should be answered first:

Which parameters affect the fatigue life of the rib-to-deck plate joint at the crossbeam?

The second objective is the fatigue assessment of the rib-to-deck plate joint near the crossbeam. To find an optimized design of the detail, an accurate fatigue assessment is preferred. This results in the second research question and should be used to find an answer on the first question.

For which fatigue assessment method, the prediction of the amount of load cycles to failure is most close to experimental results if the rib-to-deck plate joint at the crossbeam is considered?

In the end, an overview of the accuracy and ease of applicability of the assessment methods will be given and recommendations about dimensions of OSDs for traffic category 2 will be described.

1.3. Methodology

For this research, two finite element (FE) models are build in ABAQUS software. The first model consists of shell elements. The second model is a small solid element sub model of the joint and is included in the shell element model to provide enough boundary conditions. Validation of the models is provided according to available experimental results, carried out by Wu et al. [37]. This validation makes sure that the outcomes are reliable. The fatigue life of a bridge deck segment is determined with different fatigue assessment approaches. Approaches which are used are the nominal, hot spot and effective notch stress method, which are based on the S-N curve and an assessment based on a local critical plane approach using the swt-curve is applied.

For a standard design of the bridge segment, different influencing parameters are analyzed. Using a case study, four alternatives for a design of the bridge deck are determined. The damage value for these alternatives is calculated. Fatigue assessment methods, discussed in the first part of the report are used. The alternatives are used to draw conclusions about the possibilities for weight reduction of an OSD for traffic category 2.

1.4. Limitations

The focus of fatigue assessment will be on the trough web-to-deck plate joint near the crossbeam, because, as stated in paragraph 1.1, this joint is most frequently observed and is seen as most harmful.

Only movable bridges are considered in this report. This is because of the importance of reduction of self weight. Reduction of self weight is important for bridges in general, because it will lead to reduced load in the foundation and therefore, in an overall reduction of weight and thus a reduction of costs. For movable bridges, it is extra beneficial during opening and closing of the bridge. The required counterweight will reduce as well which leads to an extra reduction of weight at the foundation.

Stresses in the bridge deck due to opening and closing are not considered. These stresses are mainly in the longitudinal direction while the stress in the detail is affected by stresses in transverse direction caused by local wheel loads.

1.5. Report outline

Chapter 2 gives an overview of the literature study. For understanding of the problem, some general information about OSDs and about fatigue is collected. Subsequently, literature related to the rib-to-deck plate joint at the crossbeam is discussed and an overview of the fatigue assessment methods is provided.

After the literature study, the FE model is discussed in chapter 3. A deck segment with 'standard' dimensions is used. Experimental data from a deck segment with same dimensions is available [37] and used for validation of the FE model. Two models are created, one with shell elements and one with solid elements. The size of

the elements which results in a stable result is investigated so that a reliable FE model is created.

A simplified 2D model, the shell element model and the solid element sub model are used to determine the load cycles to failure for a certain load range in chapter 4. The fatigue life is determined with different fatigue assessment methods. In the end, the results are compared to each other and to the experimental results which makes it possible to find an answer on the research question.

An assumption for taking care of residual stresses is discussed in chapter 5. Fatigue assessment which is based on the swt model is made.

In chapter 6, the load for fatigue is given, the most unfavorable wheel location and the influence on the transverse wheel position is discussed and the effect of different parameters on the hot spot stress is analyzed.

The outcomes from the parameter study are used to determine some alternatives for a case bridge, discussed in chapter 7. The damage values for these alternatives is determined and the possibilities for weight reduction is discussed. Influences for some assumptions which are made in the report are analysed and discussed.

In the end, the conclusions are drawn and recommendations are given in chapter 8.

2

Literature review

In this chapter, information from literature is given. The literature study can be divided into three parts. In the first part, the behaviour of an OSD during loading is described. Some general information about fatigue is given and the fatigue crack initiation with respect to the rib to deck plate joint at the crossbeam is discussed. The second part gives information about the design of an OSD according to the Eurocode and some improvements and recommendations from literature is given. The last topic of the literature study provides an overview of different methods to determine the stress at the weld root and describes how the fatigue life of a detail can be assessed.

2.1. Behaviour of OSDs

An orthotropic steel deck is an integral deck, consisting of a deck plate, troughs, crossbeams, and main girders. In figure 2.1, a typical deck is shown. The troughs are continuous or welded between two crossbeams. A cope hole in the crossbeams is sometimes applied.

During traffic loading, the deck deforms. This causes axial, bending and shear stresses in the global system including the main girders. Because the deck consists of different elements, all elements behave different and should be checked locally.

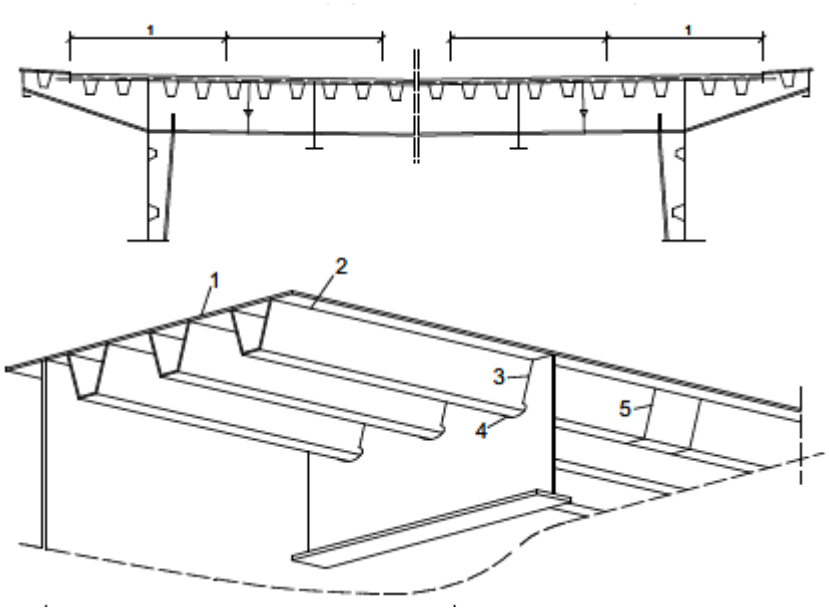

Figure 2.1: Standard OSD. 1. Deck plate, 2. Connection trough web to deck plate, 3. Connection trough web to crossbeam, 4. Cope hole, 5. Splice joint connection [30, fig. C.1]

The crossbeam is a beam supported between two main girders. Loading of the crossbeam results in in-plane deformation, figure 2.2(a).

The trough can be seen as a continuous beam supported between the crossbeams. If a load is applied at the trough in span between crossbeams, the trough web rotates near the crossbeam. Because the troughs are welded to the crossbeams, the crossbeam will deform as well, which is out-of-plane deformation, as shown in figure 2.2(b).

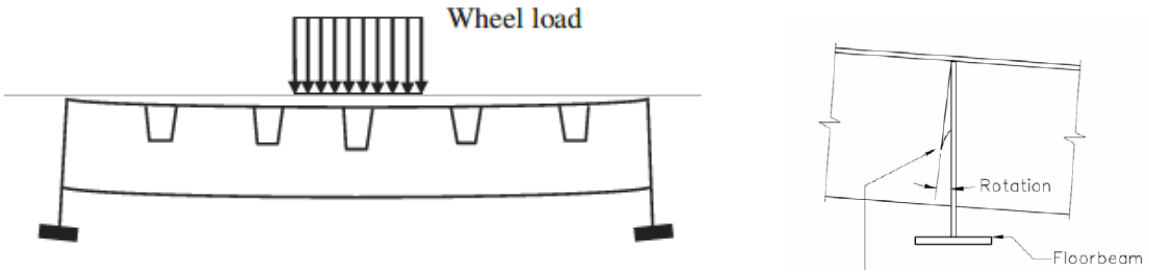

(a) In-plane (b) Out-of-plane

Figure 2.2: Crossbeam deformation [3]

The deck plate is supported by the troughs. Due to a local wheel load, the deck plate will deform locally between the trough webs, 2.3. This results in bending stresses at the connection of the deck plate with the trough. At the location of the crossbeam, the connection is much stiffer than in span. As a consequence, the deck plate will deform between the trough webs only and the local bending stress is higher, see figure 2.4.

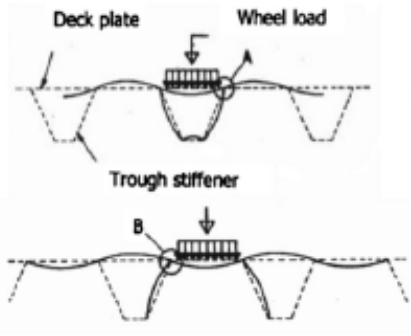

Figure 2.3: Local deflection of deck plate and trough in span between crossbeams [11]

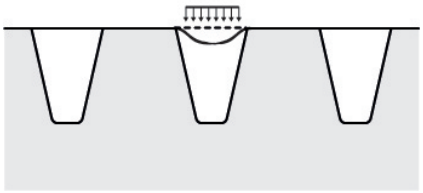

Figure 2.4: Local deflection of deck plate at the crossbeam

2.2. Introduction to fatigue

Fatigue in steel structures is the phenomenon which occurs if a structure is exposed to cyclic loading. Traffic load leads to a variation in stresses during life. The height of this stress range is the most important factor for the fatigue life. Fatigue damages is caused before the yield stress is reached. Therefore, only elastic stresses should be considered in fatigue calculations generally.

Fatigue crack growth takes place in three phases; crack initiation, crack propagation and the final fracture. An overview is given in figure 2.5. Crack initiation takes place at points where the stress range is large. Local increase in stress range is caused by stress concentration effects due to geometric discontinuities in the detail, the shape and size of the weld and local weld defects [1].

After the crack is initiated, it grows to a macro crack. Among other things, the way the crack will propagate depends on the geometry and stiffness of the detail and on the material properties. Other important influencing factors are the stress range and number of load cycles.

Generally speaking, final failure is the point in which the crack will grow unstable. This point is reached if the stress intensity factor is equal to or larger than the fracture toughness factor (K_{IC}).

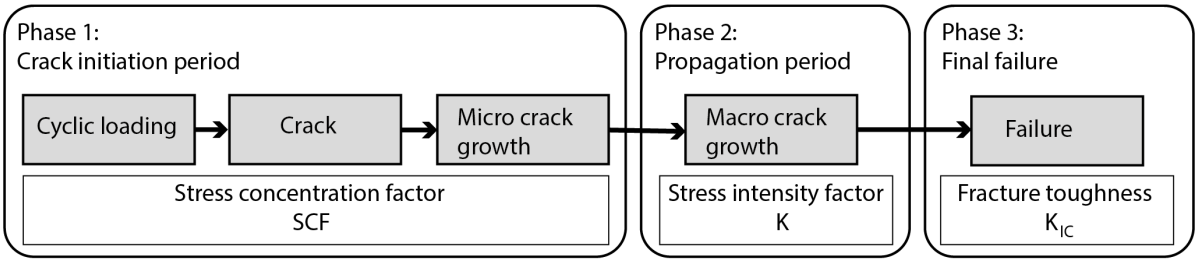

Figure 2.5: Fatigue phases - overview

2.3. Fatigue cracks in the rib-to-deck plate joint

Due to a wheel load from a vehicle, the deck plate deforms locally between the trough webs as discussed in paragraph 2.1. As a result, bending stresses will arise at the connection between the deck plate and trough web. The height of the stress range at the joint is influenced by the transverse wheel location and the wheel contact area.

There are four different crack paths for the trough web-to-deck plate joint near the crossbeam or in span, shown in figure 2.6. Location a and b initiates at the weld root and toe respectively and propagates through the deck plate. The crack at location c initiates at the weld toe and propagates through the stiffener and at location d, the crack initiates at weld root and grows through the weld bead.

The crack paths at location b and c are visible during inspection. The crack in the weld will be visible if it is propagated through the weld bead. A crack at location a is not visible. It will only become visible if there is a crack in the surface layer as well.

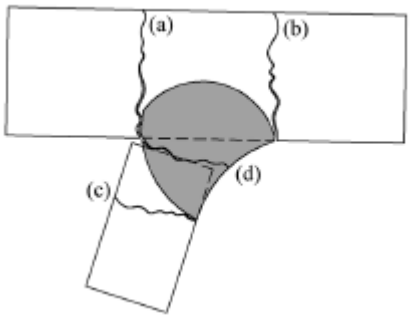

Figure 2.6: Crack paths in the rib-to-deck joint [26]

2.3.1. Crack initiation

The initiation and propagation of the crack types for the rib-to-deck plate joint are investigated by many researchers. A summary of some studies is given in this section.

The research of Leendertz [18] contains a description of different crack possibilities in OSD bridges. A conclusion is that in existing bridges as well as in test specimens cracks are found in the weld bead, figure 2.6 location d, and in the deck plate, location a. Both cracks initiates at the weld root. The crack through the weld bead is found in the joint in span between two crossbeams and is dominant in bridges which have a high truck

intensity. The crack propagation through the deck plate is present near the crossbeam and is detected in bridges where a thin wearing course is applied. In some cases, if the value of heavy traffic is high, this crack type is also found in bridges with a thick wearing course.

Murakoshi et al. [24] and Nagy et al. [26] stated that cracks will initiate at the weld root and propagation will take place in the deck plate or the weld. In a couple of existing bridges, these cracks are found in span between two crossbeams.

According to a research of Murakoshi et al. [24], both the joint at mid span and near the crossbeam are investigated and there can be concluded that the minimum principal stress is much higher in the joint near the crossbeam. Therefore, the fatigue life will be lower for this detail. This conclusion is similar to the statement of Wu et al. [37], which says that fatigue cracks in the trough web-to-deck plate joint will initiate and propagate earlier near the crossbeam than in span.

According to the different studies, there can be concluded that the crack initiates at weld root and propagation is expected in the weld bead for the joint in span and through the deck plate for the joint near the crossbeam. It is likely that the crack at the crossbeam initiates first.

2.3.2. Crack propagation and final failure

The crack through the deck plate in the rib-to-deck plate joint near the crossbeam, which initiates at weld root, propagates through the deck plate in vertical direction first. Subsequently, it will grow in longitudinal direction, parallel to the longitudinal trough. The crack usually has a semi elliptical surface [8]. The crack in the deck plate between the crossbeams propagates in a similar way. The difference is that this crack grows in vertical and longitudinal direction at the same time.

2.4. OSD design according to NEN-EN 1993-2

Eurocode 3 part 2 [30] and the corresponding Dutch national annex [31] give some limitations about the design of OSD bridges. For the deck plate thickness, the surface wearing influences the fatigue performance and therefore, it is taken into account in the recommendation. The minimum thickness of the deck plate (t) for heavy traffic is:

$t \geq 14$ mm	if the asphalt layer is ≥ 70 mm
$t \geq 16$ mm	if the asphalt layer is ≥ 40 mm.

The fatigue strength of a detail is influenced by the number of heavy vehicles which enters the bridge. A thicker deck plate results in a longer fatigue life for the same heavy vehicle intensity. Because this intensity differs per road type, the deck plate thickness is determined for each traffic category separately. The values are given in table 2.1. For traffic category 1, the design life is 100 years and for the other categories 50 years.

In some cases, a reduced traffic load can be used for traffic category 2, 3 and 4. For these cases, the deck plate thickness can also be reduced.

Table 2.1: Deck plate thickness according to NEN-EN 1993-2/NB table NB.5 and NB.6 [31]

Traffic category	**Design life**	**Deck plate thickness** (mm)	
		Asphalt or hpc layer, minimum thickness of 60 mm	Epoxy layer, minimum thickness of 8 mm
1. Highways and roads with two or more lanes per direction and with heavy truck intensity	100 years	18	22
2. Roads with average truck intensity	50 years	18 / 16*	20 / 18*
3. Roads with low truck intensity	50 years	16 / 14*	18 / 16*
4. Roads with low truck intensity and only traffic for destination	50 years	14 / 12*	15 / 14*

* Reduced value of the deck plate thickness

According to Eurocode 3 part 2 [30], the distance between the troughs web at the top (e) should be e ≤ 300 mm. The relation between the distance between the trough webs and the deck plate thickness (t) should be limited to e/t ≤ 25. The thickness of the trough should always be $t_{stiff} \geq 6$ mm.

Eurocode 3 part 2, Dutch national annex, chapter C.1.2.2 [31] gives recommendations about the distance between the crossbeams related to the moment of inertia of the longitudinal stiffener including the deck plate. This recommendation should prevent cracks in the surface layer due to deformations of the deck plate. The maximum distance between the crossbeams can be found in figure 2.7. Curve B should be used for longitudinal stiffeners within a distance of 1.20 meter from the main girder web and which are loaded by a heavy traffic lane and. For other cases, curve A is sufficient.

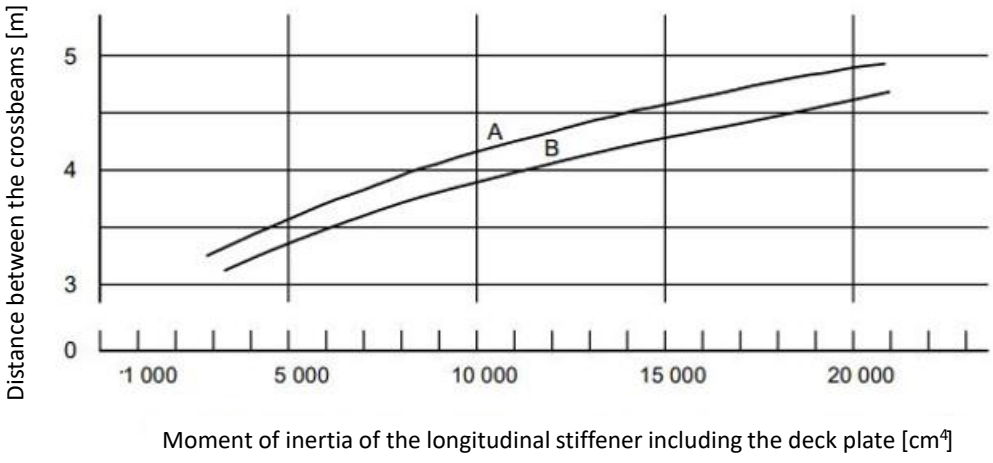

Figure 2.7: Relation moment of inertia and distance between crossbeams

2.5. Design parameters with respect to fatigue performance

The dimensions of the OSD influence the fatigue life. Besides this, the geometry of the weld may also influence the local peak stresses in the details prone to fatigue. Different geometrical aspects of the decks are already investigated by many researchers. A description of a couple of studies is given below.

The deck plate and trough thickness, the width between trough webs and the penetration ratio are related to the rib-to-deck plate weld at the crossbeam and in span. The trough shape and influence of cope holes are related to the trough-to-crossbeam weld at the bottom of the trough and the crossbeams is related to both joints.

2.5.1. Deck plate thickness and thickness of troughs

Murakoshi et al. [24] studied the rib-to-deck plate joint at the crossbeam and in span. A finite element model, made of solid elements, is used to analyze the local principal stresses at the joints for different parameters. Eight alternatives are considered. Half of the alternatives have a trough thickness of 6 mm and the other half a thickness of 8 mm. The deck plate thickness is equal to 12 mm, 14 mm, 16 mm and 19 mm.

The deck segments are loaded with a double tyre and a wheel load of 150 kN both at the crossbeam location and in the middle between two crossbeams. Resulting minimum principal stress at the weld root is given in figure 2.8.

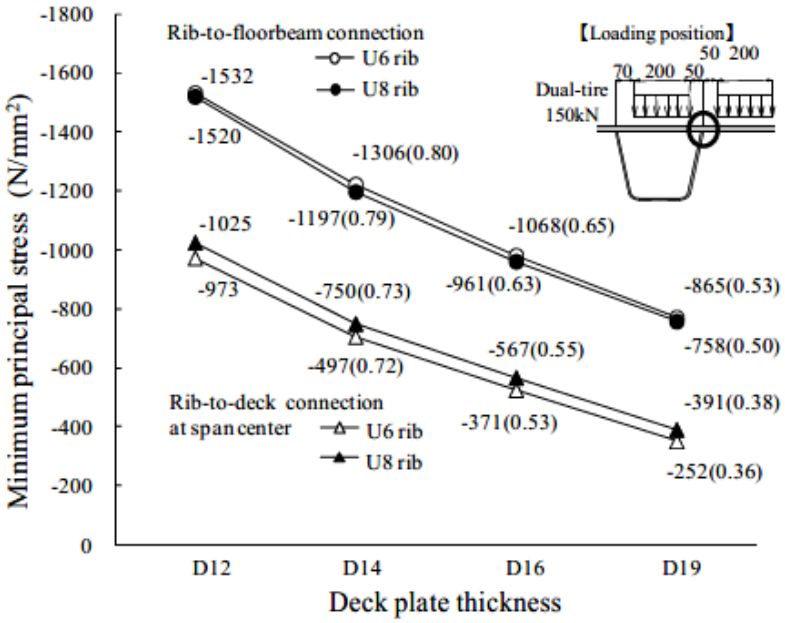

Figure 2.8: Minimum principal stress versus deck plate thickness [24, fig. 11]

A conclusion of the research is that an increased deck plate thickness results in lower maximum principal stresses and the trough thickness does not have a large influence on the principal stress. Highest stresses are found in the rib-to-deck plate joint at the crossbeam.

Another study to the rib-to-deck plate joint is made by de Backer et al. [6]. A full-scale finite element model made of shell elements is used. Three alternatives are compared at the location at the crossbeam and in span between the crossbeams. All alternatives have a same trough thickness of 8 mm. A deck plate thickness of 14 mm, 16 mm and 18 mm are considered. A cope hole is applied in the crossbeam.

The fatigue life is determined using the nominal stress method and the hot spot stress method according to the Eurocode. Fatigue load model 4 is used to determine the fatigue life. The conclusion for both locations of the joint is that a thicker deck plate thickness results in an increased fatigue life.

Terao (as cited in Kolstein [17, p. 267]) investigated the influence of the deck plate thickness and trough web thickness on the stress range near the weld root using a finite element model. The trough web and deck plate are connected with a filled weld and a gab between the element of 0.5 mm. a load of 10 kN is applied at a load area of 500 x 200 mm^2. The results for a deck plate thickness of 12 mm and 24 mm and a trough thickness of 6 mm and 8 mm is given in table 2.2.

Table 2.2: Peak stress at the weld root of the rib-to-deck plate joint at the crossbeam. (Reproduced from Kolstein [17])

Deck plate thickness [mm]	**Trough thickness [mm]**	
	6	8
12	580 MPa	580 MPa
24	300 MPa	300 MPa

There can be concluded that a deck plate thickness of 24 mm results in lower peak stresses compared to a deck plate thickness of 12 mm. The trough web thickness does not have an influence on the stress if a same deck plate thickness is considered.

Summary

An overall conclusion from the different studies is that the bending stresses in the deck plate influence the fatigue life of the detail. An increased deck plate thickness results in an decreased bending stress. Increase of the thickness of the trough web does not significantly affect the bending stress in the deck plate both at the crossbeam location and between crossbeams and thus has no influence on the fatigue life.

2.5.2. Width between troughs

Fettahoglu [11] investigated different parameters of an OSD. A finite element model made with shell elements is used. Welds are not included in the model. An oval cope hole is present. For a reference deck plate thickness of 12 mm, a distance between the trough webs of 150, 225, 300, 375 and 450 mm are compared. For all alternatives, the displacement and the Von Mises stress at the rib-to-deck plate joint in span between two crossbeams are analyzed. Results are shown in figure 2.9.

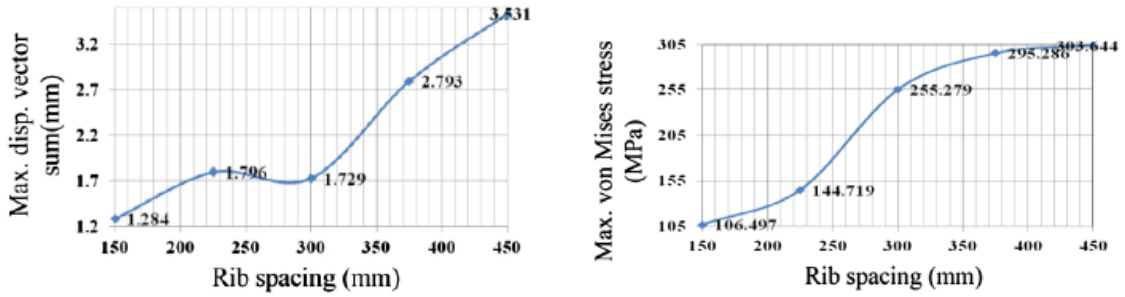

(a) Displacement versus rib spacing

(b) Von Mises stress versus rib spacing

Figure 2.9: Effect of rib spacing [11, p. 18]

The Von Mises stress increases for a distance between the webs of 150 mm to 300 mm. A distance larger than 300 mm leads to only a bit higher Von Mises stress compared to the distance of 300 mm.

For the deformation, it is the other way around. For 150 mm to 300 mm distance between the webs, the deformation does not increase significant, while if the distance becomes larger than 300 mm, the deformation increases a lot. On the other hand, the deformation becomes smaller if the deck plate thickness increases, because the moment of inertia of the deck plate increases. The deformation for an increased deck plate thickness in combination with a larger trough web space is not investigated.

2.5.3. Trough to deck plate weld design

In the past, a fillet weld without penetration was used generally. Nowadays, a full penetrated weld is required. For the ease of welding, a lack of penetration is acceptable but should be smaller than 1 mm according to table NB.7 of the Ducth national annex of Eurocode 3 part 2 [31].

Miki (as cited in Kolstein [17, p. 263]) did research to the penetration ratio of the weld root for the rib-to-deck plate weld. A deck plate thickness of 12 mm and a trough thickness of 6 mm are used. The penetration depth of 1.5, 3.0, 4.5 and 6 mm are compared. The 6 mm depth is full weld penetration. Terao (as cited in Kolstein [17, p. 267]) studied the penetration ratio in a similar way using same dimensions for the deck segment which is used for the experiment. The penetration depths which is considered is 0 mm (no penetration), 2 mm, 3 mm, 4 mm and 6 mm (full penetration). From both studies, the conclusion was that full penetration results in the lowest stress range at the deck plate. According to Terao, a full penetration can reduce the stress with 25% compared to a fillet weld.

Dung et al. [10] did research to the influence on the stresses for different weld penetration ratios in the rib to deck plate and crossbeam joint. The specimens have a deck plate thickness of 12 mm and a trough thickness of 6 mm.

A finite element model, consisting of a global shell element model and solid element sub model, are used for the analysis of the weld penetration. The effective notch stress at the weld root is determined. Results are given in figure 2.10. Concluded can be that increase of the weld penetration ratio results in slightly higher stresses. However, a full penetration results in lowest effective notch stress. The difference between the models is small. A full penetrated weld results in only a 3.8% lower stress value compared to 75% penetration ratio.

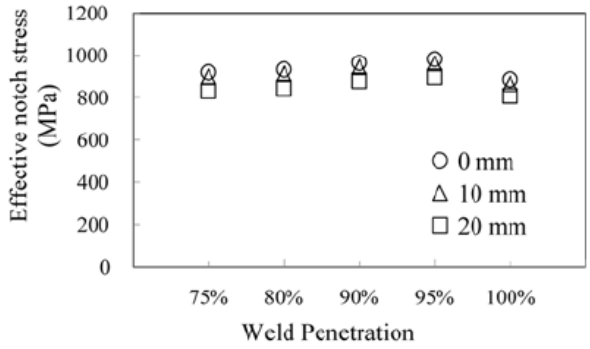

Figure 2.10: Effective notch stress versus weld penetration ratio. (Effective notch stress evaluated at 0, 10, and 20 mm from the midpoint of the weld line). [10, fig. 20]

Summary

From the different studies, there can be concluded that a full penetrated weld results in lower stresses compared to a filled weld. As discussed above, a lack of penetration of 1.5 mm (75% penetration ratio) leads to only a small increase of stress. However, according to the Eurocode, the lack of penetration should be limited to a maximum of 1 mm.

2.5.4. Trough shape

Closed stiffeners used in an OSD generally have a V-, U-, or trapezoidal shape, as shown in figure 2.11. For engineers and the world wide steel industry, the trapezoidal shape is the most useful one, and therefore most common applied [3]. However, from test results [15] it is clear that this profile is susceptible to higher stress concentrations in the crossbeam around the lower corner of the trough compared to the other two shapes. The stresses in the rib-to-deck plate detail are not considered.

For the experiment, a full scale finite element model made of shell elements is used. No cope hole is considered. Two single tire wheel loads are applied with a contact area of 200 mm x and a distance of 1200 mm between them. A load of 250 kN is applied. The principal stress in the crossbeams is analysed. There can be concluded that from the three shapes, the V-shaped profile results in the lowest maximum stress in longitudinal and transverse direction. The relation between the stress distribution for all types if a cope hole is used is not considered.

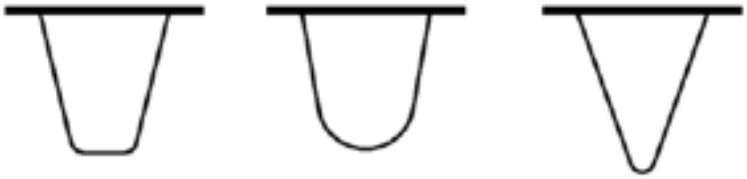

Figure 2.11: Typical trough shapes; left: trapezoidal, middle: U-shape, right: V-shape [3]

Generally, continuous troughs are used. However, it is possible to use troughs which are welded between the crossbeams. In this case, the welded trough-to-crossbeam connection is more sensitive to fatigue than if continuous troughs are used. Therefore, it can be applied only for specific cases, like if the overall depth of the deck must be minimized and if the amount of load cycles from heavy traffic is limited [17].

2.5.5. Crossbeams

The in-plane deformation of the crossbeam affects the stress range in the deck plate at the rib-to-deck joint at the crossbeam [17]. Due to in-plane deformation of the crossbeam, the deck plate has to deform as well. This results in relatively high peak stresses in the deck plate at the connection to the crossbeam and thus affects the fatigue life of the rib-to-deck plate joint. According to the research, there is concluded that for a relative shallow crossbeam, this in-plane deformation should be taken into account in the fatigue life calculation for the rib-to-deck plate joint.

The distance between and the thickness of the crossbeams may influence the stresses in the bridge deck [38]. If the distance between crossbeams becomes larger, the deflection of the deck becomes larger which leads to larger out-of-plane deformation of the crossbeam. As a consequence, the stress range around the rib-to-crossbeam joint at the bottom of the trough will increase. By increasing the thickness of the crossbeam, the in-plane stresses may decrease. From tests made by Wang [36], it follows that the out-of-plane distortion still determines the fatigue strength of the rib-to-crossbeam joint.

2.5.6. Use of cope holes

In some cases, it is beneficial to include a cope hole in the crossbeam. This cut-out leads to lower peak stresses around the lower corner of the trapezoidal trough, and should increase the fatigue life of that detail. However, this detail is still prone to fatigue cracks. If a cope hole is present, cracks may initiate at the bottom end of the weld toe of the rib-to-crossbeam joint [36].

It is recommended to use a cope hole only if the depth of the crossbeam is larger than 1200 mm and the crossbeam thickness is larger than 12 mm. For example, this is often the case in box girders. The shape of the cope hole can be oval. An improved shape is the ‘Haibach’ type, which is recommended to use by the [32].

Kolstein [17] investigated the benefits of using a cope hole and he stated that it may is never preferable to use. A cope hole in the crossbeam at the rib-to-deck plate connection should always be avoided.

2.6. Examples of dimensions of OSD

For a couple of bascule bridges with an OSD, the dimensions of the bridge deck and crossbeams are given in table2.3. Information is derived from Iv-infra, unless otherwise stated.

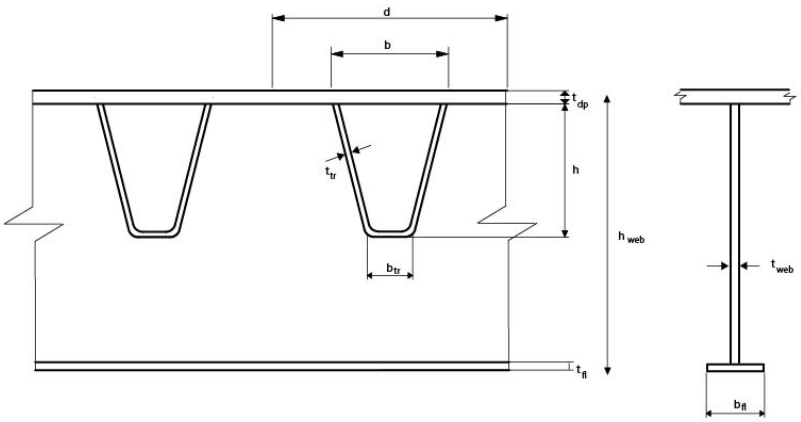
d
b
t_{dp}
h
h_{web}
t_{tr}
b_{tr}
t_{web}
t_{fl}
b_{fl}

Table 2.3: Dimensions of bridges with an OSD (mm)

Bridge	**Type**	**Traffic category**	**Deck plate**		**Trough**	**Crossbeam**			**Copehole**
			d	b x t_{dp}	h x b_{tr}	h_{web} x t_{web}	b_{fl} x t_{fl}	c.t.c.	
Julianabridge Groningen	Movable	1.	600	300 x 16	350x 180 x 8	n/a	n/a	2662	no (troughs welded between crossbeams)
Giessenbridge Rotterdam	Movable	1.	600	300 x 16	350 x 180 x 8	1230 x 12	400 x 30	2800	no
Bridge by Kanne Belgium	fixed	2.	600	300 x 14	300 x 200 x 6	800 x 30	500 x 30	n/a	yes
Temse Bridge Belgium [[25]]	Movable	2.	600	300 x 12	350 x 90 x 8	n/a	n/a	n/a	yes (and in top of crossbeam at the rib-to-deck plate joint)
Vollenhoverbridge Flevoland	Movable	2.	600	300 x 16	350 x 180 x 8	n/a	n/a	n/a	no (troughs welded between crossbeams)
Sebastiaanbridge Delft	Movable	3. (and tram line)	550	300 x 18	350 x 160 x 6	1500 x 15	350 x 25	2256	no (troughs welded between crossbeams)
Wilheminabrug Zaandam	Movable	3.	612.5	- x 18	350 x 120 x 6	1200 x 12	300 x 25	2960	n/a

2.7. The S-N curve

The stress ranges determined according to the approaches discussed in this chapter can be assessed according to the S-N curve given in Eurocode 3 part 1-9 [29]. The S-N curve gives a relation between the stress range (S) and the load cycles to failure (N). It describes the resistance limit and is determined for each specific welding detail separately.

A detail category gives the stress range which causes failure at 2 million load cycles. For each specific joint, the detail category should be determined from experimental results. All influencing factors which are not included in the design stress range are taken into account in the detail category. Factors which are taken into account are the weld imperfections and residual stresses due to welding. Depending on the method used to determine the stress range, the structural stress concentrations due to the geometry of the detail and due to weld geometry are taken into account either by the design stress or the detail category.

The S-N curve is determined from the experimental results. The mean curve is the averaged line between the experimental results. These experimental results generally give a large scatter. Therefore, a design or characteristic curve with a survival probability of 97.7% is statistically determined from the mean curve. Figure 2.12 gives an example of the mean and design curve. The detail categories are determined for the design curve.

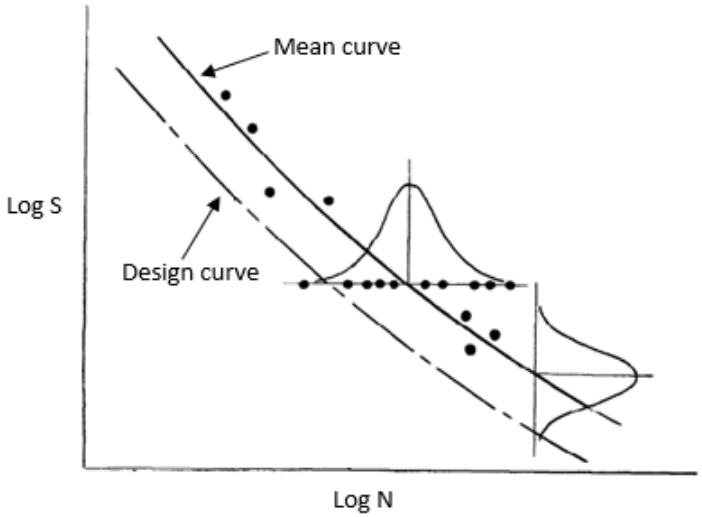

Figure 2.12: SN curve mean and 97.7% survival probability [2]

Figure 2.13 gives standard S-N curves for different details. The points 1, 2 and 3 are the detail category, the constant amplitude fatigue limit (CAFL) and the cutt-off limit respectively. The stress range at CAFL ($\Delta\sigma_D$) corresponds to $N_D = 5 * 10^6$ load cycles. The stress range at cut-off limit ($\Delta\sigma_L$) should be determined at $N_L = 1 * 10^8$ load cycles. The stress ranges can be calculated according to equations 2.1 and 2.2.

When a stress range with constant amplitude is considered, the fatigue life will be infinite if the stress range is below the stress value at the CAFL. When the amplitude is variable, fatigue life will be infinite if the stress range is lower than the cut-off limit and the value of m changes after the CAFL is reached.

$$\Delta\sigma_D = (\frac{2}{5})^{\frac{1}{3}} * \Delta\sigma_C \tag{2.1}$$

$$\Delta\sigma_L = (\frac{5}{100})^{\frac{1}{5}} * \Delta\sigma_D \tag{2.2}$$

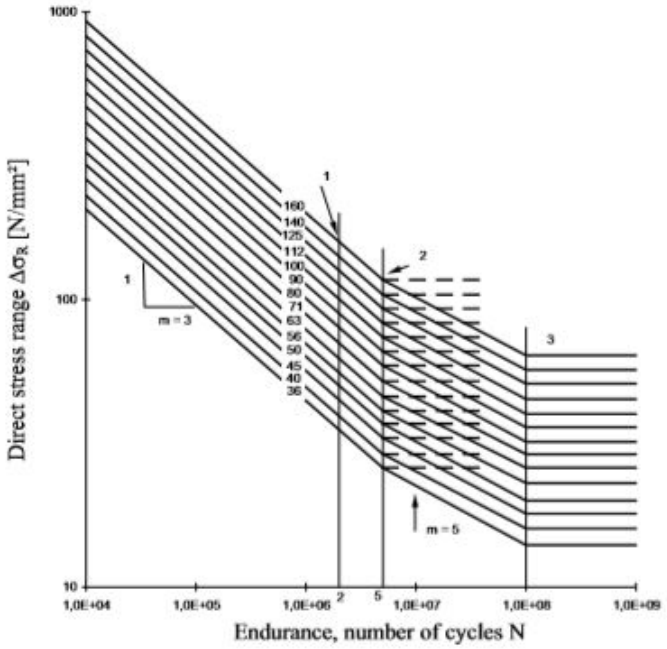

Figure 2.13: Standard S-N curves according to the Eurocode [29, fig 7.1]

The design fatigue life N_R corresponding to the design stress range $\Delta\sigma_R$ can be determined according to equations 2.3.

$$N_R = \min \begin{cases} (\frac{\Delta\sigma_C}{\Delta\sigma_R})^3 * N_C & \text{for } \Delta\sigma_R \leq \Delta\sigma_D \\ (\frac{\Delta\sigma_D}{\Delta\sigma_R})^5 * N_D & \text{for} \Delta\sigma_D < \Delta\sigma_R \leq \Delta\sigma_L \\ \infty & \text{for } \Delta\sigma_R \geq \Delta\sigma_L \end{cases} \tag{2.3}$$

Palmgren-Miner cumulative damage rule

Most structures have a variable stress range. Each stress range results in a different value of load cycles to failure. The total damage of the detail is a summation of all different damage values corresponding to the stress ranges and is called the Palmgren-Miner cumulative damage rule, as given in equation 2.4 [29, p 39].

$$D \leq \frac{n_i}{N_i} = \sum \frac{n_1}{N_1} + \frac{n_2}{N_2} + \frac{n_3}{N_3} + \frac{n_4}{N_4} + ... \leq 1.0 \tag{2.4}$$

where:

- D is the damage value,
- n_i is the design number of load cycles for load F_i,
- N_i is the number of load cycles corresponding to the design stress range $\Delta\sigma_i$ for load F_i.

2.8. Stress based fatigue assessment procedures

To determine the fatigue life of details based on the S-N curve, the stress range at the weld root and toe should be determined. Therefore, different methods are developed to calculate the stress range which can be used to estimate the fatigue life. Eurocode 3 part 1-9 [29] describes two methods, which are the (modified) nominal stress method and the hot spot stress method. The nominal stress method is generally used for simple details and if the geometry of a detail is more complex, the structural hot spot stress is recommended. An improved method, described by the International Institute of Welding (IIW) [12], is the effective notch stress method.

For all three methods, a prediction of the stress range will be made. Figure 2.14 shows the distribution of the different stresses. Dependent on the method, the geometry of the structure, the geometry of the weld and

welding defects are taken into account in the calculated stress or in the S-N curve.

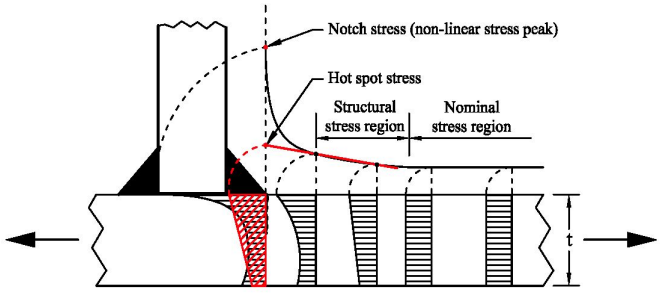

Figure 2.14: Stress in detail according to different methods [20]

2.8.1. (modified) Nominal stress method

The nominal stress method discussed in this paragraph is according to Eurocode 3 part 1-9 [29].

The nominal stress method uses the nominal stress in the weld or parent material of the considered detail to determine the fatigue life. Because only the nominal stresses are take into account, the local stress raising effect at notches is not included in the stress range. Stress concentrations due to the local weld profile and weld imperfections are also not included and should therefore be included in the detail category.

The modified nominal stress method can be used if stress raising factors should be taken into account. These factors are eccentricities, misalignment's and geometric discontinuities, like a hole or a plate with fillets and are included in the stress concentration factor k_f. To determine the modified nominal stress, the nominal stress should be multiplied by the stress concentration factor.

Detail category

The value of the detail categories for the nominal stress method for OSDs with closed stiffeners are given in table 8.8 of EC 3 part 1-9 [29]. For the trough web-to-deck plate joint near the crossbeam, a distinction is made between a full penetrated butt weld, 2.15 detail 7 and a fillet weld, 2.15 detail 8. The detail category for the butt weld is equal to 71 MPa and for the filled weld it is 50 MPa.

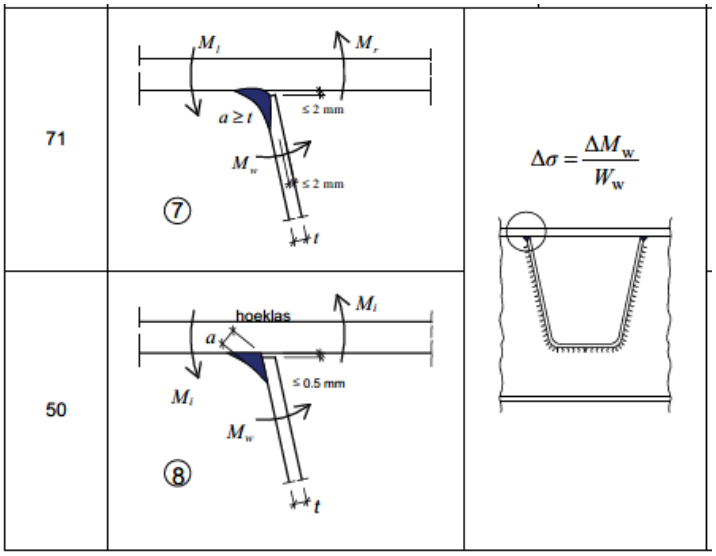

Figure 2.15: Detail 7 and 8 [29, table 8.8]

2.8.2. Hot spot stress method

The hot spot stress is an extrapolated stress at the weld toe and can be determined by hand or by using a finite element model. For the last option, no recommendations about using it are available in the Eurocode. However, the IIW gives some recommendations about it. Generally, the method is only applicable at the weld toe. However, for the rib-to-deck plate joint with a butt weld, it is also possible to estimate the hot spot stress at the weld root.

The hot spot stress range includes the stress raising effects due to geometric complexity. Local weld discontinuities and imperfections are excluded and therefore, it is included in the S-N curve [4]. The weld geometry can easily be applied in a solid element model. For a model with shell elements, it is more difficult and therefore, generally not taken into account.

Detail category

Table NB.7 of the Dutch national annex of NEN-EN 1993-2 [31] give values for the detail categories for OSDs. For the rib-to-deck plate joint near the crossbeam which satisfies the limitations as given in 2.16, the detail category is 125 MPa. There is made no distinction for the detail category for models which includes the weld geometry and which do not.

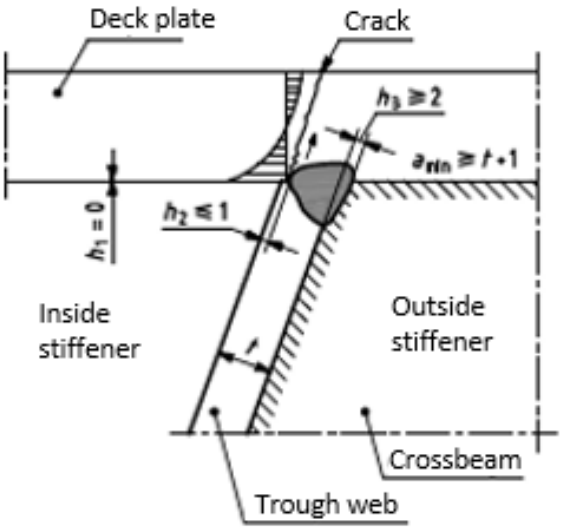

Figure 2.16: Detail 2 [31, table NB.7]

The detail category given in the Eurocode is equal to the characteristic detail category determined by Kolstein [17]. This characteristic value is equal to the mean value minus two times the standard deviation. The mean value for the detail category is 180 MPa. The failure criterion which is assumed for determining the detail category is a change of the strain value near the crack of 10%.

Finite element modelling

A 3D finite element model can be used for the calculation of the hot spot stress. Both a model with shell or solid elements is suitable. The hot spot stress is the extrapolated stress determined using reference points which are located at a certain distance from the weld toe or root.

In the report of Kolstein [17], some requirements for the reference points which corresponds to the detail category from the Eurocode are given. According to experimental results, these points should be at a distance 0.4t and 1.0t from the weld root. This results in a linear extrapolation of the hot spot stress.

The IIW [12] gives some more options for extrapolation of the hot spot stress. The hot spot stress can be

extrapolated in two ways, using type a or type b. The measuring points, and thus the stress range, determined using type a are dependent on the plate thickness, while the stress is independent of the plate thickness for type b.

The location of the reference points depends on the mesh of the model. There is made a distinction between a relative coarse and fine mesh. Table 2.4 gives the reference points.

Table 2.4: Requirements extrapolation hot spot stress according to the IIW

		Relative coarse mesh		**Relative fine mesh**	
		Shell	Solid	Shell	Solid
Type a	Element size	t	t x t	≤ 0.4t	≤ 0.4t x t
	Reference points	0.5t and 1.5t		0.4t and 1.0t	
	Hot spot stress	$\sigma_{hs} = 1.5\sigma_{0.5t} - 0.5\sigma_{1.5t}$		$\sigma_{hs} = 1.67\sigma_{0.4t} - 0.67\sigma_{1.0t}$	
Type b	Element size	10mm	10mm x 10mm	4mm	4mm x 4mm
	Reference points	5mm and 15mm		4mm, 8mm and 12mm	
	Hot spot stress	$\sigma_{hs} = 1.5\sigma_{5mm} - 0.5\sigma_{1.5mm}$		$\sigma_{hs} = 3\sigma_{4mm} - 3\sigma_{8mm} + \sigma 12mm$	

From different studies [4], [1], it follows that the results of the hot spot stress method may depend on the element type and mesh size of the FE model. The presence of welds in the model also has an influence on the results [35].

Hand calculation for the rib-to-deck plate joint

To determine the fatigue life for the rib-to-deck plate joint by hand, a 2D simplification of the real structure is used. The Dutch national annex of Eurocode 3 part 2 [31] describes how to apply the method.

The deck plate between the trough webs, figure 2.17(a), is assumed as a beam and the connection between the trough web and deck plate is taken as a fixed support. Figure 2.17(b) gives the resulting mechanical scheme. The distributed wheel load should be applied at the middle of the trough. The stress range is determined per 1 mm width of the deck plate.

The distributed wheel load is equal to equation 2.5.

$$q_{wheel} = \frac{Q_k}{2 * b_{wheel} * l_{wheel}} \tag{2.5}$$

where:

Q_k is the axle load
b_{wheel} is the width of the wheel contact area
l_{wheel} is the length of the wheel contact area

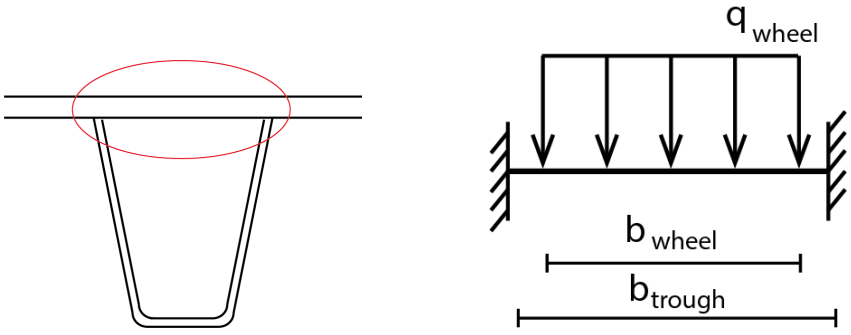

(a) Location

(b) Mechanical scheme of simplified structure

Figure 2.17: 2D simplification

The bending stress in the fixed supports should be calculated. This bending stress is the nominal stress. To determine the hot spot stress, this bending stress is multiplied by a stress concentration factor (SCF). If no asphalt layer is considered, the SCF is equal to equation 2.6. The hot spot stress can be determined with equation 2.7

$$SCF = 1.2975 - 0.00938 * t \tag{2.6}$$

$$\Delta\sigma = SCF\frac{M}{W} = SCF\frac{6 * M}{t^2} \tag{2.7}$$

2.8.3. One point hot spot stress

A simple variation of the hot spot stress method is the one point hot spot stress method. The stress at a point 0.5 times t from the weld toe should be determined, where t is the deck plate thickness. Instead of general extrapolation, the hot spot stress is determined by multiplying the reference point by a factor 1.12 [1].

A same FE model as used for the general hot spot stress approach is suitable to use. Quadratic elements with a size t x t should be applied. This element size corresponds to the type a extrapolation method with a relative coarse mesh as described by IIW.

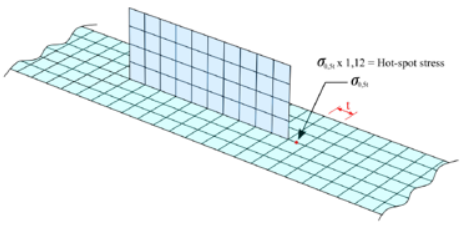

Figure 2.18: One point hot spot stress method [1]

2.8.4. Effective notch stress method

The effective notch stress method is included in the recommendations from the IIW [12]. It is an alternative method for the methods described in the Eurocode. It is applicable at both the weld toe and root. Normally, it is more time consuming than the hot spot stress method.

At the weld root and toe in a FE model, stress singularities may appear. Therefore, a realistic stress at these points is difficult to determine computational. To prevent singularities, a notch at these points is applied, figure 2.19. The effective notch stress is thus the maximum elastic stress at the notch [1].

Local stress raising effects due to geometry of the detail and geometry of the weld are included in the effective notch stress. Stress concentrations due to misalignment's and welding defects should be taken into account in the detail category.

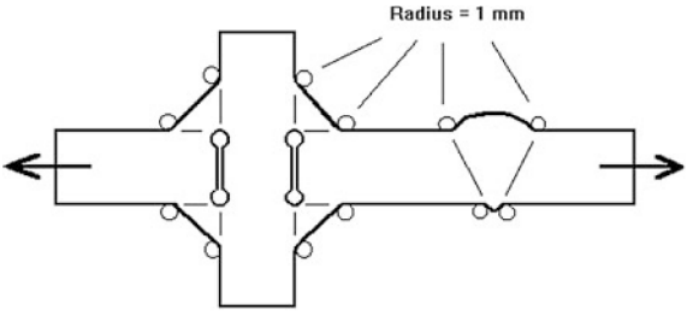

Figure 2.19: Effective notch stress method [12]

Finite element modelling

A finite element model should be used to determine the effective notch stress. Generally, this model is a 3D solid element model. However, a simplified 2D model can be used. This is possible if the stresses are mainly perpendicular to the weld and if the weld continuous, without variety of loading and geometry, over the area which is considered. [12].

The IIW recommends a notch radius of 1 mm. Like for the hot spot stress method, the value of the effective notch stress depends on the mesh size of the elements. Table 2.5 gives the required element sizes according to the IIW for a notch radius of 1mm.

Table 2.5: Element size around the notch[12]

Element type	Element size
Linear elements	≤ 0.15mm
Quadratic elements	≤ 0.25mm

Detail category

Only one detail category is needed for the effective notch stress method and can be used for each specific detail. The IIW prescribes to use a detail category of 225 MPa if the principal stress is used and 200 MPa if the von Mises stress is determined. These values are valid for filled welds with a flank angle of 45°and butt welds with a flank angle of 30°. It is limited to plates with a thickness t ≥ 5mm. The recommendations for modelling as discussed in this section should be applied.

2.8.5. Accuracy of the assessment methods

For the nominal stress method, each detail needs a specific S-N curve. More factors are taken into account by the calculation of the hot spot stress than by the nominal stress. If more factors are taken into account by the calculation of the stress range, a more accurate prediction can be made and therefore, a more accurate fatigue life may can be determined [19].

The hot spot stress method and effective notch stress method are compared with each other in several studies. According to Wang [36], analysis of the fatigue strength of fillet welds leads to similar results for both methods.

A comparison of the methods for an open stiffener-to-crossbeam joint in an OSD was made by Al-Emrani and Aygül [1]. The results for the effective notch stress where conservative. The determined value of load cycles was less than half of the cycles which was determined with the hot spot stress method (with quadratic extrapolation). The nominal stress method was analysed as well. The calculated amount of load cycles to failure was 20% lower compared to the hot spot stress method.

If a finite element model is used for the calculation of the fatigue strength, the accuracy is may influenced by the model. The mesh size and element type have a large influence on the calculated stress range. For example,

Swierstra [35] found that the hot spot stress method results in a more accurate solution if solid elements are used instead of shell elements. If the weld is included in the solid element model, the results are even more improved.

2.9. Local critical plane based fatigue assessment

Different local critical plane based models are developed. In this report, a description of the swt-parameter is given, first mentioned by Smith, Watson and Topper [33]. This model is based on the strain amplitude and the maximum stress value in a plane. Due to this maximum stress value is taken into account, not only the stress range is important for this approach but it also corrects for the maximum stresses in the material. A steel detail which is partly in compression has for example a larger fatigue life than a detail which is fully in tension.

Instead of different detail categories, this method considers one formula which determines the amount of load cycles to failure. Therefore, local material parameters should be known. The swt-parameter is described with equation 2.8.

$$swt = \Delta\epsilon * \sigma_{max} = \frac{(\sigma'_f)^2}{E}(2N_f)^{2b} + \sigma'_f\epsilon'_f(2N_f)^{b+c} \tag{2.8}$$

where:

σ_{max} is the maximum stress.
$\Delta\epsilon$ is the strain range.
$2N_f$ is the number of reversals to failure (and two reversals is equal to one load cycle).
σ'_f is the fatigue strength coefficient.
the fatigue strength exponent.
ϵ'_f ductility coefficient.
c fatigue ductility exponent.

Values for the coefficients and exponents for steel S355 are determined by de Jesus et al. [7]. Results are summarized in table 2.6.

Table 2.6: cyclic elasto-plastic and fatigue properties [7]

	σ'_f	b	ϵ'_f	c
Steel S355	952.2	-0.089	0.7371	-0.664

3

Finite element reference model

This chapter provides a description of the reference finite element (FE) model, built in Abaqus. A study to a suitable element sizes is made. To prove that the strain range near the joint derived from the FE model is similar to real values, the strain range is validated with test results from a full scale OSD specimen, performed by Wu et al. [37].

3.1. Model description

3.1.1. Dimensions

The dimensions of the FE model are the same as the dimensions of the test specimen used by Wu et al. [37], which will be used for validation. For their research to the rib-to-deck plate joint at the crossbeam, an experiment is performed at the Stevinlab II Laboratory at Delft University of Technology.

The OSD segment consists of a deck plate with a thickness of 20 mm, 8 troughs and 3 crossbeams. The total height of the deck including crossbeams is 1000 mm. The crossbeam webs have a thickness of 16 mm and the thickness of the flanges is 12 mm. By four troughs, 'Haibach' shape cope holes are included in the crossbeam. The other four troughs are fully welded to the crossbeam. An overview of the dimensions is given in figure 3.1. The red rectangle indicates the load position.

Continuous troughs are applied. Each trough has a height of 350 mm and a thickness of 6 mm. The width between the trough webs is 300 mm at the top and the flange at the bottom is 105 mm. The troughs are spaced 300 mm from each other. Figure 3.2 shows the dimensions of the trough including a cope hole.

The deck plate and trough web are connected to each other with a butt weld. The lack of penetration of the weld is 1.5 mm, see figure 3.3. The crossbeam-to-deck plate weld and the crossbeam-to-trough weld are filled welds with a throat thickness of 5 mm.

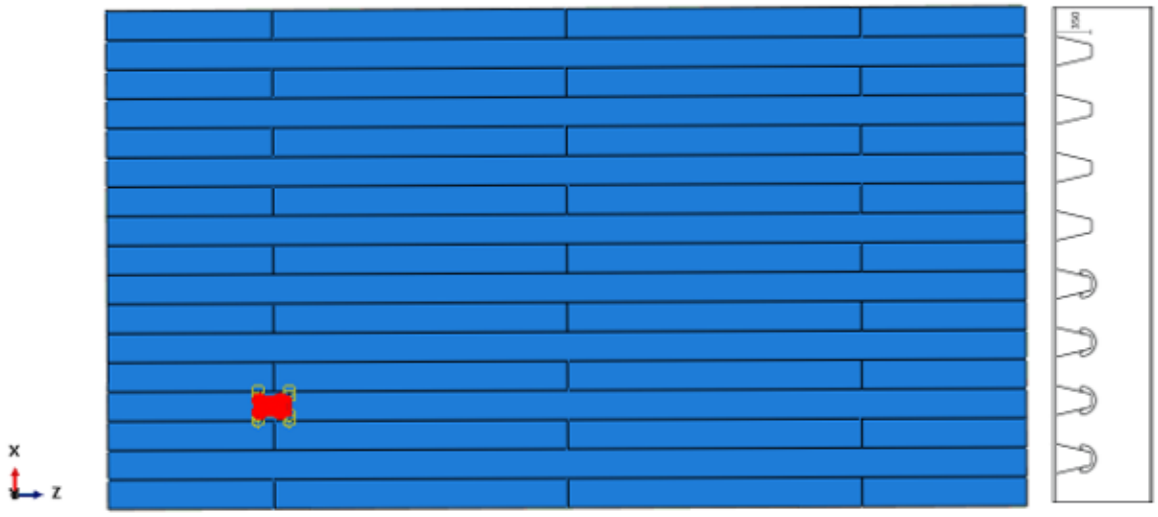

(a) Front view

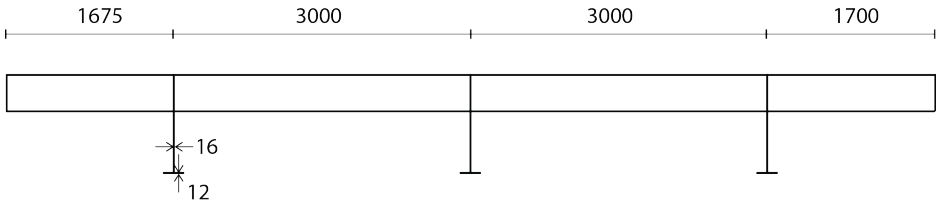

(b) Side view

Figure 3.1: Overview of the deck segment (mm) (Reproduced from Wu et al. [37])

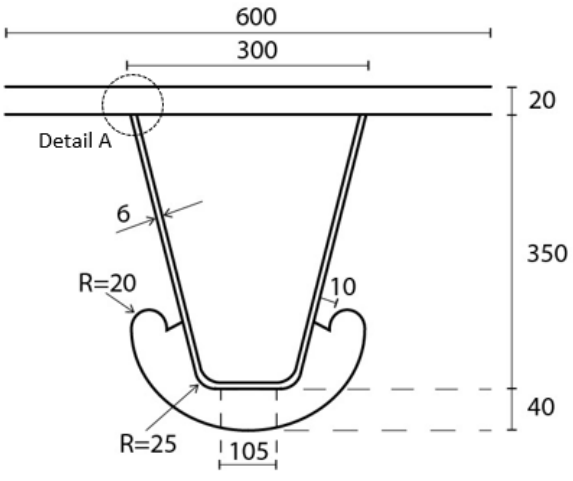

Figure 3.2: Dimensions of the trough (mm) (Reproduced from Wu et al. Wu et al. [37]

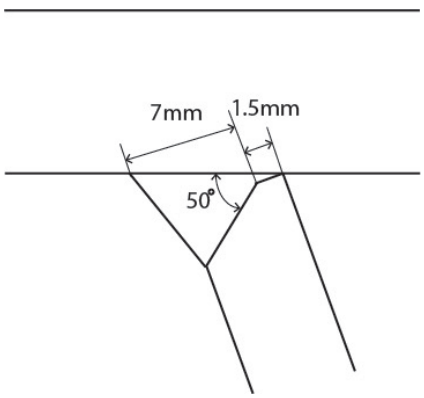

Figure 3.3: Detail A: Geometry of the weld [mm]

3.4 shows the global FE model. If a load is placed at the center of the trough, right above the crossbeam, the deck segment deforms only locally in a zone near the applied load. Therefore, it is possible to model a small part of the total segment, as shown in figure 3.5. The small part consists of only three troughs and a part of one crossbeam.

The experiment of Wu et al. [37] is performed on a trough which is automatically welded to the deck plate and a cope hole in the crossbeam is present. Therefore, this part of the model is used for the smaller FE model.

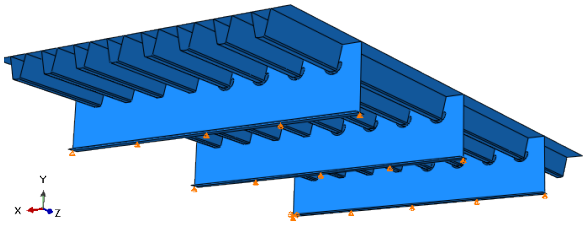

Figure 3.4: Complete global model

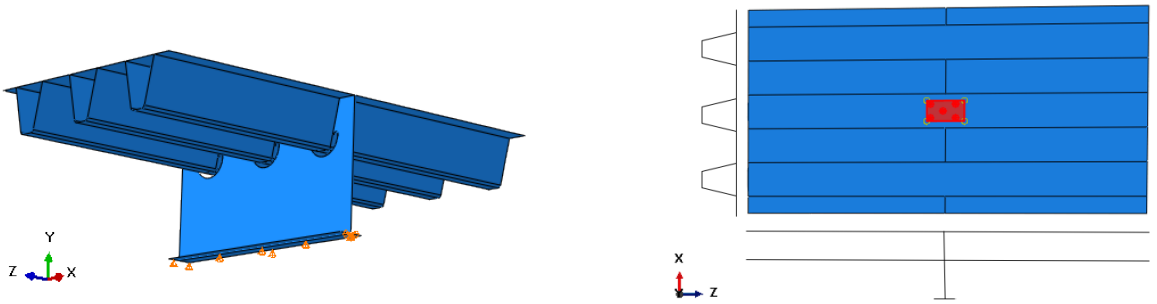

(a) 3D view (b) Top view

Figure 3.5: Three trough model part

3.1.2. Material properties

The material properties which are used for the reference model are given in table 3.1. Because fatigue problems will appear before the yield strength is reached, elastic material properties are considered only.

Table 3.1: Material properties

Modulus of elasticity	210,000 MPa
Poison ratio	0.3

3.1.3. Boundary conditions

The crossbeam flange is fixed in translation in y-direction, see figure 3.5(a). This is similar to the test specimen, which is supported over the full length of the crossbeam by a beam with an IPE-profile. At one point, the FE model is translational fixed in x- and z-direction.

3.1.4. Load

The load from the static loading test is modelled as a distributed load. The contact area of the loading plate is 180 mm x 320 mm. The loading range is 140 kN, which leads to a distributed load equal to 2.43 N/mm^2. The load is placed in the center of the trough, right above the crossbeam, see figure 3.5(b).

3.1.5. Element mesh

Shell elements of the type S8R, which is quadratic interpolation, are applied. The global element size is 100 mm. To make it possible to find the increased concentrated stresses at the joint, a local finer mesh is used at the trough where the load is put on. There are two options considered, a relative coarse mesh, figures 3.6 and a relative fine mesh, figure 3.7.

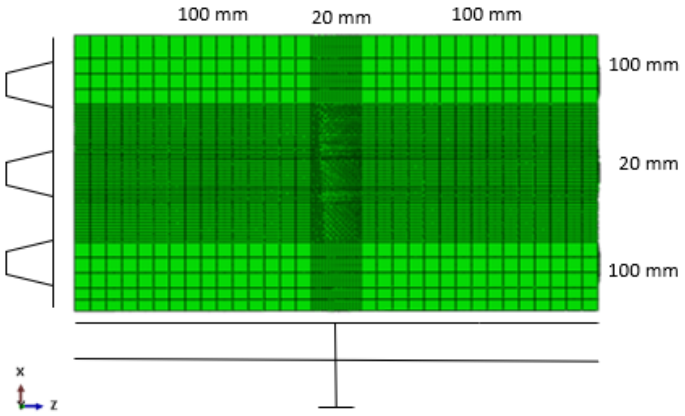

Figure 3.6: Global model with relative coarse shell element size

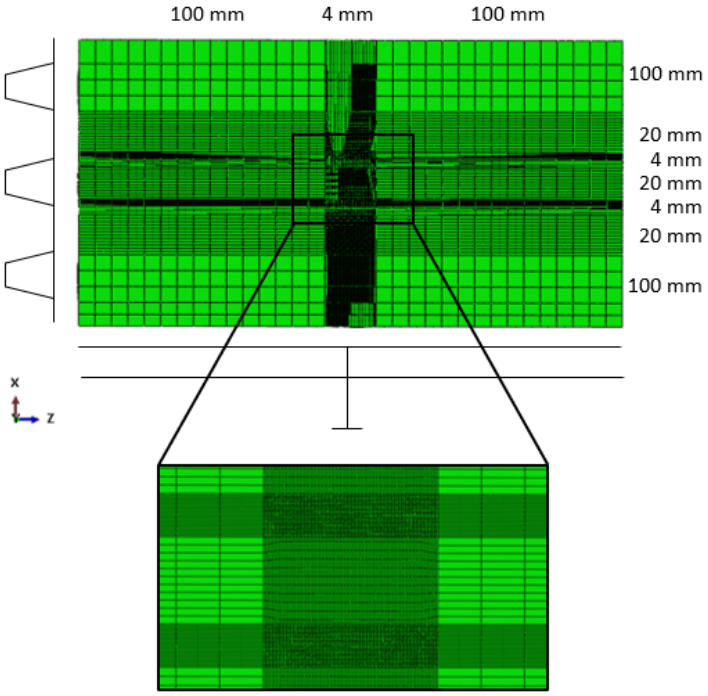

Figure 3.7: Global model with relative fine shell element size

3.1.6. Solid element sub model

For a better prediction of the strain ranges, a solid element model is build. A solid element model generally needs more computational time. To limit this, only a small part of the deck segment is modelled with solid elements. To create a good support, the model is included in the global shell element model, see figure 3.8. The solid elements are connected to the shell element model with a special shell-to-solid coupling constraint. The weld geometry is included in the sub model. In paragraph 2.5.3 is concluded that the effect of the weld penetration ratio only has a small effect on the total stress in the joint. For simplicity of the model, the lack of penetration of 1.5 mm is not taken into account in the first place. In paragraph 3.3.2, it is investigated if this assumption is acceptable.

Linear (C3D8R) or quadratic (C3D20R) brick elements are used. The difference between the two element types is analysed in chapter 4. To create a good mesh in the welds and the rest of the sub model, a global

mesh size of 2 mm is applied.

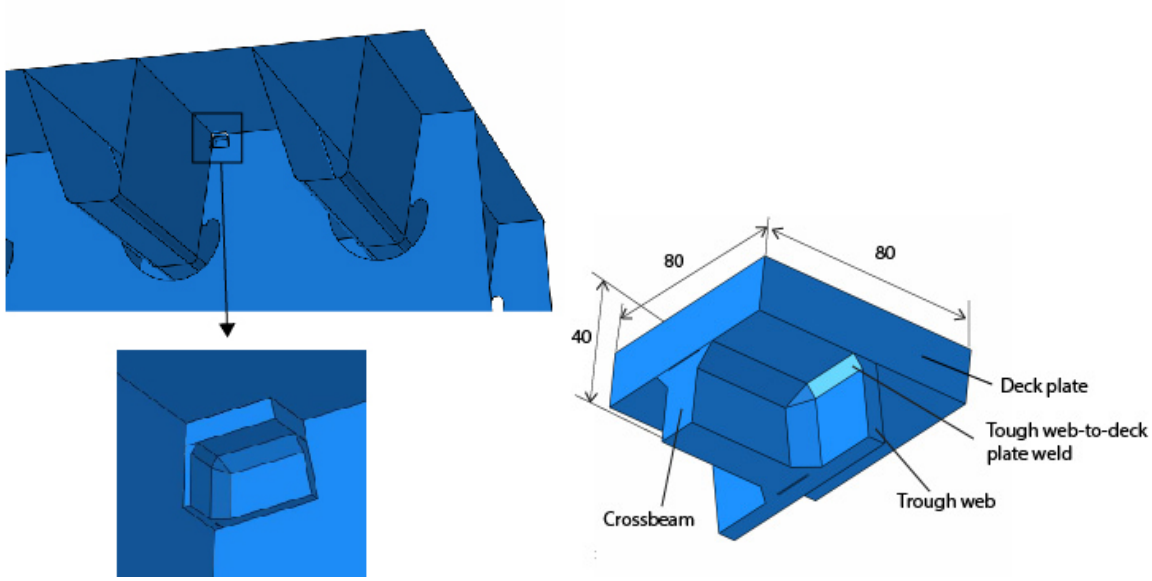

Figure 3.8: Global model and solid element sub model

3.2. Analysis global shell element model

A general analysis of the stress distribution in the global model and the model with three troughs is made. The deformation of the bridge deck due to a wheel load is given in figure 3.9. From figure 3.10, it follows that the deformation of the lower surface of the deck plate is similar for both models. This is the region which will be used for the fatigue analysis of the rib-to-deck plate joint at the crossbeam. The maximum deformation of the deck plate is found in the middle of the two trough webs and is 0.56 mm.

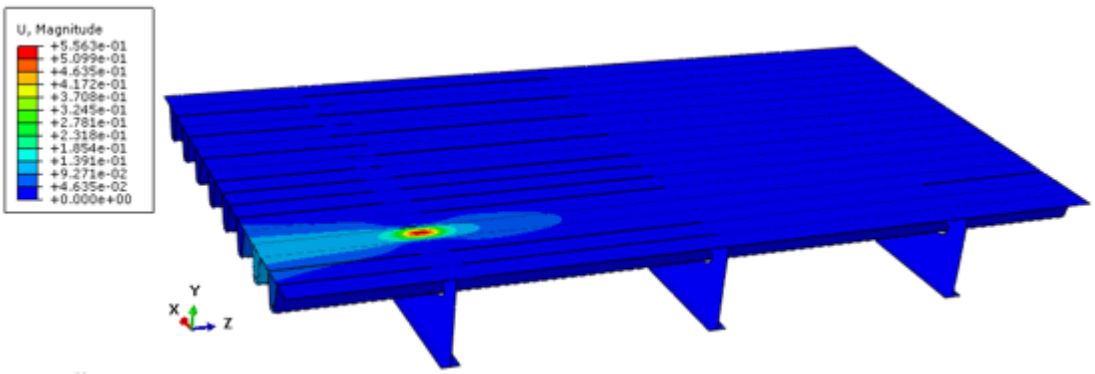

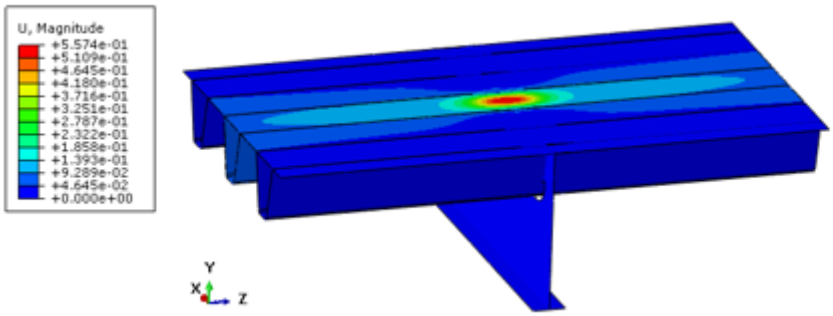

Figure 3.9: Deformation of the global and simplified model

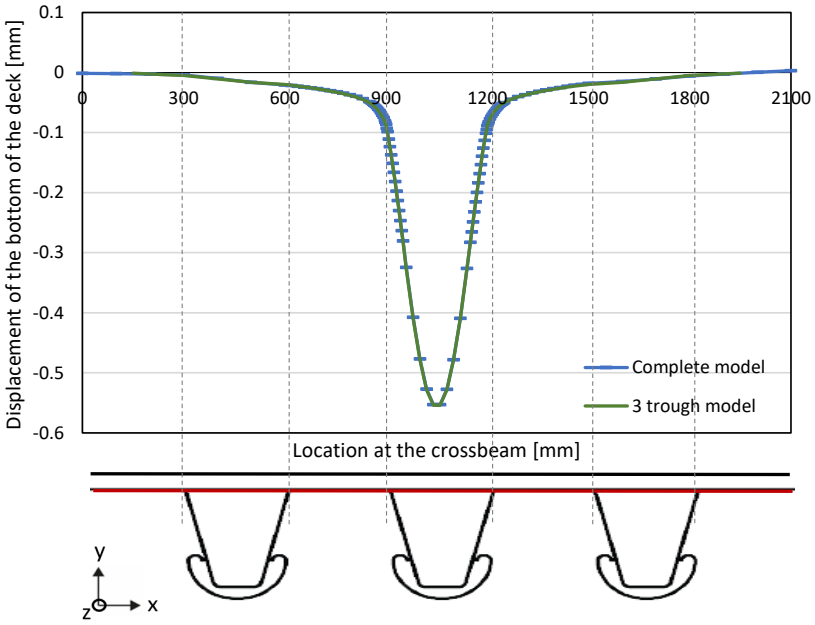

Figure 3.10: Deformation of the deck plate along the crossbeam for the global and simplified model

Because there is only a load in vertical direction, the reaction forces in horizontal direction are zero. The contour plots of the vertical reaction force of the complete and the three trough model are shown in figure 3.11.

For the complte model, there is only a reaction force in the crossbeam where the load is put on. This force is spread over a larger length than the length of the crossbeam of the model with only three troughs. However, the reactions forces in the middle of the crossbeam of the smaller model are equal to the complete model, see figure 3.12.

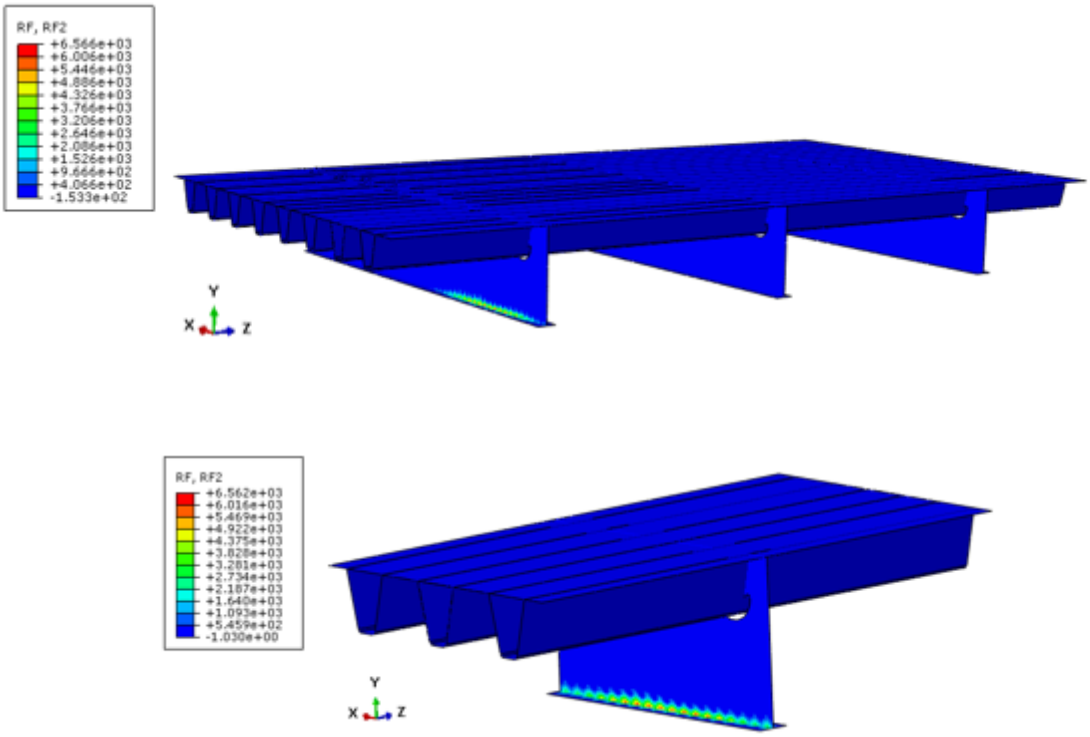

Figure 3.11: Reaction force of the global and simplified model

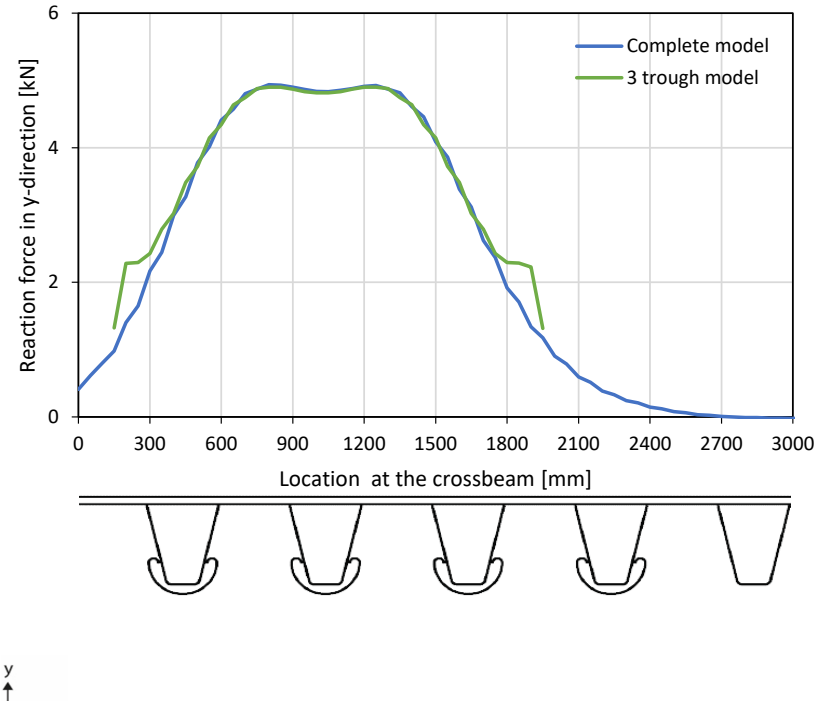

Figure 3.12: Reaction force in the crossbeam for the global and simplified model

The strain range at the bottom surface of the deck plate in longitudinal direction (z-axis) and in transverse direction (x-axis) is determined for both models, see figures 3.13 and 3.14.

For the complete model, there is no difference in strain at the left and the right joint of the trough. The strain value is similar to the strain in the joints of the three trough model. This means that the support of the rest of the model does not have an influence on the local strain range in the deck plate at the rib-to-deck plate joint.

At the crossbeam, the behaviour of the rib-to-deck plate joint at the crossbeam in the three trough model is similar to the complete model if a wheel load is placed above the center of the crossbeam. The length and support of the deck plate and troughs are not affecting the strain range and deformation. This means that the load is transferred from the deck plate, only locally in the trough around the crossbeam and directly into the crossbeam.

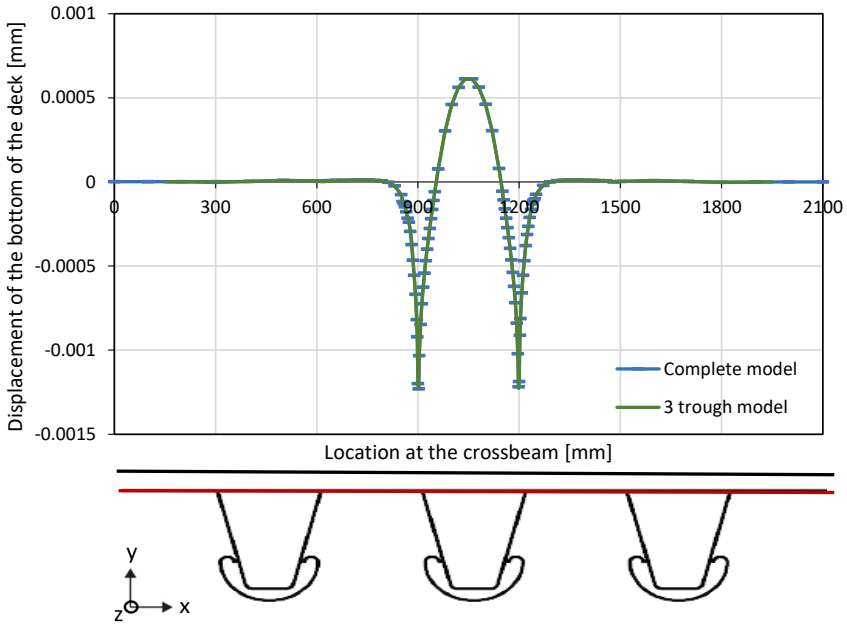

Figure 3.13: Strain range in x-direction along bottom surface of the deck plate at the center line of the crossbeam

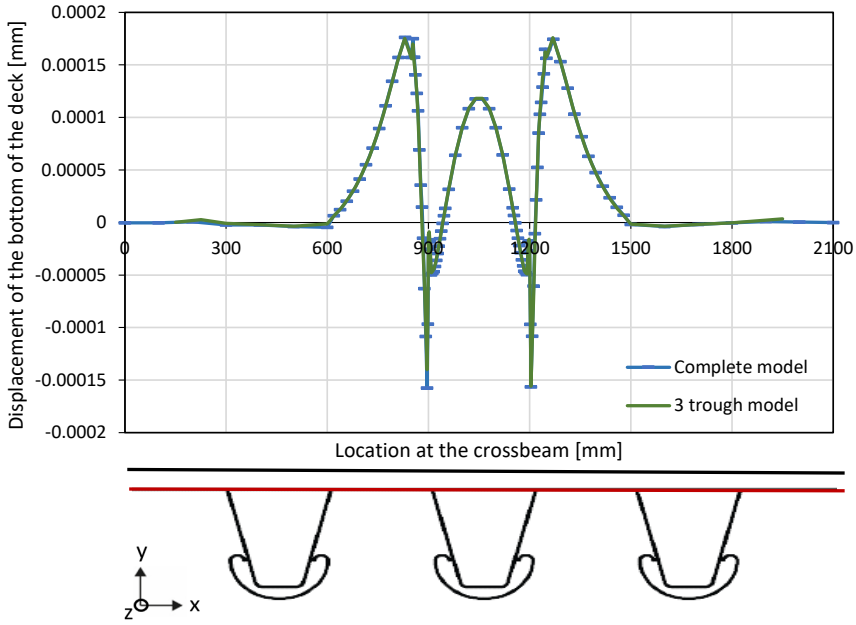

Figure 3.14: Strain range in z-direction along bottom surface of the deck plate at the center line of the crossbeam

3.3. Strain analysis near the rib-to-deck plate joint

The strain range at the lower surface of the deck plate is analyzed for the shell and solid element model and for different element sizes. A stable element size is determined for both element types.

3.3.1. Shell element model

The influence of the element size on the strain in the bottom surface of the deck plate near the weld root is analyzed. The strain range is determined for models with a local element size of 1 mm, 2 mm, 4 mm, 8 mm and 20 mm. Results are given in figure 3.15.

From the figure, it follows that a smaller element size results in a higher strain range at the weld root. A strain singularity appears at that location and if the element becomes smaller, the value of the singularity becomes larger. At a distance 4 mm away from the weld root, the models with an element size of 1 mm, 2 mm and 4 mm have a similar strain range. At 8 mm from the weld root, the model with an element mesh of 8 mm has a comparable strain range as well. The strain range of the model with an element size of 20 mm is less precise than the other models. However, at least 30 mm away from the weld root, it gives a similar strain range as the other element sizes. Therefore, the relative fine element mesh is only required for the local strain range near the weld root. A larger element size is sufficient for the rest of the model.

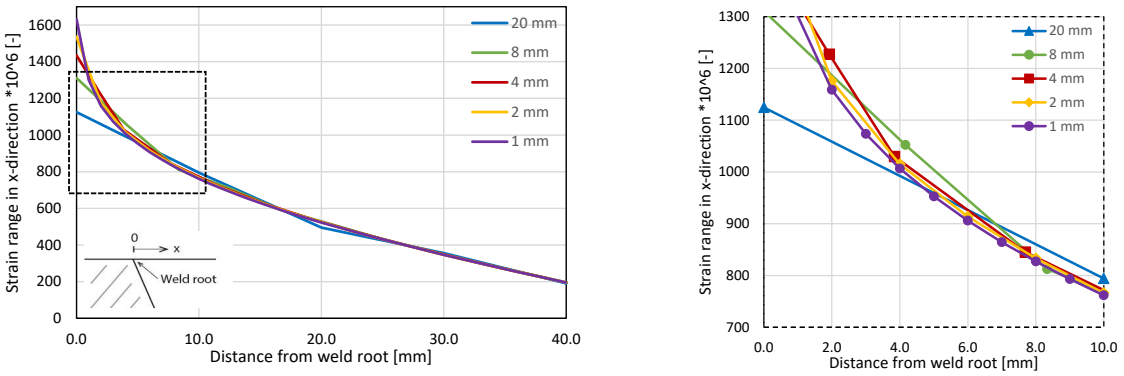

(a)

(b) Zoomed in on graph

Figure 3.15: Strain range at the bottom surface of the deck plate for the shell models with different element sizes

3.3.2. Solid element sub model

Weld penetration

As mentioned in paragraph 3.1.6, the influence of the ratio of the weld penetration is analyzed. A lack of penetration of 1.5 mm, which is a 75% weld penetration ratio in this case, is added to the model, see figure 3.16. The gab between the deck plate and the trough web is modelled as 0.2 mm.

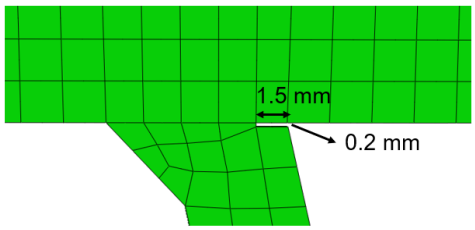

Figure 3.16: Geometry weld with 75% weld penetration ratio

The strain at the bottom surface of the deck plate for this model is compared to the model with a full penetrated weld. Contour plots of the strain are given in figures 3.17 and 3.18. The strain is shown at the location where the stress value is highest, which is section AA'. The strain range at the bottom surface of the deck plate is given in figure 3.19.

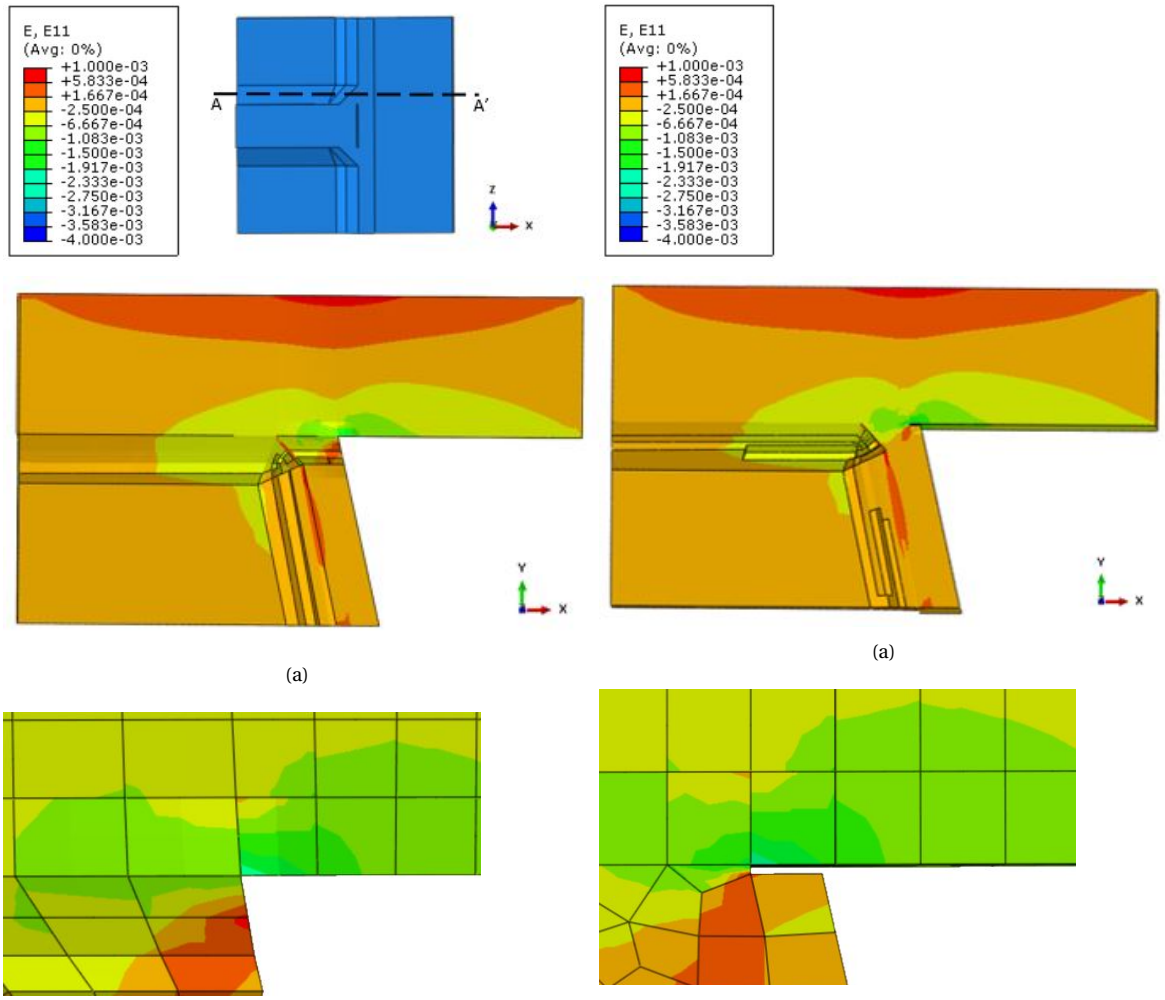

(a)

(b) Zoomed in at the weld root

Figure 3.17: Strain value in x-direction at section AA' - full weld penetration

(a)

(b) Zoomed in at the weld root

Figure 3.18: Strain value in x-direction at section AA' - 75% weld penetration

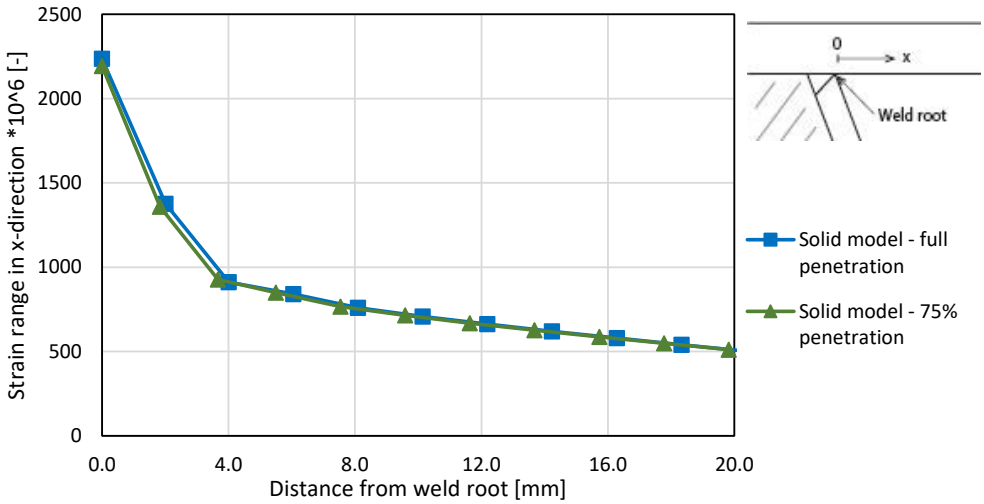

Figure 3.19: Strain range at the lower surface of the deck plate of the solid element sub models

From literature, a small increase of 3.8% in strain value was expected if the weld is not fully penetrated. However, there is found no difference between the strain range in both models.

Elements

The element size of the solid element model with 75% weld penetration is investigated. Alternatives with quadratic elements with a size in the zone around the weld is 4 mm, 2 mm, 1 mm and 0.5 mm are compared. The strain range at bottom surface of the deck plate is determined and given in figure 3.21.

In figure 3.20, the strain in the solid element model with an element size of 0.5 mm is given. The global strain in the model is similar to the strains in the models with an element size of 2 mm. However, around the weld root, the strain is much larger.

Like for the shell element model, a higher strain range at the weld root is found for a smaller element size. Therefore, a same conclusion about the strain singularity as for the shell element model can be made. Smaller elements leads to a larger singularity but at a certain distance from the weld root, the strain values are similar to larger element sizes.

The models with an element size of 0.5 mm and 1 mm result in a strain range which is similar to each other till a distance of about 2 mm away from the weld root. At a distance 4 mm away from weld root, the model with 2 mm mesh results in a comparable result as well. At 8 mm distance from the weld root, the 4 mm mesh gives a good comparison with the other models.

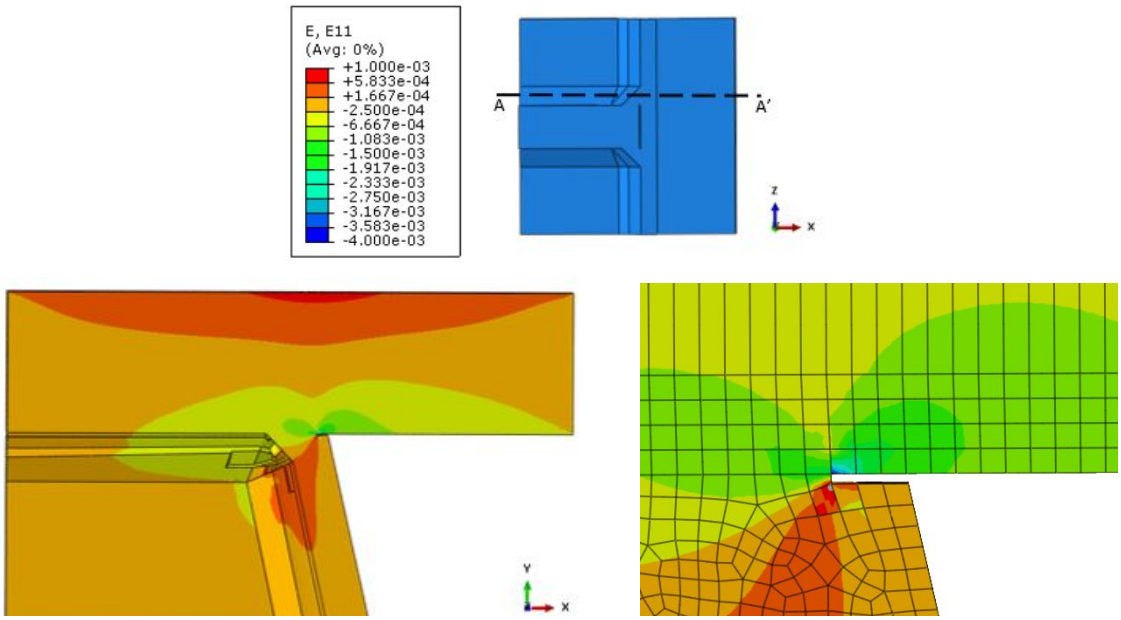

(a) Contour plot (b) Zoomed in on the weld root

Figure 3.20: Strain value in x-direction at the section AA'. Local element size is 0.5 mm

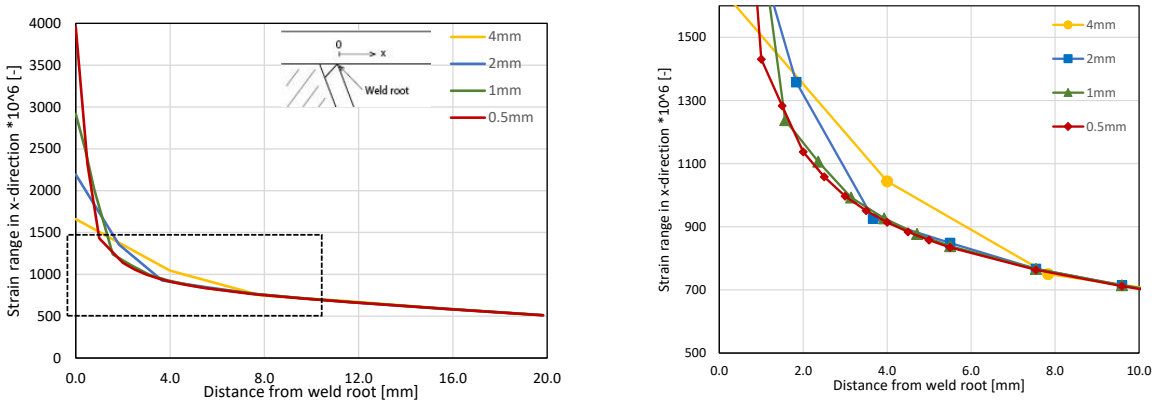

(a)

(b) Zoomed in on part of the graph

Figure 3.21: Strain range at the bottom surface of the deck plate for the solid models with different element sizes

3.3.3. Strain validation

Bottom surface of the deck plate

Strain values measured during the experiment of Wu et al. [37] are used for validation of the FE models both with shell and solid elements. The strains during loading are measured with strain gauges which are placed at the top and bottom surface of the deck plate, see figure 3.22. At the bottom surface, location c, the strain gauges are placed at a distance 0.2t, 0.6t and 1.0t from the weld root, where t is the deck plate thickness which is 20 mm. The strain gauges are placed in the center line of the crossbeam. This is also the case for the strain gauge at the top surface right above the trough, location a. At location b, 25 mm away from the trough, the strain is measured not only at the center line but also at 25, 50, 75 and 100 mm away from the center in longitudinal direction

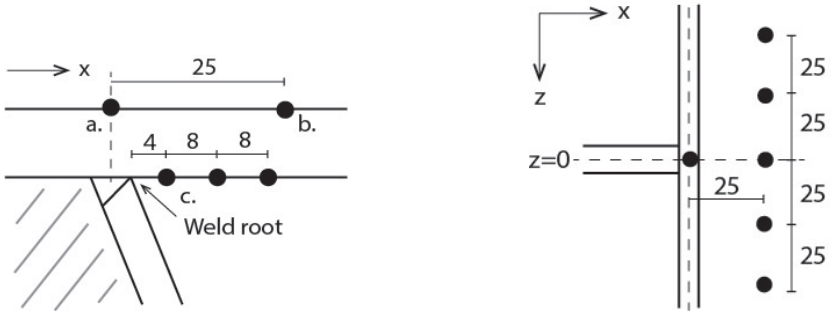

(a) Side view

(b) Top view

Figure 3.22: Locations of the strain gauges during the experiment of Wu et al. [37]

The computational results are compared to the experimental results. The experiment is done on one trough, which results in two test specimens. Both results and an averaged value of the strain from the two joints is used for validation. The strain range derived from the FE model is acceptable if the deviation is not more than 10% from the experimental results.

Figure 3.23 shows the strain range for a shell element model with a relative coarse mesh of 20 mm and relative fine mesh of 4 mm and for a solid element model with 2 mm. For the solid element model, an analysis with linear and quadratic elements is made. Because the lack of weld penetration does not influence the strain

range, the model with a full weld penetration is considered.

The strain range of the solid element model with quadratic elements is in agreement with the result from the experiment. Using linear elements results in a strain range which is lower than the strain in the test specimen. This means that calculations with this model results in unconservative stress and strain values.

The shell element model with a relative fine mesh gives a good strain range, except at a distance 4 mm from the weld root. At this point, the strain range is higher than the 10% deviation.

The shell element model with an element size of 20 mm results in a higher strain range compared to the model with a fine mesh. At 20 mm away from the weld root, the strain range is comparable to other values, but closer to the weld root, the strain is higher. Therefore, the increase of the strain value (slope of the graph) is larger compared to the other graphs.

Because of the presence of a singularity in all models, it is not possible to determine the strain range at the weld root directly from the FEM output.

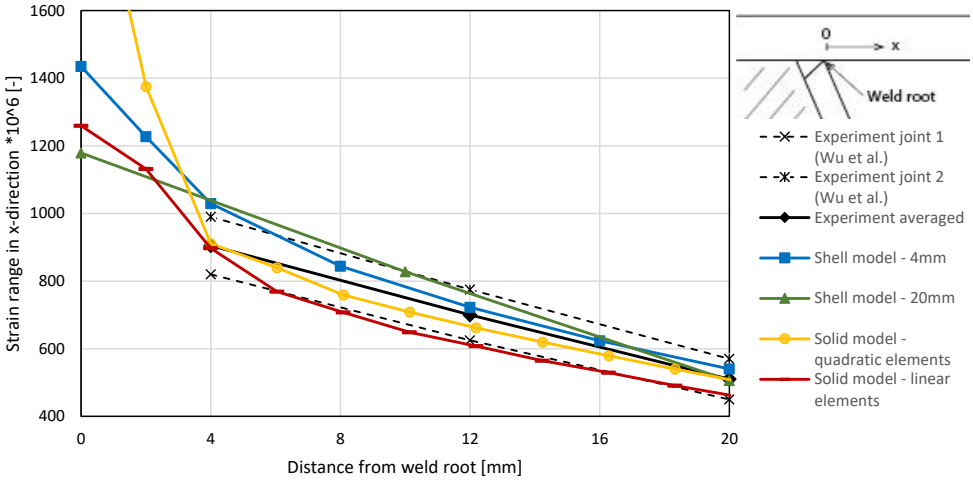

Figure 3.23: Strain validation of the FE model at the lower surface of the deck plate

Top surface of the deck plate

The strain at the top surface of the deck plate is compared to the test results. This is done for the solid element sub model with quadratic solid elements with and without including the lack of penetration. Figures 3.24(a) and 3.24(b) show the strain range right above the middle of the trough, figure 3.22 location a, and at a distance of 25 mm from the trough web, figure 3.22 location b. A contour plot of the strain value is added in appendix A

The strain range right above the trough web is higher for the model with a penetration ratio of 75%. A reason for this is because the maximum strain range at the weld root is more close to the middle of the trough and therefore, also more close to the measure point at the top of the deck plate. At location b, the strains are similar for the two models. At both locations, the computed strain is slightly lower than the experimental result but for both models, it is within 10% of the strain range measured during experiment, which means that the results from the FE model are acceptable.

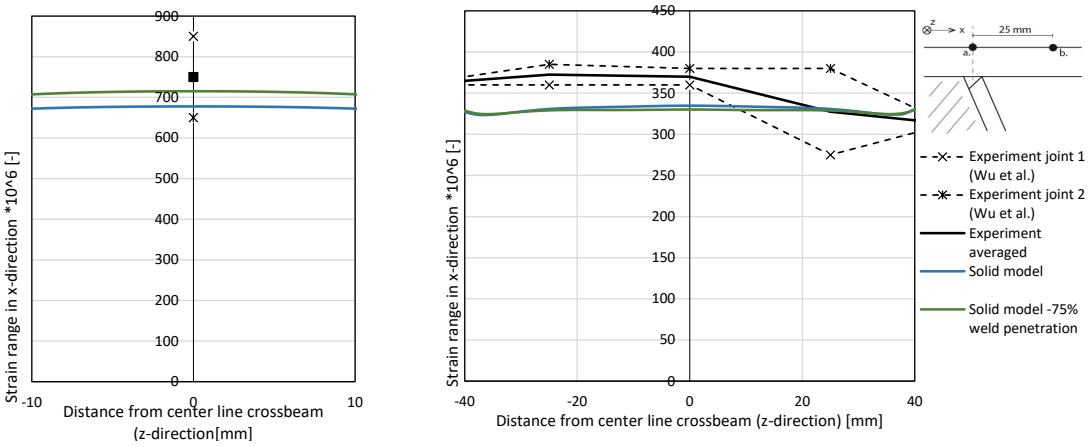

(a) Location a

(b) Location b

Figure 3.24: Strain validation top surface of deck plate

4

Stress based fatigue assessment of the reference model

In this chapter, there is searched for an answer on the question which fatigue assessment method results in a fatigue life most close to experimental results. A simple 2D model and the reference models, discussed in chapter 3, are used. The nominal, hot spot- and effective notch stress method, as described in paragraph 2.8.1, 2.8.2 and 2.8.4, are considered. The amount of load cycles to failure is determined using the S-N curve, see paragraph 2.7.

Table 4.1 gives an overview of which assessment procedures per model are discussed in this chapter.

Table 4.1: Overview methods used to determine load cycles to failure

	Nominal stress	**Hot spot stress**	**Effective notch stress**
Hand calculation	X	X	
Shell element model		X	
Solid element model		X	X

4.1. Nominal stress method

A simple 2D model, as described in paragraph 2.8.2, is used to determine the load cycles to failure of the rib to deck plate and crossbeam joint.

The bending moment in the deck plate at the joint is determined with MatrixFrame Software, see appendix B, and is equal to 14.4*10^3 Nmm.

The nominal stress at the connection is determined with equation 4.1.

$$\Delta\sigma_{nom} = \frac{M}{W} = \frac{6 * M}{t^2} = \frac{6 * 14.4 * 10^3}{20^2} = 217 N/mm^2 \tag{4.1}$$

The detail category is 71 MPa, figure 2.15. The fatigue life is determined in eq 4.2:

$$N_{nom} = (\frac{\Delta\sigma_c}{\Delta\sigma_{nom}})^3 * 2 * 10^6 = 7.1 * 10^4 \tag{4.2}$$

Table 4.2: Hot spot stress and load cycles to failure for the analytical model

Approach	$\Delta\sigma_{hotspot}$**[MPa]**	**N - mean**	**N - mean-2sd**
Nominal stress	217	-	7.1*10^4

4.2. Hot spot stress method

For different models, the hot spot stress is determined and the amount of load cycles to failure is calculated. Because there are only two experimental results, it would be conservative to determine a design value from the experimental results. Therefore, the mean value for the detail category determined by Kolstein [17] as discussed in section 2.8.2 is used to determine the mean fatigue life. This detail category is 180 MPa and a change in strain range of 10% is assumed as failure criterion. This is also the case for the experimental result used for comparison. The design detail category is 125 MPa.

4.2.1. 2D model

The stress concentration factor (SCF) for a deck plate thickness of 20 mm is determined with equation 4.3 [31, table NB.10]) and is equal to 1.11.

$$SCF = 1.2975 - 0.00938 * t \tag{4.3}$$

The hot spot stress at the connection is determined with equation 4.4.

$$\Delta\sigma_{hs} = SCF * \frac{6 * M}{t^2} = 1.11 * \frac{6 * 14.4^3}{20^2} = 240 N/mm^2 \tag{4.4}$$

In table 4.3, the hot spot stress value and corresponding amount of load cycles are given.

Table 4.3: Hot spot stress and load cycles to failure for the analytical model

Approach	$\Delta\sigma_{hotspot}$ **[MPa]**	**N - mean**	**N - mean-2sd**
Hot spot stress	240	8.4*10^5	2.8*10^5

4.2.2. Finite element model

In chapter 3, concluded is that there will be a singularity at the weld root. The hot spot stress method uses the reference points at a certain distance from the weld root. As a consequence, stresses which are not dependent on a singularity can be used for fatigue assessment.

Extrapolation of the stresses is possible for different element sizes and using different reference points, as discussed in paragraph 2.8.2. Kolstein [17] suggests to use the measure points at a distance of 0.4t and 1.0t from the weld root, where t is the deck plate thickness. This extrapolation method is the same method as the 'type a' method with a relative fine element mesh from the IIW [12]. Another suggestion for the extrapolation points given by the IIW is called 'type b' extrapolation. The first reference point is located at 4 mm from the weld root. Discussed in paragraph 3.3.3 is that the strain value is not accurate determined with the FE model at that location compared to the strain measured during the experiment. Therefore, this extrapolation type is not considered in this report. Because both Kolstein and the IIW suggests to extrapolate according to type a, this method is used.

For a comparison of a relative fine and coarse mesh, the extrapolation type a method with a relative coarse element size is analyzed as well. The element size is equal to the deck plate thickness. This method is applied at the shell element model only, because for the solid element model, it is not possible to create a mesh with this element size.

Figures 4.1(a) and 4.1(b) show the locations of the reference points for the shell element models and in figure 4.1(c) for the solid element model. The equation which is used for the extrapolation of the stress are given in table 2.4.

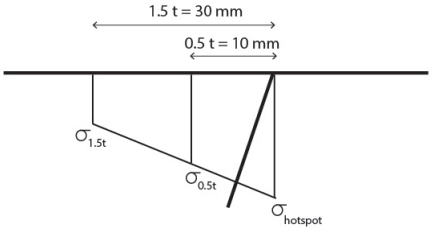

(a) Shell elements, coarse mesh

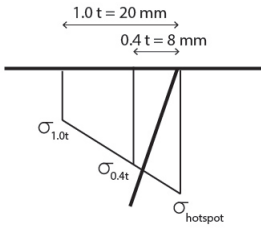

(b) Shell elements, fine mesh

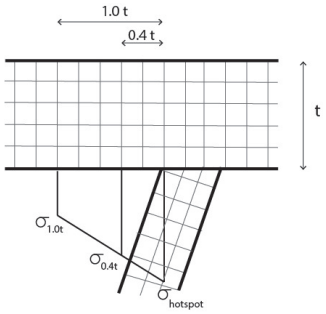

(c) Solid elements, fine mesh

Figure 4.1: Overview extrapolation of the hot spot stress

For the shell element model, the strain at the lower surface of the deck plate is not dependent on the element size anymore if an element size of 8 mm or smaller is used, as discussed in paragraph 3.3.1. An element size of 4 mm is used for the fine mesh for the shell element model and a size of 20 mm for the coarse mesh.

Concluded in paragraph 3.3.2 is that the solid element model gives a stable strain range at 8 mm from the weld root if an element size smaller than 4 mm is chosen. The amount of load cycles for the solid element model is determined for the solid element model which has full weld penetration and 75% weld penetration. To create a good element shape around the weld root if the 75% penetration ratio is taken into account, an element size of 2 mm instead of 4 mm is chosen for the solid element models.

The hot spot stress for the two shell element models and the solid element model is determined and the amount of load cycles to failure is calculated. For the shell element model with 4 mm element size, the minimum principal stress at the lower surface of the deck plate is shown in figure 4.2. The stress output, calculated hot spot stress and corresponding load cycles to failure for all models is summarised in table 4.4.

To determine the one point hot spot stress, a shell element model with an element size equal to the deck plate thickness is recommended to used, see paragraph 2.8.3. Therefore, the shell element model with a relative coarse mesh is used to calculate the hot spot stress. The result is given in table 4.4 as well.

Table 4.4: Hot spot stress and load cycles to failure

	$\Delta\sigma_{1.5t}$ [MPa]	$\Delta\sigma_{0.5t}$ [MPa]	$\Delta\sigma_{hotspot}$ [MPa]	**N - mean**	**N - mean-2sd**
Shell - 'Coarse' mesh	85	195	250	$7.5 * 10^5$	$2.5 * 10^5$
Shell - 1 point hot spot		195	218	$1.1 * 10^6$	$3.7 * 10^5$
	$\Delta\sigma_{1.0t}$ [MPa]	$\Delta\sigma_{0.4t}$ [MPa]	$\Delta\sigma_{hotspot}$ [MPa]	**N - mean**	**N - mean-2sd**
Shell - 'Fine' mesh	128	198	245	$7.9 * 10^5$	$2.7 * 10^5$
Solid - full penetration	118	177	216	$1.2 * 10^6$	$3.9 * 10^5$
Solid - 75% penetration	120	178	217	$1.1 * 10^6$	$3.8 * 10^6$

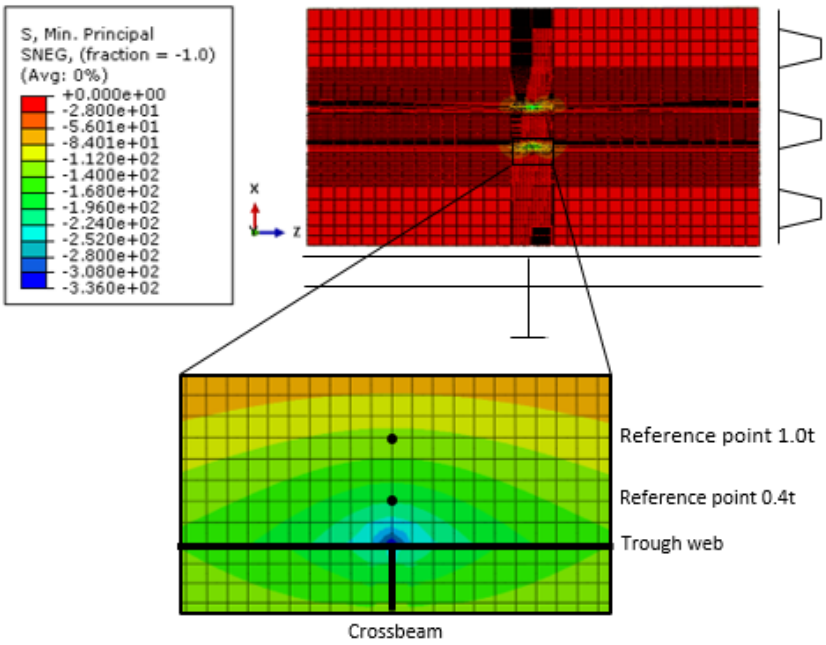

Figure 4.2: Stress at the lower surface of the deck plate for the shell element model with 4 mm element size.

The lowest hot spot stress value, which causes the highest stress range, is found in the center of the crossbeam for the shell element model. For the solid element model, the highest strain range is found at the location where the crossbeam is welded to the deck plate and trough web.

4.2.3. Hot spot stress method for the test specimen

Wu et al. [37] determined the hot spot stress from the extrapolated strains. The hot spot stress is equal to 206 MPa.

Using the S-N curve and a detail category of 125 MPa, the load cycles to failure is equal to $4.5*10^5$. For a detail category of 180 MPa, the amount of load cycles to failure is $1.3*10^6$.

4.3. Effective notch stress method

According to the recommendations described by the IIW, as given in paragraph 2.8.4, a notch with a radius of 1 mm is made in the solid element model. This notch is placed exactly at the weld root, see figure 4.3. The lack of penetration is taken into account.

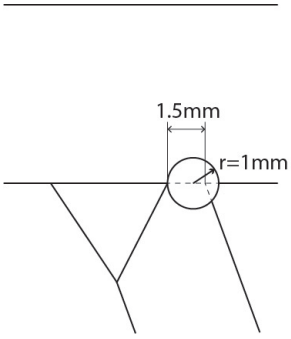

Figure 4.3: Location of the effective notch (not on scale)

The IIW [12] suggests to use an element size around the notch of 0.25 mm for a model with quadratic elements,see paragraph 2.8.4. Therefore, this size is used in this report. The minimum principal stress in the notch is determined. Figure 4.4 shows the stress in the solid element sub model. Like for the hot spot stress

determined with a solid element model, the highest stress range is found at the location where the crossbeam is welded to the deck plate and trough web. The effective notch stress range ($\Delta\sigma_{eff}$) is equal to 1080 MPa.

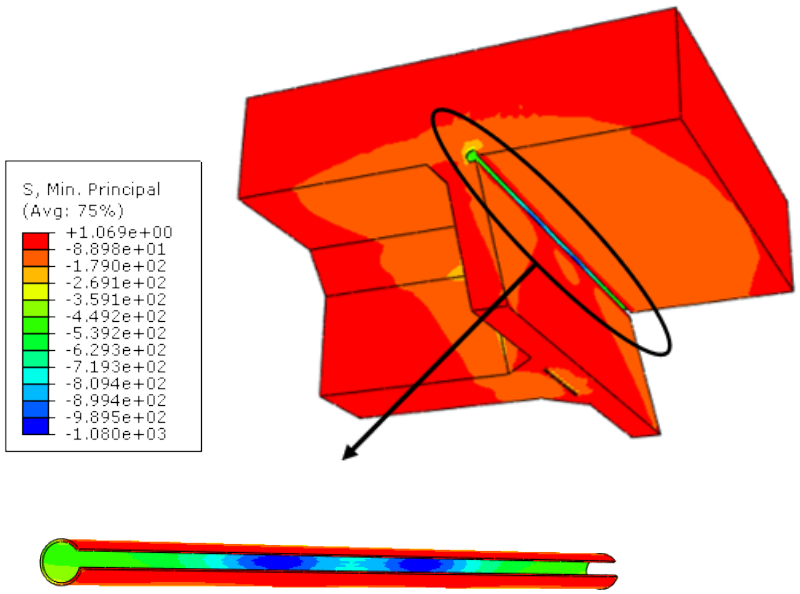

Figure 4.4: Minimum principal stress in the effective notch. Top: solid sub model. Bottom: zoomed in on the notch

Using a detail category of 225 MPa, see paragraph 2.8.4, the amount of load cycles to failure is determined. The result is summarized in table 4.5

Table 4.5: Stress range and load cycles to failure for the analytical model according to the effective notch stress approach

Approach	$\Delta\sigma_{eff}$ **[MPa]**	**N - mean-2sd**
Effective notch stress	1080	$1.8*10^4$

4.3.1. Improvement of method

Concluded can be that the determined load cycles to failure is low compared to the results from the hot spot stress method and the experimental results. According to the IIW, the detail category is valid for a butt weld which has an flank angle of 30°. In this case, the angle is 46°. A greater flank angle results in an other stress value and therefore, the detail category may is not applicable for this specific joint. The method can be improved by increasing the value of the detail category. The amount of load cycles to failure determined with the experiment is used.

For the mean value, the new detail category is equal to 796 MPa, see appendix C.

Two methods are used to determine the design load cycles to failure and a new corresponding detail category. The most easy method is to determine the standard deviation from the experimental result and subsequently, determine the amount of load cycles, which is equal to the mean value minus two time the standard deviation. The method should give a survival probability of 97.7%.

According to this method, the design life is equal to $4.5*10^4$. The new proposed design detail category is 305 MPa. For calculations, see appendix C.1.

Chapter 4.5 of the IIW [12] describes another method to determine the design amount of load cycles to failure from experimental results. Equation 4.5 should be used.

$$N_d \leq \frac{N_T}{F} \tag{4.5}$$

where:

N_d is design value for the amount of load cycles to failure.
N_T is the amount of load cycles to failure of the test specimens.
F is a factor dependent on the number of test results available.

The design life is equal to $1.5*10^5$. The new proposed detail category is 418 MPa. See appendix C.2 for the calculation.

4.4. Comparison of the approaches

Results from the FE model are compared to the experimental results from Wu et al. [37]. The result for the hot spot stress is shown in figure 4.5 and for the effective notch stress, it is given in figure 4.6

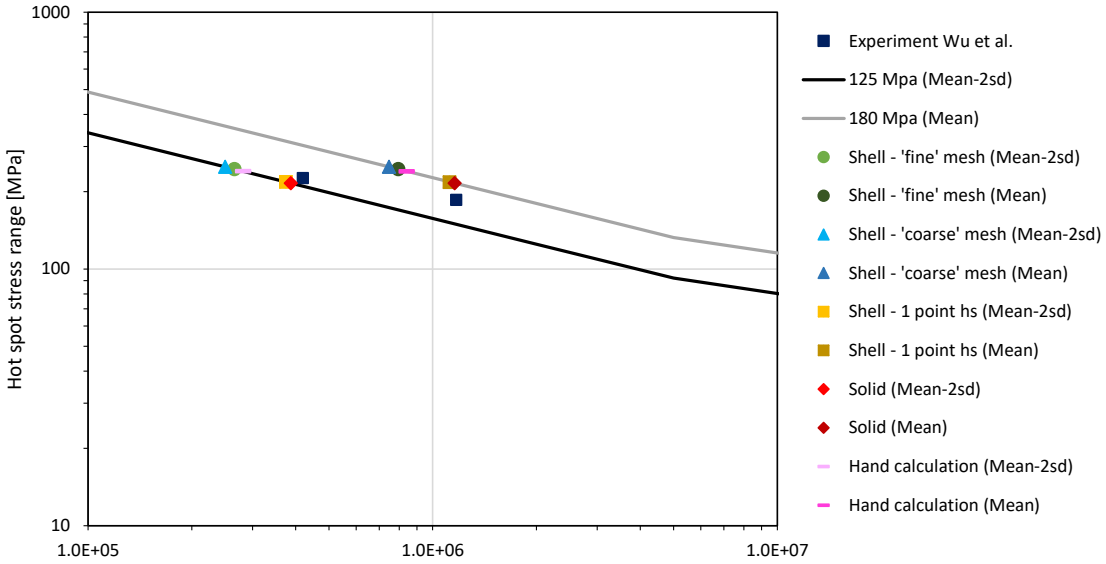

Figure 4.5: Relation hot spot stress and load cycles to failure

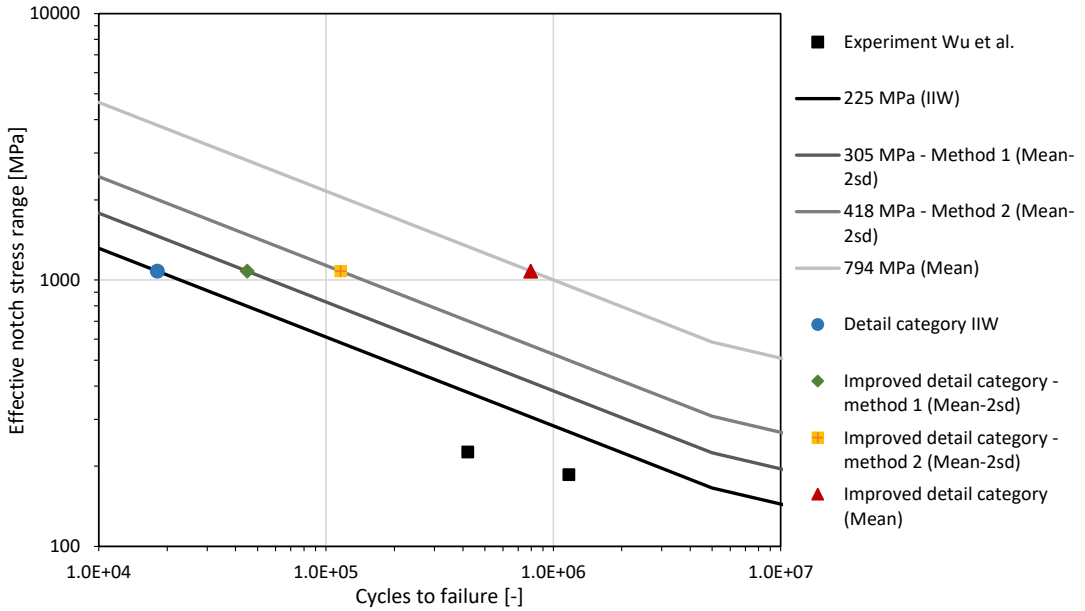

Figure 4.6: Relation effective notch stress and load cycles to failure

Table 4.6 gives an overview of which factors are taken into account in the stress value of each model. The hot spot stress is abbreviated to HHS. If a factor is not included in the stress range, it is taken into account in the SN-curve.

Table 4.6: Summary of the approaches

		Stress raising effect due to:		
		Geometry joint	Geometry weld	Weld discontinuities
Nominal stress	Analytical	x	x	x
HSS	Analytical	Yes	x	x
	FEA - Shell elements	Yes	x	x
	FEA - Solid elements	Yes	Yes	x
1point HSS	Shell elements	Yes	x	x
Effective notch stress	FEA - Solid elements	yes	Yes	x
Experiment HSS	Measured strain	Yes	Yes	Yes*

*If is present in specimen

The mean value for the load cycles to failure is used to compare the computational result with experiments.

The hand calculation and the shell element model with a relative coarse or fine mesh give all a similar fatigue life. The mean value is in between the two experimental results. There should be noticed that the hand calculation approach does not take into account influences of the shape of the bridge deck, except from the

deck plate thickness and the width between the trough webs at the top.

The hot spot stress approach with a relative coarse mesh results in a slightly higher hot spot stress than when the fine mesh is used, because the model gives a less precise stress range as mentioned in paragraph 3.3.3. However, the difference in hot spot stress is only 2%, which results in 6% less load cycles.

Use of a solid element model for the hot spot stress method results in a longer fatigue life than when shell elements are used. The determined fatigue life is 44% longer compared to the shell element model with a relative fine mesh. This solid model includes not only the geometry of the joint but also the geometry of the weld, as can be seen in table 4.6.

The fatigue life determined with the one point hot spot stress method is similar to the fatigue life determined with the solid element model. However, the fatigue life determined according to this approach is dependent on a factor. This factor is independent on the geometry of the weld. As a consequence, the fatigue life is less reliable than the fatigue life determined with the solid element model.

Expected is that taking into account more stress raising effect in the stress range instead of in the detail category should lead to a more accurate fatigue life and this is true for the hot spot stress method. Nevertheless, the fatigue life determined with the effective notch stress method is less than 10% of the fatigue life determined with the hot spot stress approach. Because no mean value for the detail category is available, the design values from both methods are compared. There can be concluded that the effective notch stress method is conservative for the assessment of the rib-to-deck plate joint at the crossbeam.

After improvement of the detail category used for the effective notch stress method, the predicted amount of load cycles is still conservative, because the fatigue life is still less than half of the value of the hot spot stress with shell elements.

There are only two specimen available from experimental results. These results are lower than the S-N curve for the detail category 180 MPa (mean value) determined by Kolstein [17]. Those two reasons makes the new proposed detail category still conservative. More experimental data is required to determine a more accurate design detail category.

If the design detail category of 125 MPa is used for the hot spot stress method, all models give a shorter fatigue life than the experiment. This means that no model results in an unsafe estimation. Because the solid element model results in longest fatigue life, this model is most accurate compared to the experimental result.

There should be noticed that the stresses used for the stress range are all stresses in compression. However, fatigue cracks will grow due to load cycles which cause tension in the detail. Therefore, it is likely that there are residual stresses in the joint due to welding. These residual stresses cause a tensile stress range in unloaded situation.

5

Residual stresses

It follows from chapter 4 that there is only a compressive stress range in the rib-to-deck plate joint at the crossbeam. However, fatigue crack initiation is caused by tensile stress cycles. Therefore, it is likely that there are residual stresses due to welding in the detail.

In this chapter, an estimation of the fatigue life of the deck segment as discussed in chapter 3 is made and the residual stresses due to welding are included. The detail category used for assessment with the S-N curve includes the residual stresses already. Therefore, these stress based models are not suitable to use. The Smith, Watson, Topper (swt) local critical plane method, see paragraph 2.9, is used as alternative. In this model, the residual stresses can be included in the stress range.

This method is dependent on the strain range and maximum stress as discussed in paragraph 2.9. Using this method without including residual stress results in an infinite fatigue life, because the maximum principal stress is almost zero. However, from the experiment it follows that a fatigue crack will initiate.

5.1. Introduction to residual stress

Due to the presence of residual stress, there are initial tensile stresses in the zone around the weld which can be equal to the yield strength. The stress range in the joint will be similar, but the mean stress value increases if the residual stresses are considered. Figure 5.1 gives an overview of the effect of residual stresses on a stress range in general.

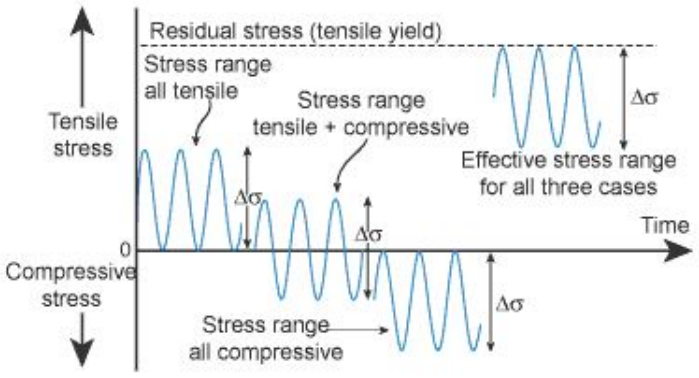

Figure 5.1: Effect of the residual stress on the total stress range [22]

5.2. Input in the FE model

Spyridoni et al. [34] did research to the residual stresses in the rib-to-deck plate joint in span. An approximation of the residual stress value in longitudinal direction in the deck plate and trough webs is proposed, see figure 5.2. This is valid for automatic welding.

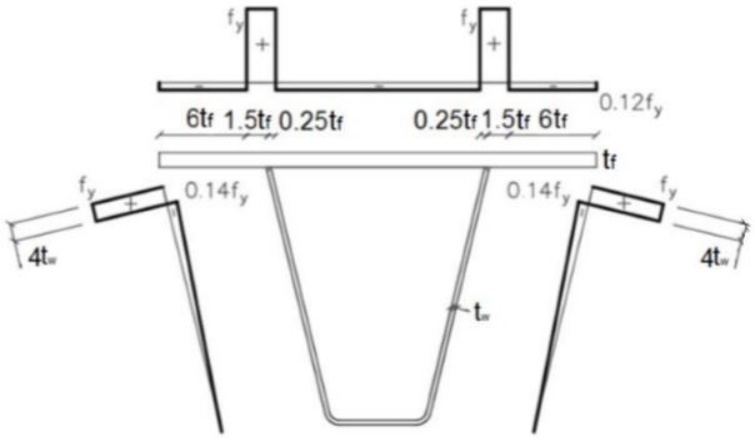

Figure 5.2: Approximation of the residual stress in the trough and deck plate [34]

Assumed is that the residual stress around the rib-to-deck plate joint at the crossbeam is similar to the stress range for the joint in span. The possibility of the presence of extra residual stresses due to welding of the crossbeam to the deck plate and trough is neglected. Because of this assumption, it is possible to use the residual stress value as given in figure 5.2.

The residual stress value is included in the total FE model by applying a prescribed stress value, see figures 5.3 and 5.4. This stress value is included in the shell element and solid element model part. To avoid the stress singularity at the weld root, the solid element model with effective notch is used.

After the prescribed stress is applied, the stress and strain value for the unloaded situation is determined, called step 1. Then, the deck segment is loaded with a wheel load of 140 kN on a load area of 180 mm x 320 mm, step 2. This load is similar to the load used in chapter 4.

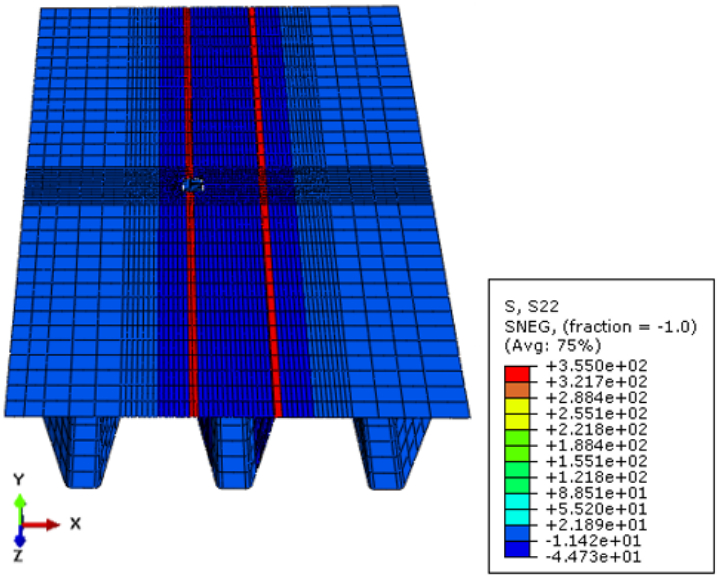

Figure 5.3: Including the residual stress in the deck plate

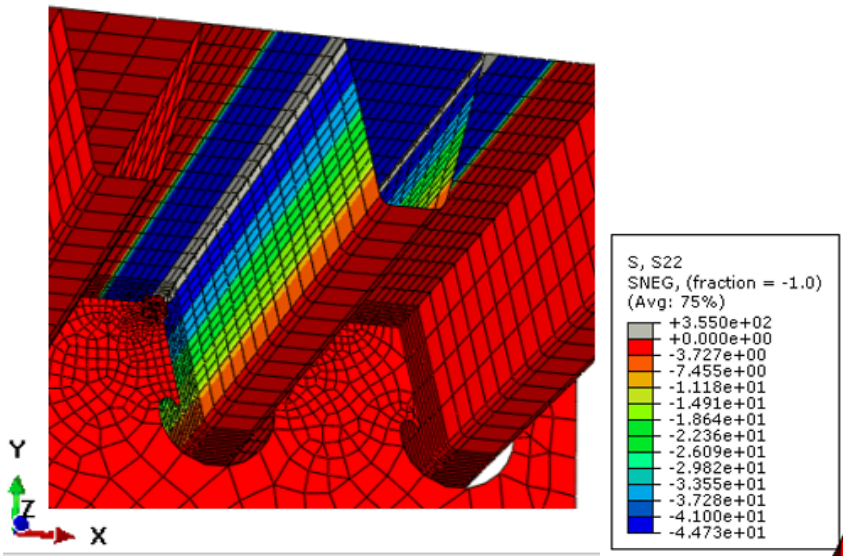

Figure 5.4: Including the residual stress in the trough

The output from the model is given in figures 5.5 and 5.6. A summary of stress and strain output which results in the largest swt-parameter is given in table 5.1. The maximum value is found at the location where the crossbeam is welded to the trough web. This is the same location as where maximum stress values are found for the hot spot stress approach with the solid model and the effective notch stress approach based on the S-N curve.

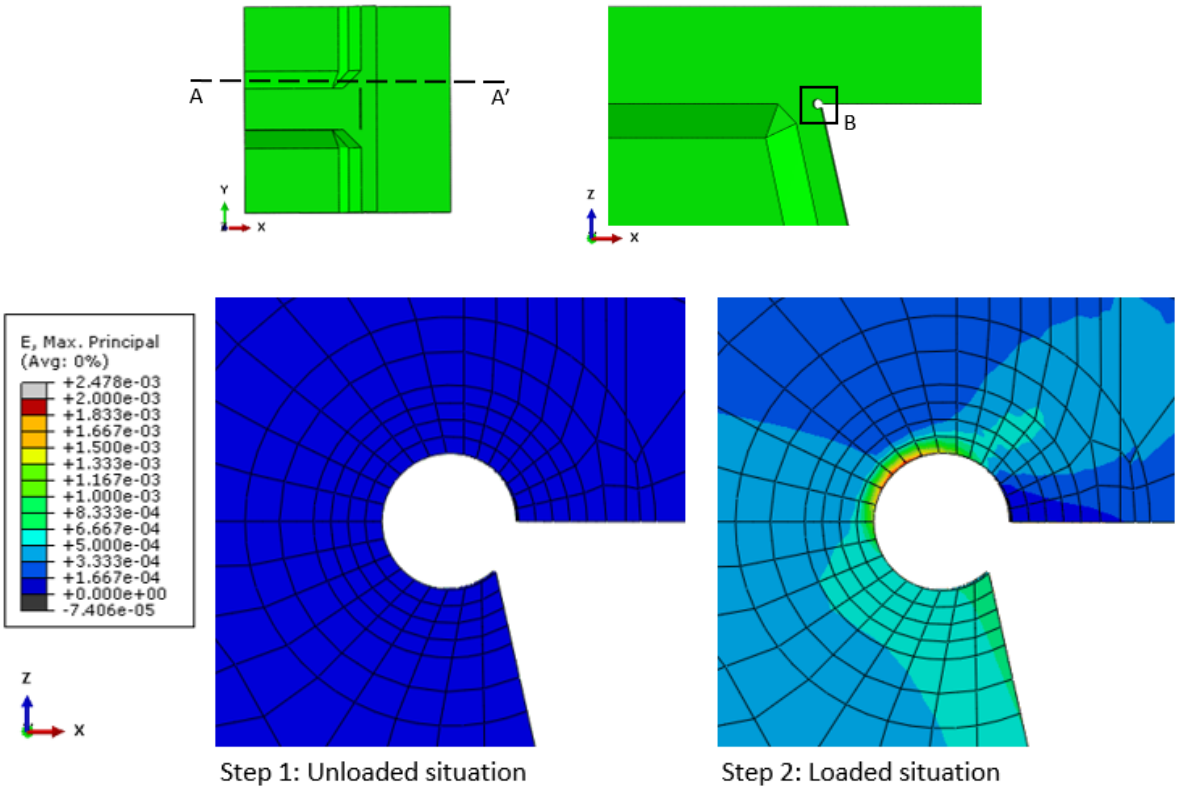

Figure 5.5: Maximum principal strain around the notch at section AA'

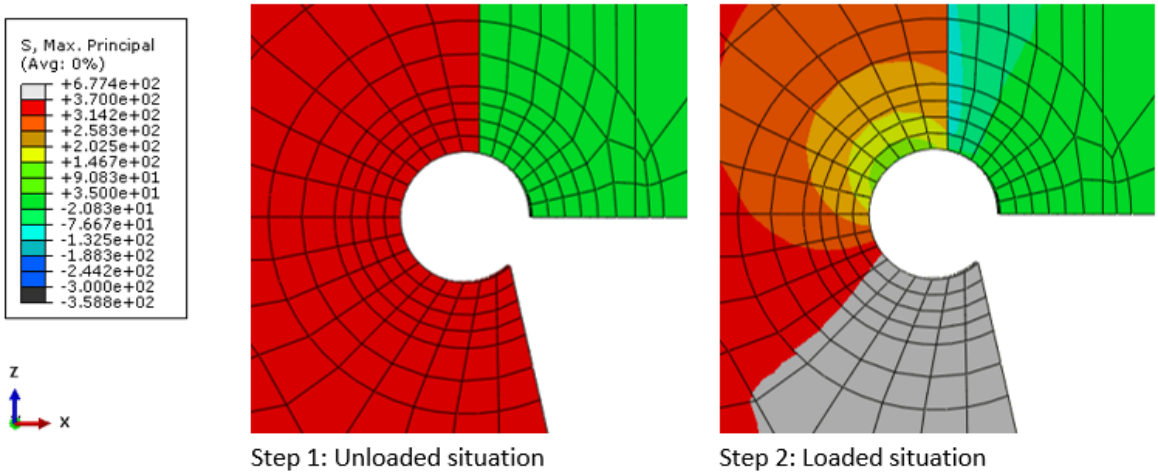

Figure 5.6: Maximum principal stress around the notch at section AA'

Table 5.1: Strain and stress output at location which results in highest swt-parameter

	$\epsilon_{maxPrincipal}$ [-]	$\sigma_{maxPrincipal}$ [MPa]
Step 1	6.2*410^{-4}	362
Step 2	1.93*10^{-3}	90
	$\Delta\epsilon = 9.97 * 10^{-4}$	σ_{max} = 362 MPa

Using equation 2.8 and the material factors from table 2.6, the swt parameter is calculated and equal to 0.36. This results in the value for the reversals $2N_f$ is $*10^6$ and thus is the amount of load cycles to failure N = $7.4*10^5$.

5.3. Conclusion

The averaged amount of load cycles to failure determined from experiments made by Wu et al. [37] is $8.0 * 10^5$. The calculated amount of load cycles to failure is within 10% of the result from the experiment. Therefore, this method is a suitable approach for the prediction of the fatigue life if residual stresses are included.

After the initial stress input is applied, an equilibrium for the stresses and strains is found by the FE software. A stress of 362 MPa instead of 355 MPa is found at the location where the maximum swt-parameter is found. This is because the applied stress value is only an assumption of the residuals stress and no initial strain input is considered. Assumed is that the stress value is equal over the total thickness, while from experiments made by Kainuma et al. [14] there is found that it will differ over the thickness.

To improve the input for residual stress, the initial deformation instead of initial stress input can be used. Another option is applying the heat input in the model. However, this last method is time consuming and weld information should be available.

6

Parameter study

In this chapter, the influence of the size of different parameters on the fatigue life is investigated. Therefore, the most unfavourable wheel position is determined and different wheel types are analysed.

In chapter 4 it is concluded that the effective notch stress method results in a conservative fatigue life prediction of the rib-to-deck plate joint at the crossbeam. The hot spot stress method is a suitable method for the fatigue assessment of the joint. Using a solid element sub model including the weld geometry results in a slightly better fatigue life prediction than if a shell element model is used. However, this way of modelling is more time consuming. The hand calculation using a simple 2D model results in a similar amount of load cycles compared to the shell element model, but only the deck plate thickness and width between the troughs are considered in this model. In this chapter, the influence of other parameters on the stress range in the joint is investigated and therefore, a 3D FE model is required.

The shell element model with a relative fine element size of 4 mm is used in this chapter because it results in an accurate fatigue life prediction and is more easy to apply compared to solid elements. The model as discussed in chapter 3 is used. To make it more easy to change parameters and because it is expected that it has negligible influence on the hot spot stress in the rib to deck plate joint, the cope hole is not modelled.

6.1. Traffic load on bridge decks

6.1.1. Traffic categories

The Eurocode 1 part 2 makes a distinction between four traffic categories, varying from a low to a high heavy traffic intensity. The traffic intensity (N) is the value of lorries per year for a slow-lane with a maximum lorry load larger than 100 kN. For each category, the value of N is estimated and for the Netherlands, the values are given in the Dutch national annex table NB.5-4.5(n) of Eurocode 1 part 2 [28], see table 6.1.

Table 6.1: Value of lorries per lane per year [28]

Traffic category		**N**
1.	Highways and roads with two or more lanes per direction and with heavy truck intensity	$2 * 10^6$
2.	Roads with average truck intensity	$0.5 * 10^6$
3.	Roads with low truck intensity	$0.125 * 10^6$
4.	Roads with low truck intensity and only traffic for destination	$0.05 * 10^6$

6.1.2. Fatigue load models

If road bridges are considered, there are 5 different fatigue load models which can be used to determine fatigue life according to NEN-EN 1991-2 [27]. Fatigue load model (FLM) 1 and 2 should be used to determine

an infinite fatigue life for a given constant amplitude fatigue limit. FLM 3, 4 and 5 should be used to design a safe life.

In this report, a safe life design will be analyzed and therefore, FLM 1 and FLM 2 are disregarded in this chapter. FLM 5 is based on measured truck intercity and will therefore also not be discussed further. FLM 3 determines fatigue life using a constant stress range with a minimum and maximum stress. FLM 4 include a spectrum of stresses considering loads of different trucks on the bridge.

Eurocode 1 part 2 [27] states that FLM 4 is more accurate than FLM 3, assuming that the presence of more vehicles on the bridge can be neglected. The ROK [32] prescribes to use always FLM 4. For these reasons, FLM 4 will be used as load model for fatigue in this report.

Fatigue load model 4

This load model represents a composition of 5 common used truck types, which should be considered all separately. The damage due to stress cycles can be determined for each truck. Using a cumulative damage model, the total damage can be determined. This should be smaller than 1. In this FLM, it is assumed that each lorry enters the bridge without the presence of another vehicle.

Each truck has his own specifications, which are the distance between the axles, load per axle, wheel type and the percentage of that lorry type from the total amount of lorries per year. All information is collected in table 6.2. The wheel contact area for the wheel types is given in figure 6.3.

Table 6.2: Lorry type, load and percentage of total amount - FLM4a (reproduced from NEN-EN 1991-2 table NB.6 [28]

Lorry type			**Percentage of lorries**			
Image	**Distance between axles** [m]	**Axle load** [kN]	**Traffic category 1** [%]	**Traffic category 2 and 3** [%]	**Traffic category 4** [%]	**Wheel type**
	4.50	70	20	50	80	A
		130				B
	4.20	70	5	5	5	A
	1.30	120				B
		120				B
	3.20	70	40	20	5	A
	5.20	150				B
	1.30	90				C
	1.30	90				C
		90				C
	3.40	70	25	15	5	A
	6.00	140				B
	1.80	90				C
		90				C
	4.80	70	10	10	5	A
	3.60	130				B
	4.40	90				C
	1.30	80				C
		80				C

Table 6.3: Wheel types and load

Wheel type	Wheel contact area [mm] and corresponding distributed load [N/mm^2]
A	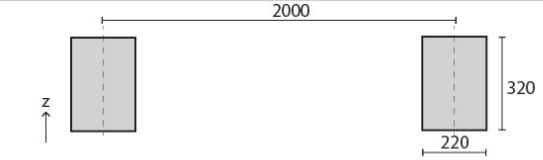
B	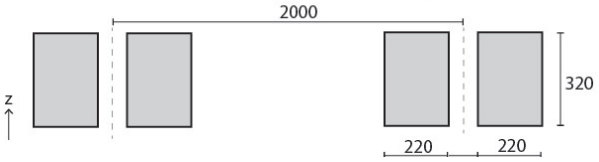
C	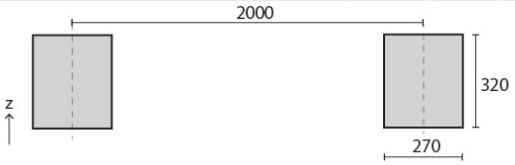

FLM 4 gives the axle loads for each truck. For the rib-to-deck plate joint, the local stress due to wheel loading is important. This distributed wheel load (q_{wheel}) can be determine with equation 6.1.

$$q_{wheel} = \frac{Q_k}{2 * l_1 * l_2} \tag{6.1}$$

where:

Q_k is the axle load.
l_1 is the width of the wheel.
l_2 is the length of the wheel.

Eurocode 1 part 2 paragraph 4.3.6(3) states that the local load dispersal from the top of the surface layer till the middle plane of the structural steel plate can be taken into account. This load is spread under an angle of 45°, which means that for every centimeter surface layer the wheel contact area will become 1 centimeter larger at each side. Figure 6.1 shows the resulting wheel contact area, where s is the thickness of the surface layer and t is the deck plate thickness. This should be taken into account both in the length and width of the wheel contact area and therefore, b is the width or length of the wheel print mentioned in 6.3.

For movable bridges, an epoxy layer of 8 mm is a common surface layer. Therefore, this value is used as the thickness of the surface layer in this report.

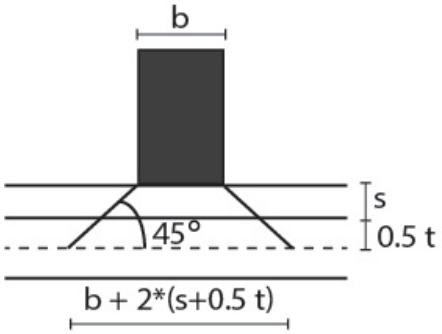

Figure 6.1: Wheel contact area due to load dispersal through epoxy layer and steel plate

The wheel contact area and distributed load for the different wheel types from table 6.2 are given in table 6.4. It includes the contact size from the Eurocode and the one which takes into account the load dispers.

Table 6.4: Wheel contact area and load distribution load

		General wheel contact area		**Including load dispersal**	
Wheel type	**Axle load** [kN]	**Wheel contact area**	**q** [N/mm^2]	**Wheel contact area**	**q** [N/mm^2]
A	70	220x320	0.50	256x356	0.38
B	120	220x320	0.43	256x356	0.33
	130		0.46		0.36
	140		0.50		0.38
	150		0.53		0.41
C	80	270x320	0.46	306x356	0.37
	90		0.52		0.41

The transverse wheel position has a large influence on the fatigue life of OSDs. According to Eurocode 1 part 2 paragraph 4.6.1(5), an approximation of the transverse distribution of trucks is given, see figure 6.2.

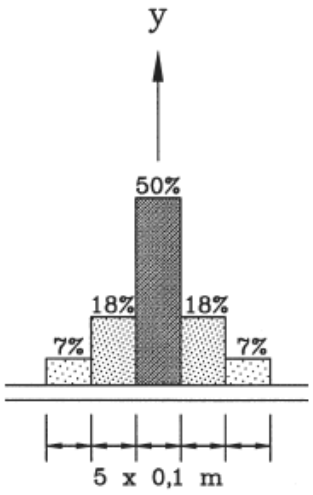

Figure 6.2: Distribution of the vehicle position in transverse direction [27, fig 4.6]

6.1.3. Stress range

The stress in transverse direction is responsible for the fatigue cracks. The bending moment and resulting stresses in transverse direction are largest if the wheel load is placed right above the crossbeam. In this report, there is assumed that the stress will become zero after one axle is passed and before the second axle will pass. As a consequence, each axle results in an individual stress range independent of another wheel axle. In this way, the stress range per truck is determined. In paragraph 7.5, this assumption is analyzed.

6.1.4. Partial safety factor

According to paragraph 9.3 of the Dutch national annex of Eurocode 3 part 2 [31], a partial safety factor (γ_{Mf}) of 1.15 should be used for fatigue calculations of OSDs. This factor is valid for a safe life assessment method and the consequences of failure should not influence the main structure. The partial factor for fatigue loads γ_{Ff} is given in Eurocode 3 part 2 paragraph 9.3 [30] and should be taken as 1.

6.2. Damage value calculation

The damage value gives how much damage the detail will give for the chosen design life. If the damage value is larger than 1, fatigue failure will occur.

Combining the information for extrapolation of the hot spot stress method with a relative fine mesh, section 2.8.2, the calculations for the amount of load cycles, section 2.7 and the design amount of load cycles according to FLM 4, section 6.1.2, the following flow chart is used for calculations of the damage value.

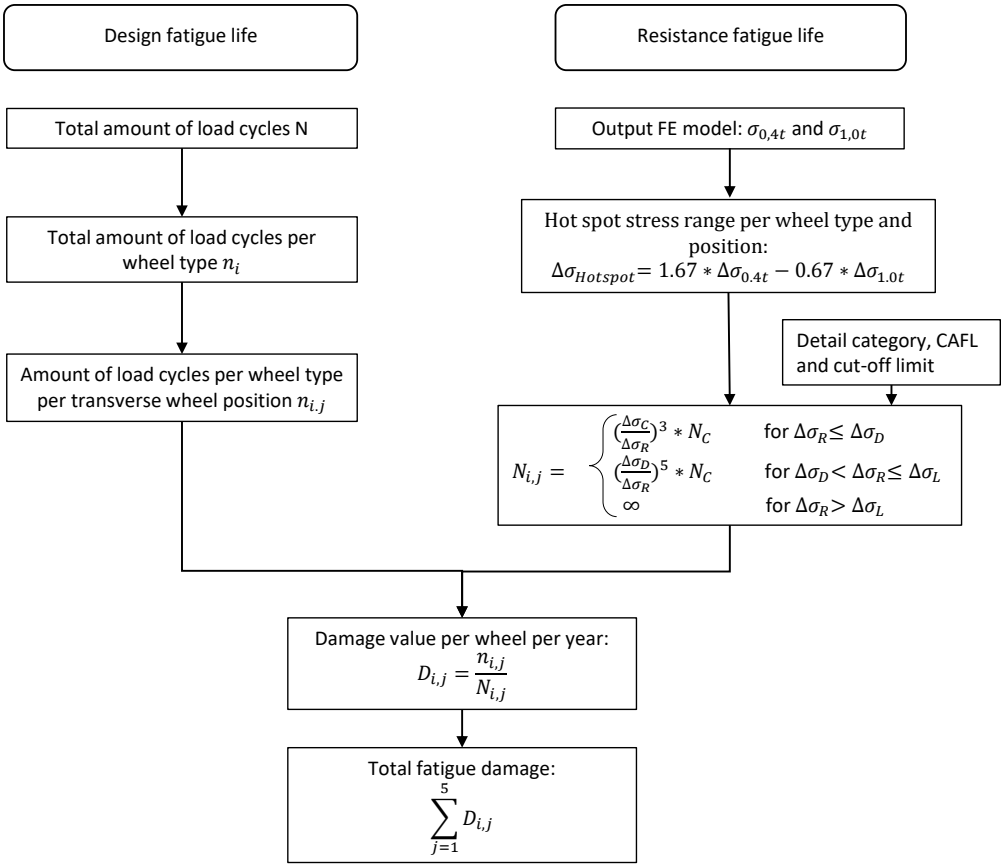

Figure 6.3: Flow chart calculation of damage value

The damage values in this chapter are calculated in Excel, see appendix D for the in- and output.

6.3. Wheel positions

The most unfavourable wheel position in transverse direction is determined using an influence line. The wheel loads are placed at locations above the crossbeam. The assumed center position of the wheel is shown in figure 6.4(a) for a single tyre, which corresponds to wheel type A and C, and in figure 6.4(b) for a double tyre, wheel type B. The hot spot stress at the deck plate of the rib-to-deck plate joint, figure 6.4 point A, is determined. The influence lines for wheel type C with an axle load of 90 kN and wheel type B with an axle load of 150 kN are given in figure 6.5.

For a single tyre, the bending stress at the lower surface of the deck plate is highest if the wheel is places in the center of the trough. If a wheel is placed not in the center of the trough, the stress range decreases drastically. Therefore, this center position is the most unfavourable wheel position for a single tyre.

For the double tyre, loading of each tyre in the center of the trough results in a peak stress at the joint. This

position results in the most unfavourable wheel location.

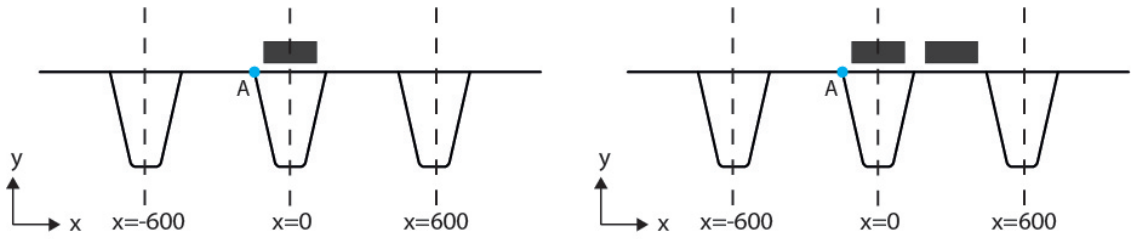

(a) Single tyre (b) Double tyre

Figure 6.4: Wheel positions

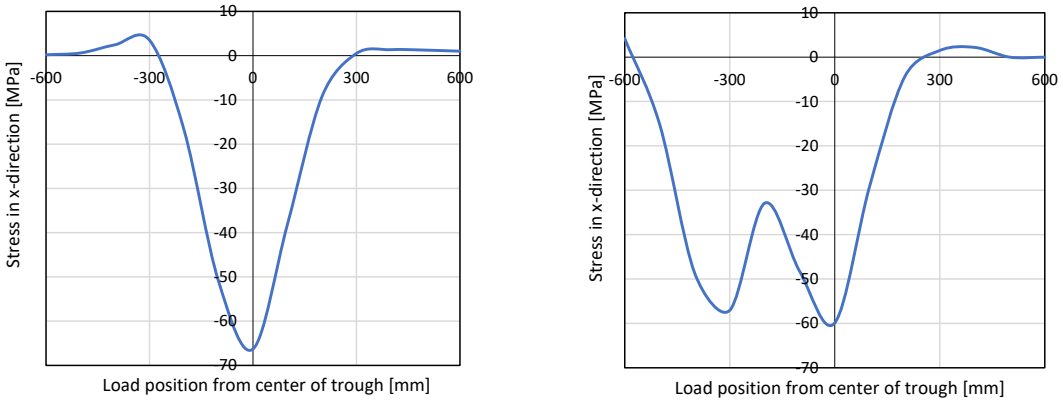

(a) Single tyre (Wheel type C) (b) Double tyre (Wheel type B)

Figure 6.5: Influence lines of the hot spot stress at location A

The total damage value, including all wheel types and axle loads as discussed in table 6.2 is determined, see table 6.5. It follows that the center position is responsible for 93% of the total damage value of the deck plate. The other damage is caused by the position -100 mm from the center. The rest of the transverse positions does not influence the fatigue damage.

The center position is responsible for only 50% of the total amount of design load cycles. Because of the large difference between the stresses if the load is placed in the center or at another position, it is important to take into account the transverse wheel positions. It results in almost half of the fatigue life compared to if all design load cycles are considered in the center.

Table 6.5: Damage value per transverse load position for a=300mm and t=20mm. $\gamma_{Mf} = 1.15$

a=300mm - t=20m					
	Location from center [mm]				
	-200	**-100**	**0**	**100**	**200**
A - 70kN	0	0	0.47	0	0
B - 120 kN	0	0	0.02	0	0
B - 130 kN	0	0	0.17	0	0
B - 140 kN	0	0.01	0.07	0	0
B - 150 kN	0	0.01	0.12	0	0
C - 80 kN	0	0.01	0.11	0	0
C - 90 kN	0	0.09	0.97	0	0
Total	0	0.13	1.9	0	0
			Total damage:		2.05
Percentage of total	0	7	93	0	0

6.4. Influence of parameters on the hot spot stress

The effect of different parameters on the deck segment is discussed in this section. Wheel type C, table 6.3, is considered and a uniform distributed wheel load $q_{wheel} = 0.52\ N/mm^2$ is applied which corresponds to an axle wheel load of 90 kN. The load dispersal through the epoxy layer is not taken into account in this parameter study.

6.4.1. Cope hole

A model with the troughs fully welded to the crossbeam is compared to a model which has a cope hole in the crossbeam. Figure 6.6 shows the stress range for both models. A cope hole results in 3% increase of the hot spot stress. This difference is small. However, there should be noticed that a small increase in stress results in a much larger increase of the fatigue life.

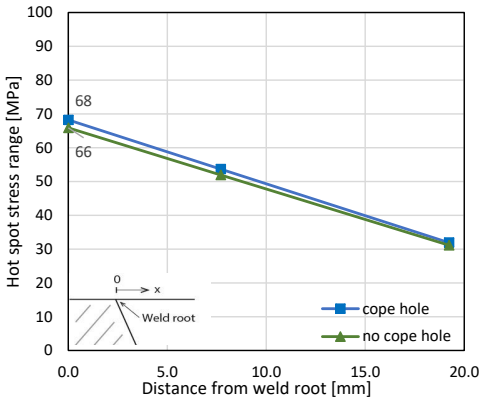

Figure 6.6: Influence of a cope hole on the hot spot stress range at the bottom surface of the deck plate

6.4.2. Thickness trough and crossbeam

Figure 6.7(a) shows the hot spot stress for the standard model which has a trough thickness of 6 mm and for a thickness of the trough of 8 mm. There is no difference in hot spot stress. This means that the fatigue life is not dependent on the trough thickness because the load is directly transferred from the deck plate to the crossbeam.

The effect on the hot spot stress for a thinner crossbeam thickness is analyzed. A crossbeam thickness of 16 mm, which is the reference model, and 12 mm are compared. The results for the hot spot stress are given in figure 6.7(b). A thinner crossbeam thickness results in a less stiff connection. As a consequence, the bending

stress is lower at the joint. The hot spot stress value reduces with 4.5%.

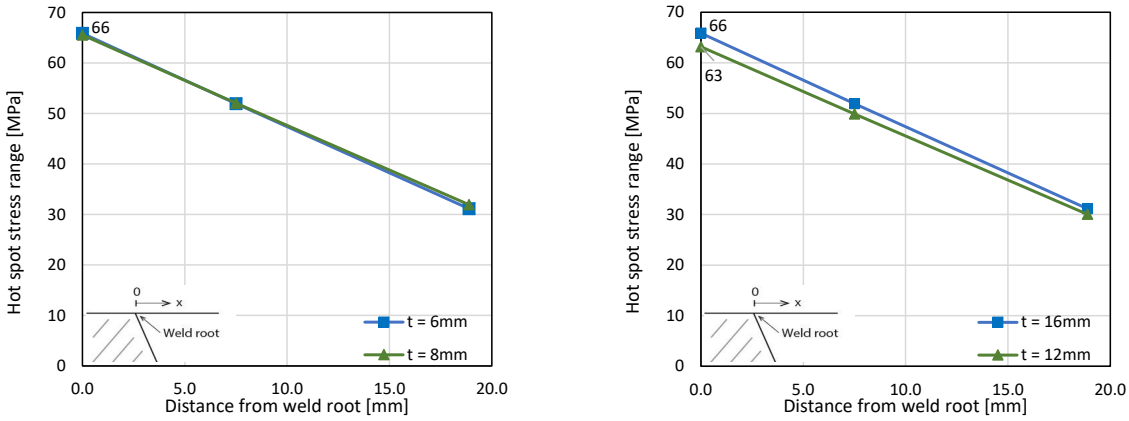

(a) Trough thickness

(b) Crossbeam thickness

Figure 6.7: Influence of parameters on the hot spot stress range

6.4.3. Trough shape

A trapezoidal shape is mostly used as trough shape. The influence of the angle of the trough web is investigated. Therefore, two alternatives for the standard model are built. The first alternative is a V-shape model which means that the width of the bottom flange is equal to zero and angle between the deck plate and trough web becomes smaller. The second alternative is a trapezoidal model with a bottom flange of 210 mm, which is 2 times the length of the standard model. See figure 6.8 for the two trough shapes.

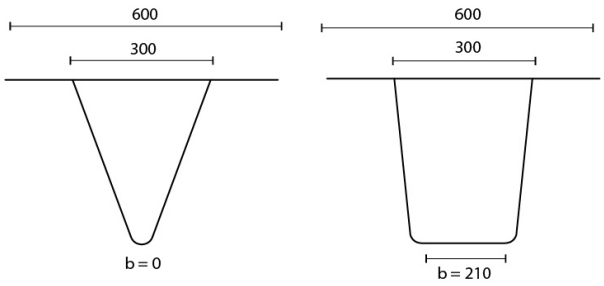

Figure 6.8: Design of a trough with b = 0 and b = 210 mm [mm]

The value of the hot spot stress is determined for the models, see figure 6.9. A larger bottom width of the trough results in a slightly lower hot spot stress range of 5% and no bottom flange results in an increase of 3% of the hot spot stress range.

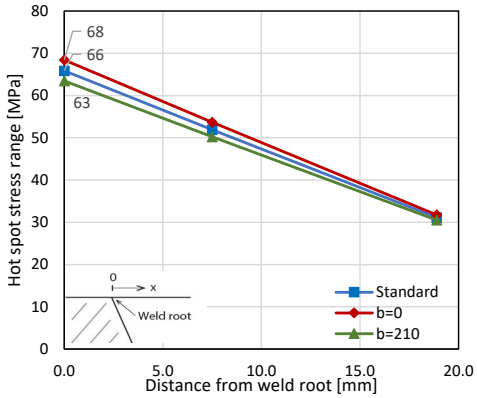

Figure 6.9: Hot spot stress due to loading with wheel type C for a trough with different width of the bottom flange

6.4.4. Deck plate thickness and width between the troughs

The influence of the width between the trough webs related to the hot spot stress range is analyzed. Four different alternatives are build which have all same parameters as the reference model as discussed in chapter 3, except for the width between the trough webs. A width of 250 mm, 300 mm, 350 mm and 400 mm are compared. The width of the bottom flange is decreases or increased with the same value as the width between the trough webs. Different deck plate thicknesses, varying between 16 mm to 24 mm, are analysed per alternative. The resulting hot spot stress due to loading is given in figure 6.10.

A larger distance between the trough webs gives a larger span between the webs and thus results in a higher hot spot stress at the rib to deck plate joint. The increase of the deck plate thickness results in lower bending stresses and as a consequence, in a lower hot spot stress. This compares to the conclusions from literature, see paragraph 2.5.1.

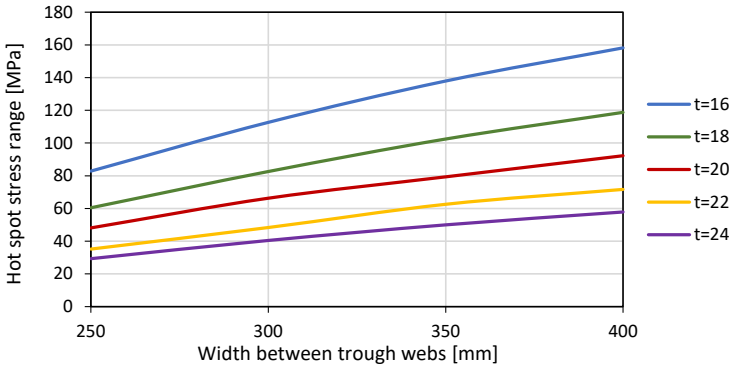

Figure 6.10: Hot spot stress at the rib-to-deck plate and crossbeam joint for varying parameters

For these parameters, the damage value per year (D_{year}) is determined. Therefore, the load dispersal through the epoxy layer is taken into account. Wheel contact area and distributed load as given in table 6.4 is used as input in the FE models. The damage value is determined only for the center position of the wheels. The transverse wheel position is taken into account by assuming that the center position is 93% of the total damage value as determined in table 6.5.

The resulting fatigue life is the amount of years for which the damage value is equal to 1. The resulting fatigue life is given in figure 6.11. The fatigue life for a deck plate thickness of 24 mm is larger than 100 years for all these situations and therefore not included in the graph.

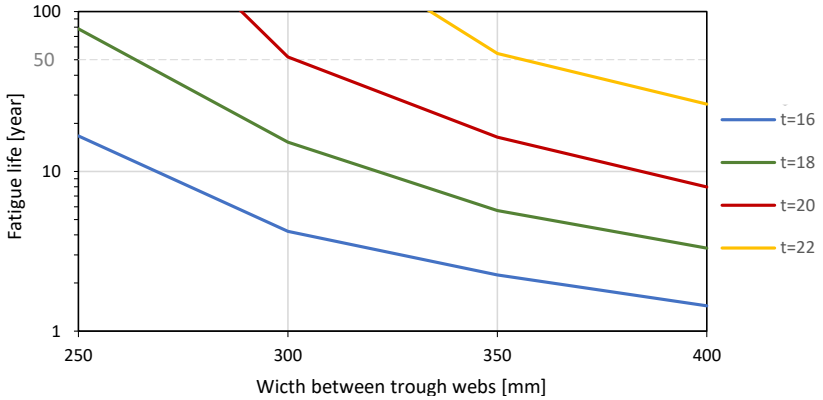

Figure 6.11: Fatigue life versus the width between the trough webs

The Eurocode gives a limitation ratio for the width between troughs (e) and the deck plate thickness (t), as discussed in paragraph 2.4. This value should be smaller than 25. Table 6.6 gives the ratio for different parameter options. A ratio of 25 corresponds to a deck plate thickness of 12 mm for the 300 mm standard width between troughs. From the table, it follows that to reach a ratio 25, the deck plate thickness should increase if a larger width between the troughs is chosen. This corresponds to the results found in this chapter.

For traffic category 2, a design life of 50 years is generally considered. For a width between the troughs (e) of 250 mm, a deck plate thickness (t) of 18 mm meets the requirement to have a fatigue life longer than 50 years, see figure 6.11. The requirement for e = 300 mm and e = 350 mm is met if respectively t = 20 mm and t = 22 mm are chosen. Considering these parameters, the ratio e/t is much lower than 25. The ratio given in the Eurocode is valid for traffic category 4 and a bridge deck which includes a thick asphalt layer. However, for higher traffic categories, a lower ratio is required and the ratio of 25 results in an unconservative fatigue design.

A suggestion is to make the ratio dependent on the traffic category, like the deck plate thickness is. For traffic category 2, the ratio e/t should be smaller than 17. However, the ratio gives only an approximation and should not be decisive.

Table 6.6: Ratio e/t. Green numbers: Possible parameters for traffic category 2.

t \e	**250**	**300**	**350**	**400**
12	20.8	25.0		
14	17.9	21.4	25.0	
16	15.6	18.8	21.9	25.0
18	13.9	16.7	19.4	22.2
20	12.5	15.0	17.5	20.0
22	11.4	13.6	15.9	18.2
24	10.4	12.5	14.6	16.7

7

Case study - Fatigue analysis for a couple of alternatives

In the previous chapter, different parameters which influence the fatigue performance of the rib-to-deck plate joint at the crossbeam are analyzed. In this chapter, there is searched for a design which combines the different influencing factors to see in which way it is possible to reduce weight. For the same reasons as mentioned in 6, the hot spot stress method for a shell element model with a relative fine mesh is used for the fatigue assessment, unless otherwise stated.

7.1. Case description

Dimensions of an existing bridge design are used for the design of four alternatives. This bridge is a bascule truss bridge in Terneuzen with a span of 55.8 meter. The bridge is designed for two lanes between the main girders. A standard distance between the troughs of 300 mm is used, which results in 12 troughs over a width of 7.2 meter. A front view of the design is shown in figure 7.1. A part of the side view is provided in figure 7.2.

In this report, the bridge deck is designed for traffic category 2. FLM 4, see paragraph 6.1.2, is used as fatigue load model. Damage values are determined for a design life of 50 years.

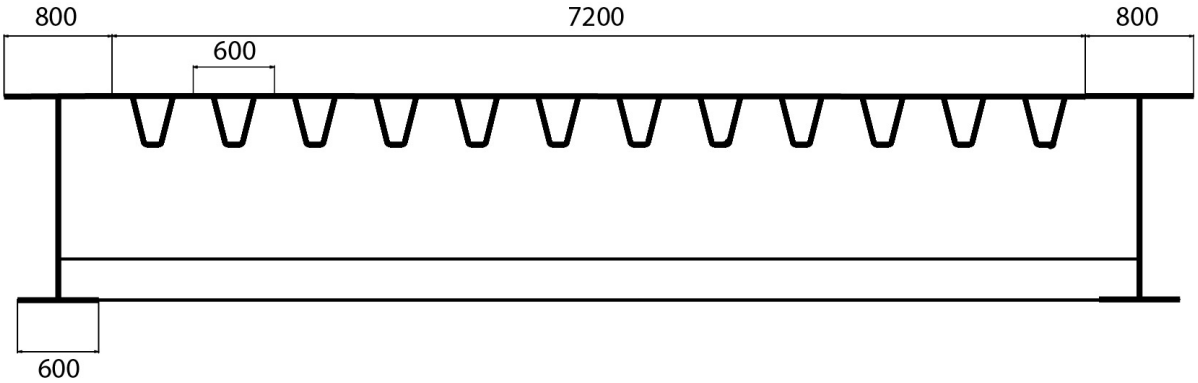

Figure 7.1: Dimensions bridge deck design. Front view (mm)

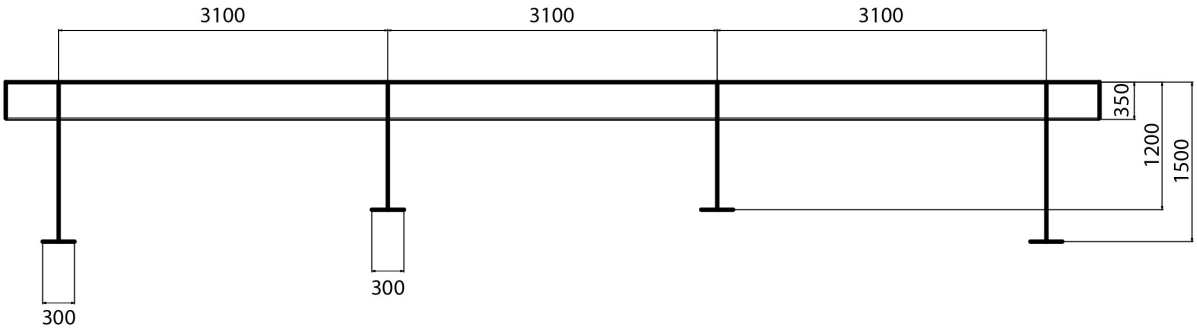

Figure 7.2: Dimensions bridge deck design. Side view (mm)

7.1.1. Design alternatives

The design of the trough as discussed in chapter 3 is used as the standard design. This design, with a width between the troughs of 300 mm and a deck plate thickness of 20 mm results in 12 troughs, see figure 7.3. Three alternatives are given for the design, all with a different amount of troughs. From paragraph 6.4.3 it followed that the influence of the trough shape only has a small effect on the hot spot stress. However, 3% stress increase results in a much larger fatigue life decrease. To exclude this effect in the design of the different alternatives, the angle between the deck plate and trough webs remains the same. As a consequence the width of the bottom flange increases or decreases with the same value as the width between the trough webs. For each alternative, the width within the trough webs is equal to the width between two webs.

The first alternative has 14 troughs. The width between the trough webs (a) is 257 mm and the deck plate thickness (t) is 18 mm, figure 7.4(a). The second alternative consists of 10 troughs, which results in a trough web distance of 360 mm and a deck plate thickness of 22 mm, figure 7.4(b). The last alternative is a variant with 9 troughs, a width of 400 mm between the trough webs and a deck plate thickness of 24 mm, figure 7.4(c). Because the stress range in the joint increases if the width between the troughs becomes larger, the deck plate thickness is increased as well. The deck plate thickness is determined using the results from figure 6.11.

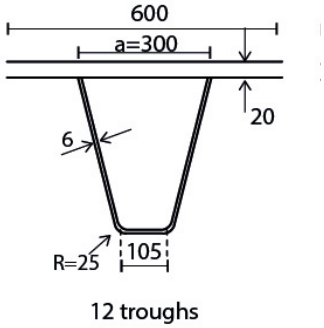

Figure 7.3: Dimensions for the design with 12 troughs [mm]

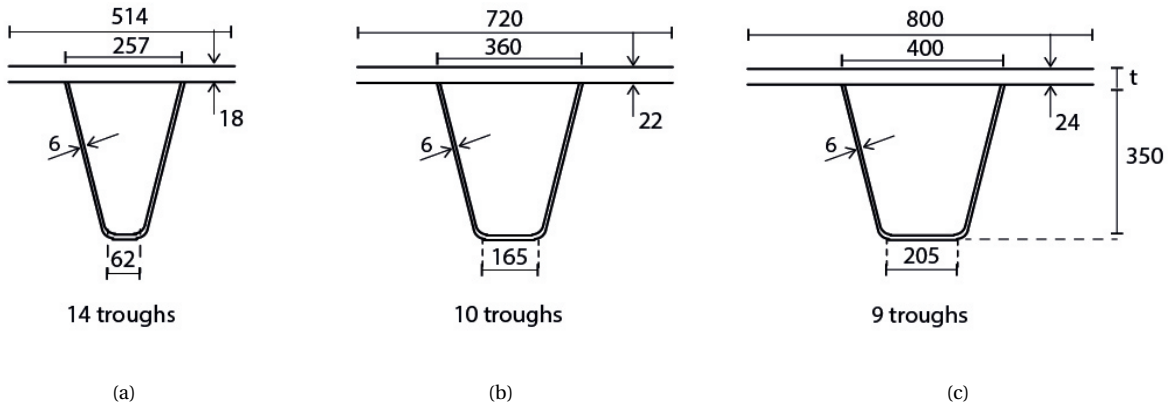

(a) (b) (c)

Figure 7.4: Dimensions of the four alternatives [mm]

In this report, the crossbeam thickness is taken as 16 mm and the trough thickness is 6 mm, which corresponds to the model as discussed in chapter 3.

A 3D view of the alternative with 12 troughs is shown in figure 7.5.

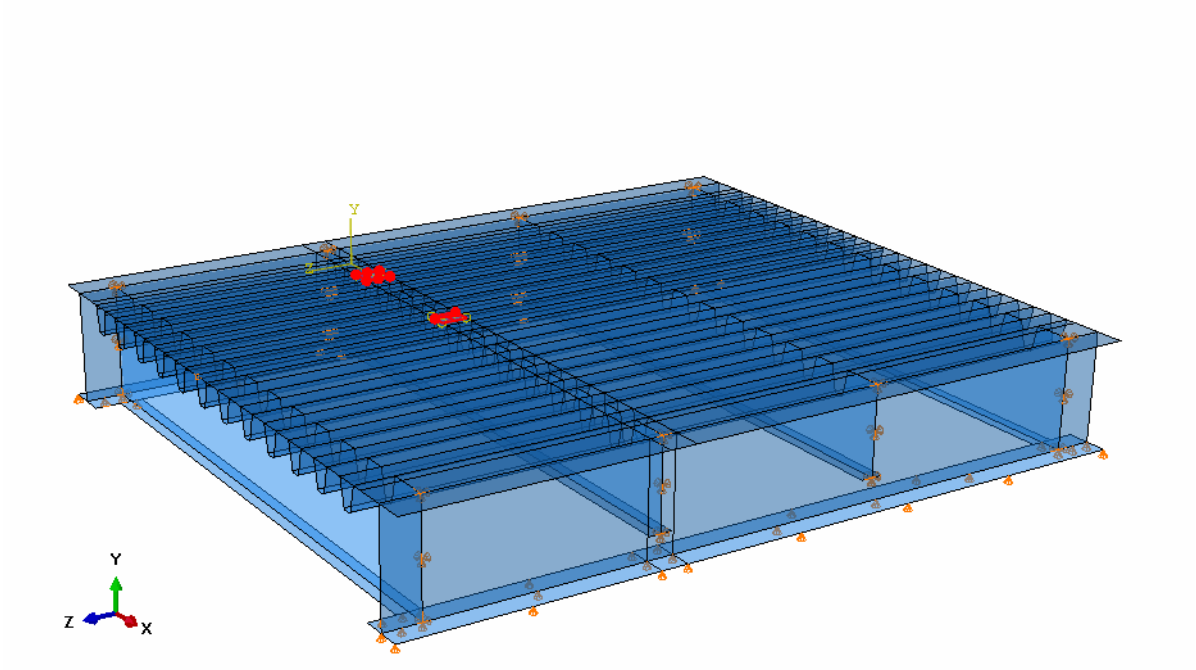

Figure 7.5: 3D view of the case model

When the load is placed right above the crossbeam and the crossbeam is fully fixed over the bottom flange, only a small part of the total bridge deck can be modelled, as discussed in paragraph 3.2. Therefore, only three troughs and one crossbeam are modelled for the different alternatives.

7.2. Damage values

In this parapgrah, the damage value is determined for the four alternatives and a design life of 50 years. To determine the damage values, the most unfavourable wheel positions as given in figure 6.4 are considered.

The influence of the load dispersal on the stress range is analyzed. The damage value is determined for the shell element model without taking into account the load dispersal, which means that the wheel contact area

as described by the Eurocode is applied and with taking into account the load dispersal. For both options, see table 6.4 for the wheel contact area and distributed load input.

To compare the results for using shell and solid elements for fatigue assessment, the damage value is determined for the model with a solid element sub model. Because of the presence of the solid element model, the increase of the wheel contact area due to load dispersal is only taken into account for the epoxy surface layer and not in the steel plate. In chapter 4, there is concluded that considering a lack of penetration of 1.5 mm does not influence the hot spot stress value. Therefore, this is not taken into account in the solid element model.

Table 7.1 gives a summary of the damage values for the different approaches. For the shell element model which includes the load dispersal, the transverse displacement in considered and loads are placed at all five positions. For the other two models, the wheel load is only applied at the center position, right above the trough. Transverse displacement is taken into account in the total amount of design load cycles to failure. Because the total damage is not only due to the center position, total damage is corrected using the percentages given in table 7.2.

Table 7.1: Damage value for traffic category 2 - $\gamma_{Mf} = 1.15$

a - t (mm)	Shell model - Standard wheel contact area	Shell model	Solid model
257 - 18	2.0	0.93	0.51
300 - 20	2.1	0.96	0.61
360 - 22	1.8	1.1	0.63
400 - 24	0.97	0.49	0.41

7.2.1. Transverse wheel position

The influence of the transverse location of the wheel on the hot spot stress at the joint is investigated for the four alternatives. For wheel type B with an axle load of 150 kN and wheel type C with an axle load of 90 kN, the hot spot stress range is given in figure 7.6. The shell element model and taking into account the load dispersal is considered.

If the distance between the troughs becomes larger, the presence of the second wheel has a larger influence on the hot spot stress if the double tire wheel is considered. Therefore, influence of this double tyre on the transverse wheel position has a larger influence on the hot spot stress range than for the single tyre wheel.
Unlike for the other models, for the model with a = 400 mm, the most unfavourable position is the location at -100 mm from the center of the trough. However, there should be noticed that the positions between the center and position -100 mm from the center are not considered, so it is possible that the exact position which leads to the highest stress value is somewhere in between these two locations.

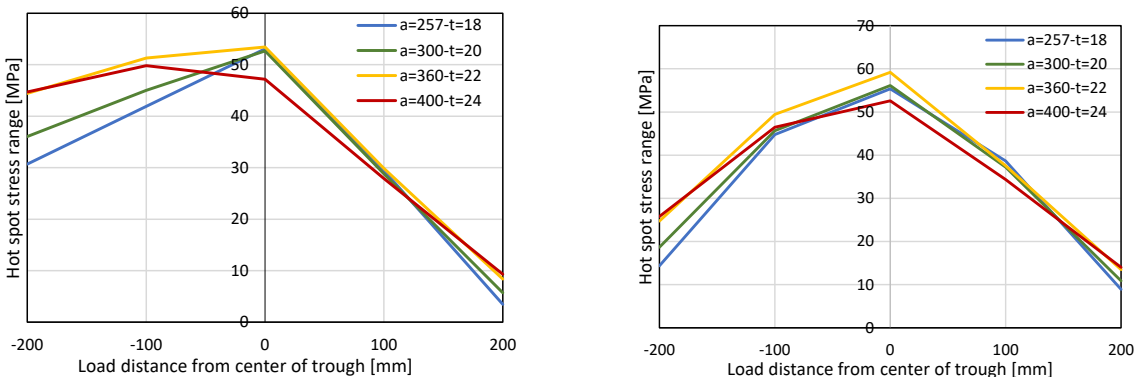

(a) Double tyre

(b) Single tyre

Figure 7.6: Influence lines of the hot spot stress range in detail A.

In section 7.2.1, the influence of the transverse wheel position on the total damage value is investigated for the alternative with a = 300 mm and there is concluded that the center position takes care of 93% of the total damage value. However, for this situation, the load dispersal was not taken into account. The percentage for the center position from the total damage is similar if the load dispersal is taken into account in the wheel contact area, see annex E. The result of the damage per transverse position for the other alternatives is also given in annex E. The percentage of the damage value caused by the center position relative to the total damage is given in table 7.2 for the four alternatives.

Table 7.2: Influence of the transverse wheel position on the total damage value

	a=257 - t=18	a=300 - t=20	a=360 - t=22	a=400 - t=24
Damage center / total damage [%]	95	93	90	83

7.2.2. Load dispersal

Taking into account the load dispersal through the surface layer by applying a larger wheel contact area generally is beneficial for bridge decks with a thick asphalt layer. However, table 7.1 shows that it is beneficial to take into account for movable bridges with a thin asphalt layer as well. Because of the load dispersal, the wheel contact area becomes larger, while the same axle load is applied. Therefore, the distributed load becomes smaller and is less concentrated. This results in a reduced hot spot stress.

For wheel type B with an axle load of 150 kN and for wheel type C with an axle load of 90 kN, the resulting stress range in the rib-to-deck plate joint, figure 6.4 point A, is given in figure 7.7. Including the load dispersal results in a stress ranges which is 10 to 15% lower at the center position than if the load dispersal is not considered. A small decrease of the stress results in a large decrease of the damage value, which is in this case reduced by about 50%, see table 7.3.

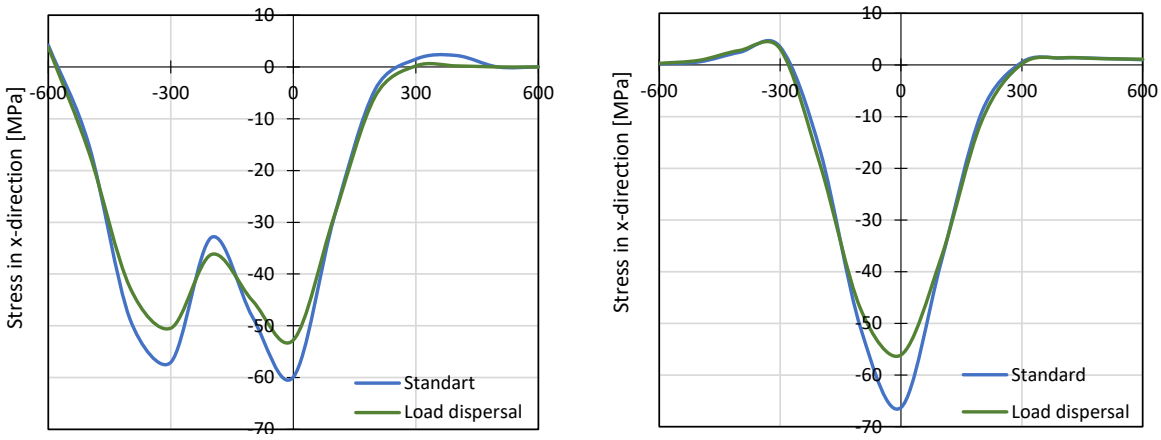

(a) Wheel type B - 150 kN axle load

(b) Wheel type C - 90 kN axle load

Figure 7.7: Hot spot stress at the deck plate

Table 7.3: Load dispersal reduction

a - t (mm)	$\mathbf{D_{Shell}/D_{Shell\text{-}standard}}$
257 - 18	52%
300 - 20	46%
360 - 22	61%
400 - 24	50%

The applicability of the load dispersal as described by the Eurocode is a discussion point. Ming et al. [23] and de Jong [8] concluded that the reduced stress range is caused by the composite action between the asphalt surface layer and the steel plate, more than due to the load dispersal. de Jong [8] states that the load dispersal as given in the Eurocode covers the load dispersal as well as the composite action of the deck plate with the surface layer. Because the last one is dependent on temperature, taking into account the load dispersal can result in an unsafe stress range prediction.

According to site measurement of a movable bridge deck with an epoxy layer of 8 mm, Kolstein [16] found for an air temperature between 0°and 7°lower stress ranges in the bride deck compared to when the air temperature was 20°to 33°. Therefore, there can be concluded that there is composite action between the epoxy layer and the steel deck plate and this influences the stress in the rib-to-deck plate joint.

de Backer [5] did research to the a thin surface layer. There is found no large difference between the fatigue life of a variant without considering a surface layer and a variant with a 7 mm surface layer with asphalt material properties. In his research, solid elements are used and the asphalt surface layer is included.

From the different studies, there can be concluded that there is a small reduction of stresses due to the surface layer, but it is likely that this is not because of the load dispersal but due to the composite action. Including the load dispersal gives an approximation of the increase of the stress but may is unconservative. Therefore, more research can be done to the actual reduction of the stress due to the epoxy layer.

7.2.3. Use of the solid element sub model

In chapter 4, there is concluded that the hot spot stress approach with a solid element sub model results in a less conservative fatigue life than using a shell element model. The ratio between the damage value determined with a solid element model and shell element model is given in table 7.4.

Table 7.4: Solid element model vs. shell element model

a - t (mm)	$\mathbf{D_{Solid}/D_{Shell}}$
257 - 18	55%
300 - 20	64%
360 - 22	64%
400 - 24	82%

Considering the alternative with a = 360 mm and t = 22 mm, the damage value is larger than 1 if the shell element model is used. From table 7.1, it follows that using the solid model results in a damage value smaller than 1. Therefore, the solid element sub model is beneficial to use in this case.

For a = 300 mm and a = 400 mm, the possibility to reduce the deck plate thickness if the detailed solid element model is used is investigated. The damage value for these alternatives is determined for a deck plate thickness of 18 mm and 22 mm respectively. The damage value is given in table 7.5. Using a solid element model instead of the shell element model leads not to a thinner deck plate thickness for these alternatives.

There can be concluded that the solid element model results in a reduced damage value compared to the shell element model. However, this method is more time consuming so it is recommended to first use the shell element model. If a damage value above 1 is found and a reduction of the damage by 50 to 80% will result in a damage value smaller than 1, then the solid element model can be used for fatigue assessment of the detail.

Table 7.5: Damage value - thickness reduction possibility

a - t (mm)	Damage value
300 - 18	2.4
400 - 22	1.8

7.2.4. Comparison to the Eurocode

The recommended value for the deck plate thickness determined by the Eurocode is 20 mm for traffic category 2, see table 2.1. If a shell element model is used and load dispersal through the surface layer is neglected, the damage value is larger than 1 for a model with a = 300 mm and t = 20. But taking into account one of the improvements results in a damage value smaller than 1. A deck plate thickness of 18 mm does not suffice, and therefore, the recommendation from the Eurocode is correct for a width between the troughs of 300 mm.

According to the Eurocode, the width between the troughs should be smaller than 300 mm. A larger width is possible as well for this joint. Nevertheless, if the width between the trough webs becomes larger, a thicker deck plate thickness is required to find a damage value smaller than 1 for traffic category 2. This should be considered if a design for an OSD bridge is made.

7.3. Weight of the bridge deck

A larger width reduces the cross section area, but a thicker deck plate thickness results in an increased cross section area. However, to reach a damage value below 1, a thicker deck plate thickness is required if the width between the trough webs is increased. In this paragraph, the effect on the weight of the bridge deck is discussed.

The weight of the elements and the total weight of the bridge deck are determined for the four alternatives. A crossbeam thickness of 12 mm and thickness of the troughs of 8 mm are assumed. The center to center span between the crossbeams is 3100 mm. These values correspond to the general design of the bascule bridge used in this case study. The main girders are not taken into account.

For the four discussed alternatives, the total weight of the bridge deck increases if less troughs are used and thus the width between the trough webs is larger. This is because the weight of the deck plate gives a large

contribution to the total weight of the bridge deck and this deck plate thickness is increased as well. Generally speaking, there can be concluded that how thinner the deck plate thickness is, how lighter the total bridge deck will be. When a deck plate thickness of 24 mm is used, the weight of the deck plate increases with 20% compared to a deck plate thickness of 20 mm and 33% compared to a deck plate thickness of 18 mm. However, the increase of the heaviest total design compared to the lightest design is only 8.5%.

From table 7.1 it follows that the damage value is not exactly the same for all models. For the case study, general thicknesses for the deck plate are chosen. The alternative with a = 400 mm and t = 24 mm has a smaller damage value which means that the fatigue life is longer compared to the other alternatives. To reach a same damage value (around D=0.95), the deck plate thickness can be made smaller, for example 23 mm or 23.5 mm. This results in a lighter deck plate and thus, a reduced total weight of the bridge is reached. The 8.5% increase of the weight compared to the lightest alternative becomes smaller. By a decrease of the deck plate thickness of 0.5 mm, the total weight is only 6.5% higher instead of 8.5%.

The design with 10 troughs and a = 360 mm has a higher damage value than around 0.95. Therefor, this alternative needs a slightly thicker deck plate to make a fair comparison. This has a negative effect on the weight, which means that the total weight will increase to almost the weight of the alternative with a = 400 mm.

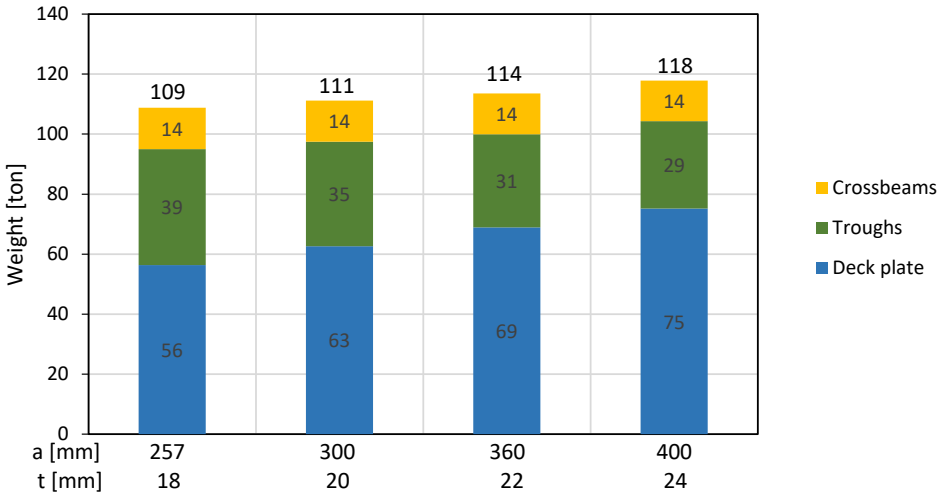

Figure 7.8: Weight of the elements of the bridge deck

Improvement possibilities

An optimization of the designs is still possible because in these designs there is assumed that the bottom flange increases with a same value as the width between the trough webs. However, the most contribution to the total weight of the bridge deck is from the deck plate. A reduction of the trough design results only in a small reduction of the total weight and thus will not have a large influence on the final conclusions of the weight reduction.

Another parameter which can be optimized further is the width between and within the webs. These values are similar to each other in this case. Because the rib-to-deck plate joint is only dependent on the width within the troughs and not on the width between two troughs, this last parameter can be increased. The fatigue life of the joint in span will be more important then. Because this joint is less susceptible for fatigue failure, higher stress ranges are acceptable for the joint at this location and therefore, an weight reduction of the deck plate may is possible.

7.3.1. Costs versus weight

Although the weight of the bridge deck increases if less troughs are used, the amount of welds for the trough web to deck plate connection decreases. In this section, an approximation of the costs for welding and for the amount of steel is made. The estimations for the costs are received from Iv-Infra and are only a rough approximation.

The welding speed it about 100 to 125 cm^3 / hour. This value is dependent on the shape of the weld and on if it is welded manually or automatically. In this report, an automatic weld is considered which will increase the speed. However, the shape of the weld is more complex than a simple filled weld which results in slower welding. Therefore, the conservative value of about 100 cm^3 per hour is assumed for the welding volume. A rough estimation of the price for labor is €80.0 per hour. Therefore, the price of one weld is about €0.80 per cm^3.

The surface area of the weld is 0.24 cm^2 and the length per trough is 55.8 m. The total volume of the weld per trough web is 1339 cm^3. Total price for the weld per web is €857 and thus €1714 per trough.

The purchase prise of 1 kilogram steel is about €1.00. The final price is about €6.00/kg steel. Then the steel structure is in the factory made ready to install at the building site. Because of the amount of welding, an OSD is relatively labor intensive to build. Therefore, this value may is a bit higher. However, the welding is considered separately in this calculation and therefore, the steel price may should be taken a bit lower. Therefore, the steel purchase price and estimated final price are considered.

Per alternative, the price for the OSD is determined by multiplying the amount of steel with the steel price. For the total weight, the deck plate and troughs are considered only. The amount of troughs is multiplied by the price of the weld per trough. Results for the total price of the deck is given in figure 7.9 for the final steel price and in figure 7.10 for the steel purchase price.

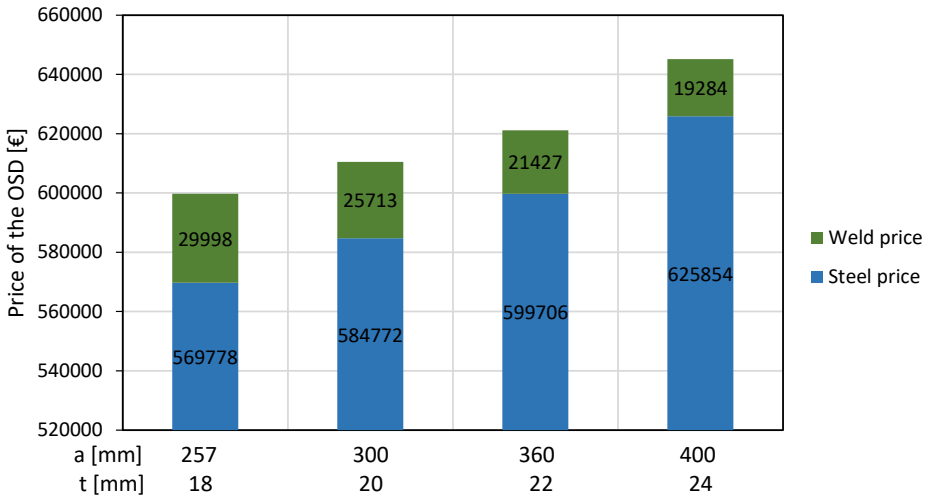

Figure 7.9: Costs per alternative - steel final price

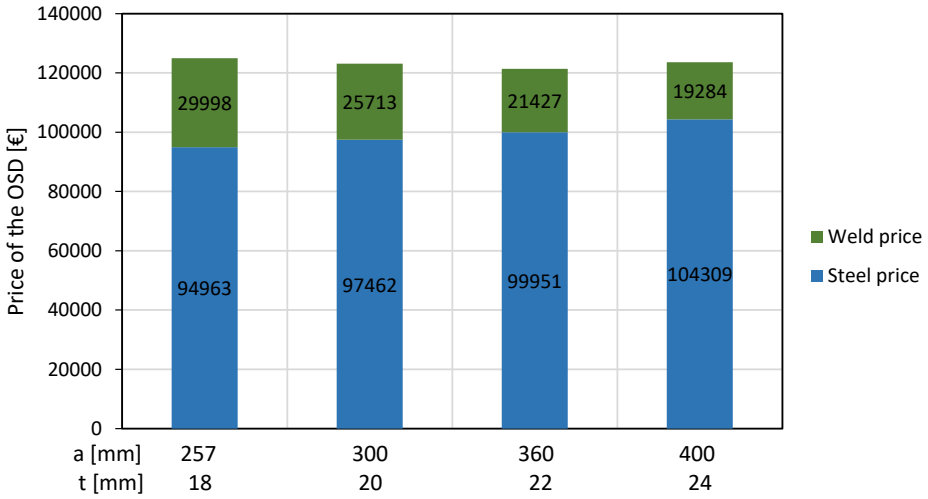

Figure 7.10: Costs per alternative - steel purchase price

When the final price for the steel is considered, the steel price has a larger influence on the total price than the welding price. Small changes in the assumptions for the weld price does not have a significant influence on the total steel price, because it is only a small value of the total price of the deck. However, if the steel price is taken much lower, the welding price is more important and a design with less troughs can reduce the total price.

There should be noticed that if the crossbeams and main girders and other elements of the bridge are also taken into account, the influence of the price of the welds becomes only smaller. As a consequence, the percentage of the costs for the welding of the trough web to deck plate joint are will become only smaller and therefore, less important, if more elements parts of the bridge are considered..

7.4. Crossbeam deformation

In this report, a fully supported crossbeam is used in the calculations. However, in a normal bridge design, the crossbeam is supported by the side edges only. The crossbeam will deform due to a truck load. Majlaars et al. [21] states that a simply supported beam results in a small increase of the hot spot stress at the deck plate compared to a crossbeam which is fully supported at the bottom flange.

The effect of the deflection of the crossbeam on the stress range for the design a = 300 mm and t = 20 mm is analyzed. For this calculation, the total width of the bridge is considered instead of the small model with only three troughs. Therefore, the total bridge part is used, see figure 7.5. Wheel contact area which includes the load dispersal is used, table 6.4. The axle wheel is considered. The end of the axle is placed in the most unfavourable wheel position right above the second trough. Because the transverse displacement only had a small influence on the damage value, only the center position is used in this section.

Three options are compared. The first option is a fully supported crossbeam in y-direction, the second option is a crossbeam which is fixed in translation in x- y- and z-direction at the side edges of the crossbeam. The last option is similar to the second option, but only one wheel at the second trough is considered instead of the wheel axle. For all options, the crossbeam thickness is 16 mm, which is the crossbeam thickness used for the alternatives. For option 2, a crossbeam thickness of 12 mm is considered as well. Table 7.6 gives the hot spot stress in trough 2 (T2) at the left and right side due to an axle load of 90 kN and wheel type C. Figure 7.11 shows the vertical deformation (y-direction) of the crossbeam of the first 2 options. The resulting damage value considering all wheel types and axle loads from FLM 4 is given in table 7.6 as well.

Considering the deformation of the crossbeam results in a damage value 2.5 times the damage value if the crossbeam is fully fixed over the crossbeam length. There should be noticed that applying a load only at T2

results in a lower stress at the left side and a higher stress at the right side of the trough than if the full axle load is applied. A conclusion is that it is important to consider the wheel axle of the truck instead of only one wheel. The in-plane deformation of the crossbeam has a large influence on the damage value of the rib-to-deck plate joint and should therefore always be taken into account in the fatigue calculation.

Expected is that increasing the thickness of the crossbeam will reduce the deformation. In paragraph 6.4.2, an increase in stress of 4.5% was found if the crossbeam thickness is 16 mm instead of 12 mm and when the deformation of the crossbeam is not considered. If the in-plane deformation is taken into account, the difference in stress is only 3%, which means that the thicker crossbeam thickness decreases the in-plane deformation and has a positive effect on the fatigue life. However, using a crossbeam thickness of 16 mm still results in a 12% shorter fatigue life than a crossbeam thickness of 12 mm.

From the calculations, there can be concluded that a simplified 2D model is not suitable for a final damage calculation of the rib-to-deck plate joint at the crossbeam. Not only the bending stress due to the local deformation of the crossbeam has an influence on the hot spot stress in the joint, but the deformation of the crossbeam is important to consider as well. This can not be taken into account in the simple 2D hand calculation.

According to paragraph 2.5.5, the in-plane deformation is only important to consider if a relative shallow crossbeam is used. No dimensions of this crossbeam is given. According to the results from the study in this report, the in-plane deformation has a large negative effect on the hot spot stress at the deck plate. Therefore, more research to the dimensions of the crossbeam is required for reduction possibilities of the effect of the in-plane deformation on the stress range at the deck plate.

Table 7.6: Hot spot stress in T2

		T2 - Left [MPa]	**T2 - Right** [MPa]	**Damage value**
Full support		-53.8	-53.7	0.89
Support at edges		-65.5	-48.3	2.3
	$T_{crossbeam}$ = 12 mm	63.7	46.0	2.0
	One wheel instead of axle	-58.6	-51.9	1.3

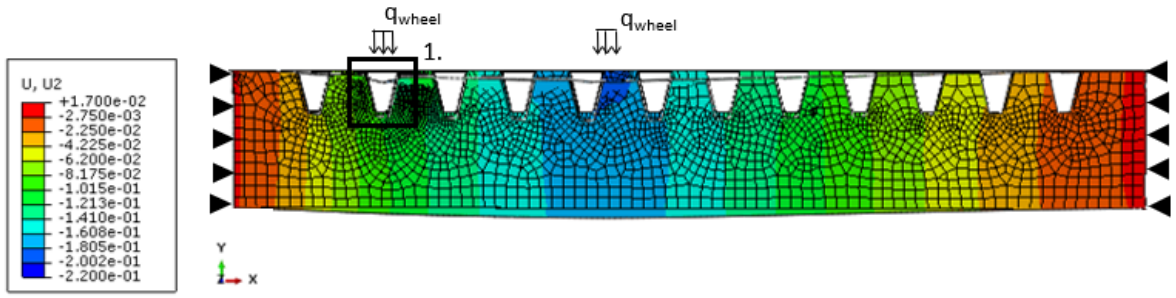

(a) Crossbeam edges supported

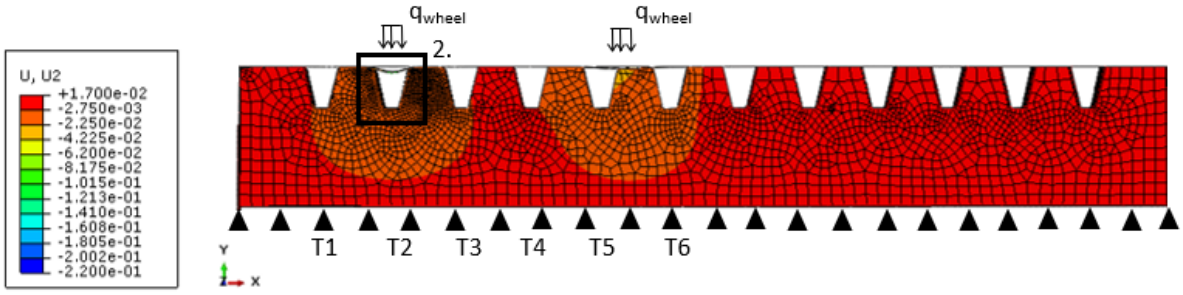

(b) Crossbeam full support

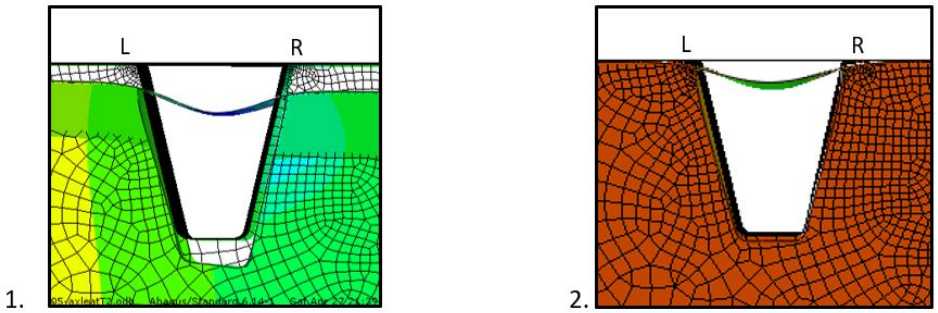

(c) Detail 1 and 2

Figure 7.11: Deformation of the crossbeam (Deformation scale factor is 500)

7.5. Stress range assumption

In the report, the wheel axles of a truck are considered separately and there is assumed that the stress range becomes zero at the moment between loading of the first and second axle of the truck. The most unfavourable wheel position is chosen for each wheel type, which means that the single tyre and double tyre are not in line of one truck, see figure 7.12 for truck 3 from FLM 4, table 6.2. In this section, this assumption is called option 1. However, if a truck enters the bridge, the position of the wheels are in a line as shown in figure 7.13 for the third truck from FLM 4. This is option 2 in this section.

Due to passing of a truck, a certain stress range will remain in the deck plate at the crossbeam at the moment the different axles of the truck passes the bridge deck. This will have an influence on the stress ranges and thus on the total damage value of the joint, called option 3.

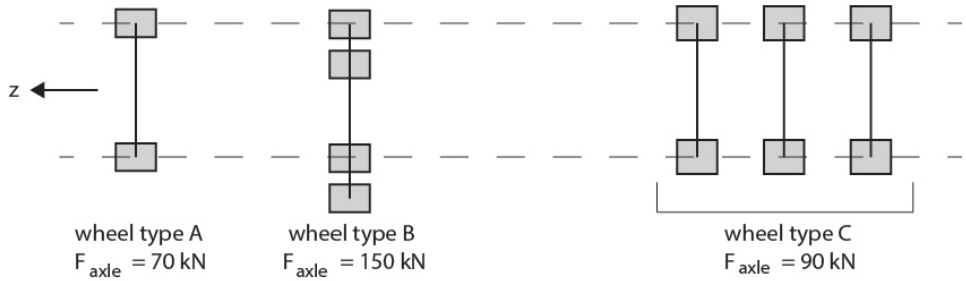

Figure 7.12: Wheel axles of truck 3 - most unfavourable wheel position assumption

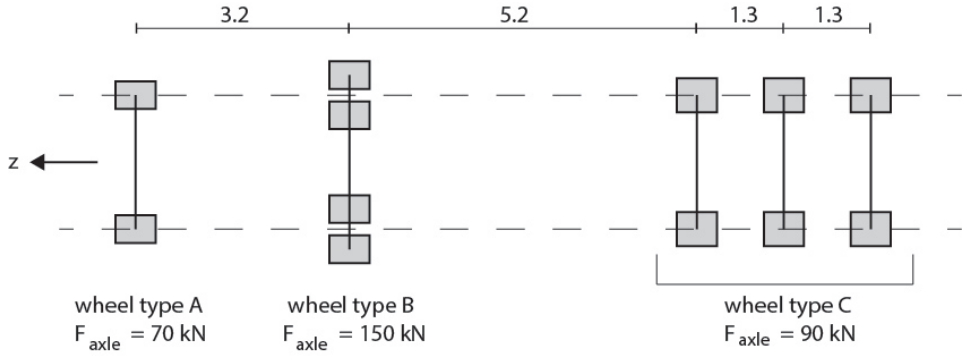

Figure 7.13: Wheel axles of truck 3

The effect of the assumptions made in this report on the damage value is analyzed in this section. The total deck segment of the model with a = 300 mm and t = 20 mm is used. The stress range and damage value is determined for truck 3 from table 6.2. Wheel contact areas from the Eurocode, table 6.4, are used. Because of considering the transverse displacement of the loads results in only a small increase of the total damage value, only the center position is considered.

The load positions which are used to determine the hot spot stress in the joint for option 3 are given in appendix F. The reservoir counting method is used for determining the stress ranges. Results are shown in figures 7.14, 7.15 and 7.16.

Considering the position of each axle in one line relative to each other results in a slightly lower damage value than when the most unfavourable positions are taken. This is because the stress range caused by the double tyre is lower. There should be noticed that the transverse displacement of the truck is more important now than for option 1. Because 50% of the total damage is related to the center position, expected is that the damage value still will be smaller for options 2 compared to option 1.

Considering the passing of a truck and the remaining stress in the deck plate, the stress ranges becomes different. The total damage value is lower than when all axles are considered separately because the remaining stress range between passing of the axles has a positive effect on the value of the stress ranges.

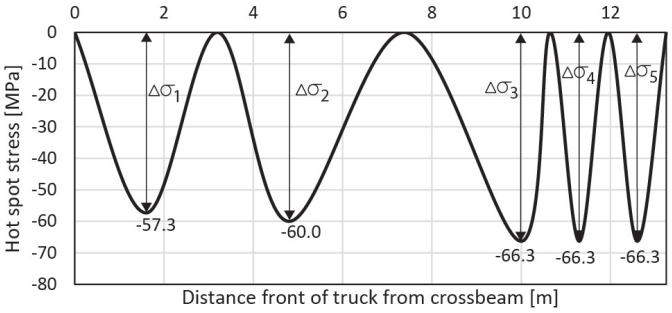

Figure 7.14: Stress range due to truck 3, option 1

Stress range	Load cycles	Damage value
$\Delta\sigma_1$= 57.3	2.7 *10^7	0.09
$\Delta\sigma_2$= 60.0	2.1 *10^7	0.12
$\Delta\sigma_3$= 66.3	1.3 *10^7	0.19
$\Delta\sigma_4$= 66.3	1.3 *10^7	0.19
$\Delta\sigma_5$= 66.3	1.3 *10^7	0.19
Total Damage value:		0.80

Table 7.7: Damage values, options 1

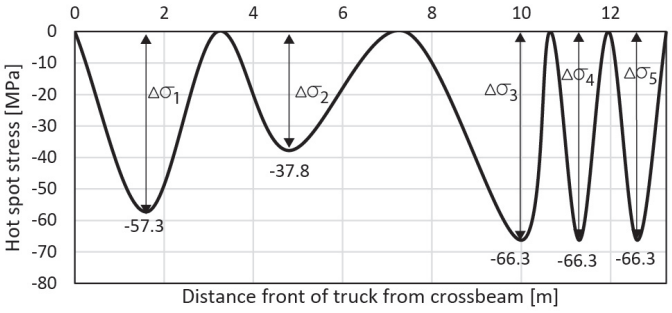

Figure 7.15: Stress range due to truck 3, option 2

Stress range	Load cycles	Damage value
$\Delta\sigma_1$= 57.3	2.7 *10^7	0.09
$\Delta\sigma_2$= 37.8	∞	0
$\Delta\sigma_3$= 66.3	1.3 *10^7	0.19
$\Delta\sigma_4$= 66.3	1.3 *10^7	0.19
$\Delta\sigma_5$= 66.3	1.3 *10^7	0.19
Total Damage value:		0.68

Table 7.8: Damage value, option 2

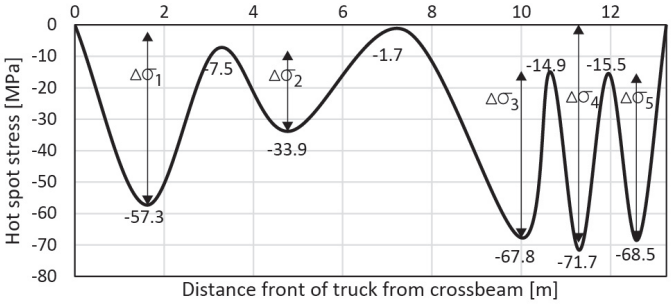

Figure 7.16: Stress range due to truck 3, option 3

Stress range	Load cycles	Damage value
$\Delta\sigma_1$= 49.8	5.4 *10^7	0.05
$\Delta\sigma_2$= 26.4	∞	0
$\Delta\sigma_3$= 52.9	4.0 *10^7	0.06
$\Delta\sigma_4$= 71.7	8.7 *10^6	0.29
$\Delta\sigma_5$= 53.0	4.0 *10^6	0.06
Total Damage value:		0.46

Table 7.9: Damage value, option 3

7.6. Stress range in the joint at mid span

The effect of rib spacing on the trough web-to-deck plate joint between two crossbeams is investigated. Therefore the stresses in the joint for the alternatives with a = 300 mm and a = 400 mm as provided in this chapter are analyzed. The larger model, see paragraph 7.4, is used.

The maximum stresses in the trough web will be found if the load is placed in the middle of the span [13]. Therefore, the load is placed at this position. All wheel loads of the trucks are considered separately, which means that there is assumed that the stress range becomes zero after one wheel is passed and the second will pass the joint. Wheel contact areas as give in the Eurocode are used.

The influence lines at location A, see figure 7.17, are determined at the deck plate either weld root or toe, which results in the largest value, and the trough at the weld root at the inner surface of the trough web, and

the weld toe, the outer surface. Figures 7.18, 7.19 and 7.20 gives the influence lines for a model with a = 300 mm and t = 20 mm and a trough thickness of 6 mm and 8 mm. Figures 7.21, 7.22 and 7.23 shows the influence lines for a model with parameter a = 400 mm, trough thickness is 6 mm and deck plate thickness is 20 mm or 24 mm.

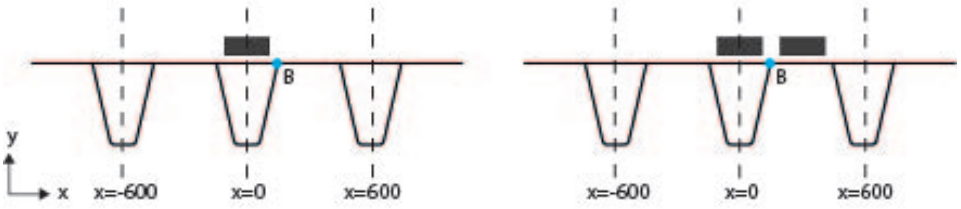

Figure 7.17: Wheel center positions

Because of the absence of the crossbeam in this detail, there is no point where stresses will concentrate so there will be no singularities in the FE model. Therefore, instead of the hot spot stress, the nominal stress can be derived from the FE model.

In span, the transverse wheel location has more influence on the stress in one joint compared to the location at the crossbeam. Because the trough-to-deck plate joint is less stiff, the peak stresses are lower than at the crossbeam.

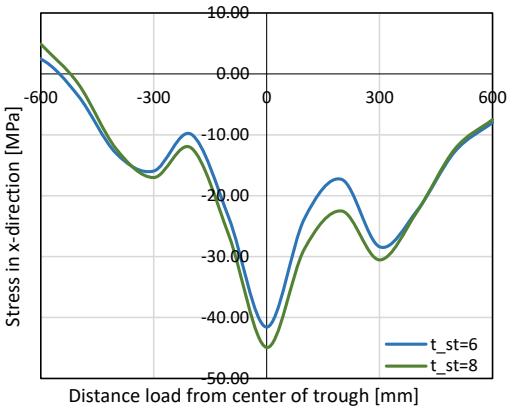

(a) Wheel type B

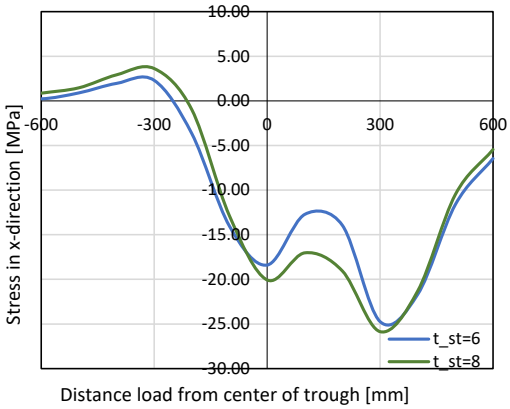

(b) Wheel type C

Figure 7.18: Influence line for the nominal stress in point B at the deck plate. a=300 mm

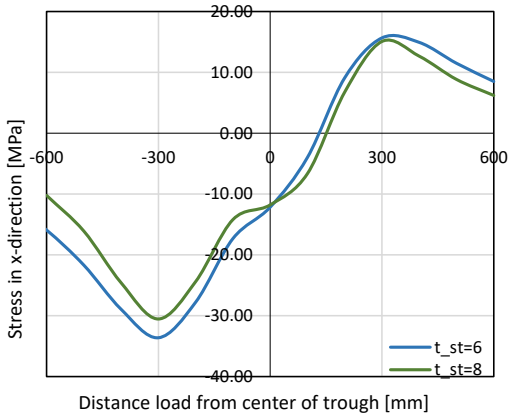

(a) Wheel type B

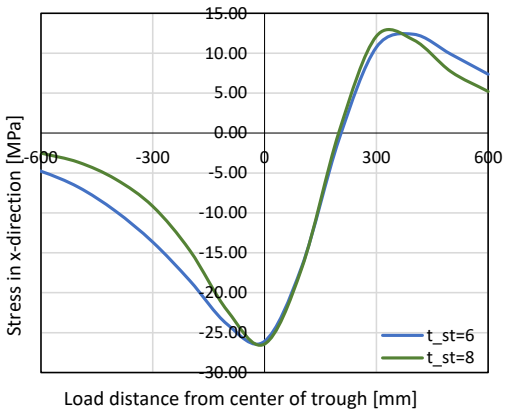

(b) Wheel type C

Figure 7.19: Influence line for the nominal stress in point B at the inner surface of the trough. a=300 mm

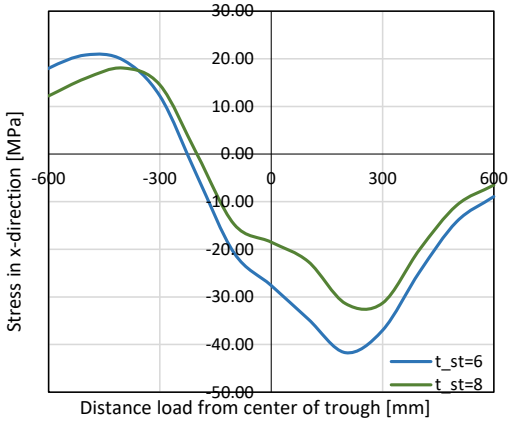

(a) Wheel type B

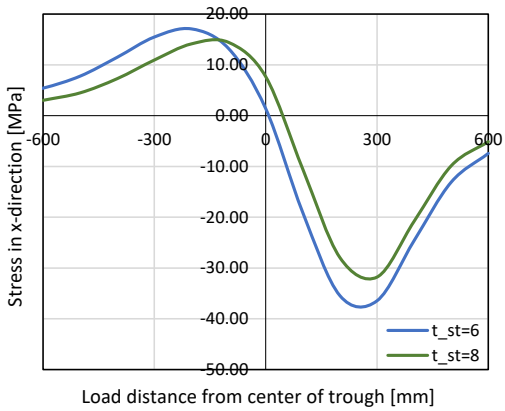

(b) Wheel type C

Figure 7.20: Influence line for the nominal stress in point B at the outer surface of the trough. a=300 mm

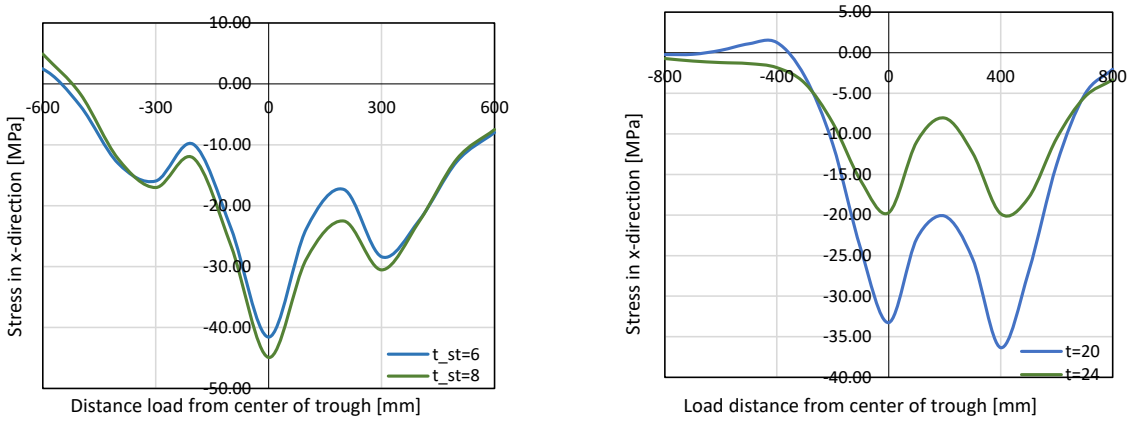

(a) Wheel type B

(b) Wheel type C

Figure 7.21: Influence line for the nominal stress in point B at the deck plate. a=400 mm

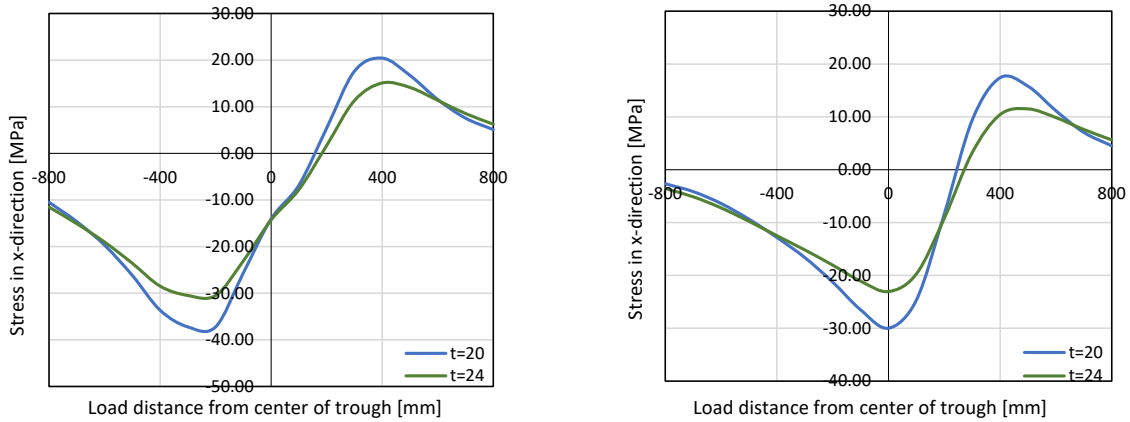

(a) Wheel type B

(b) Wheel type C

Figure 7.22: Influence line for the nominal stress in point B at the inner surface of the trough. a=400 mm

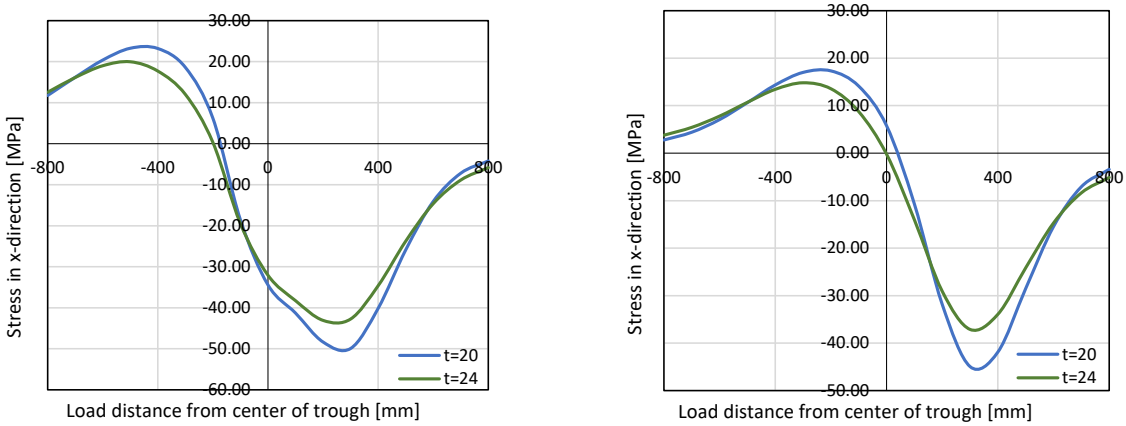

(a) Wheel type B

(b) Wheel type C

Figure 7.23: Influence line for the nominal stress in point B at the outer surface of the trough. a=400 mm

The stress range at the deck plate causes a fatigue crack through the deck plate. Detail 1 in table NB.7 of the Dutch national annex of Eurocode 3 part 2 [31] states that the detail category is 125 MPa for this crack location. Besides the stresses at the deck plate, the stress at the trough web should be checked. This stress is responsible for the weld bead crack, both at weld root (inner side of the trough) and weld toe (outer side of the trough). The detail category which should be used for this crack type is $\Delta\sigma_C = 100$ MPa, see detail 3 in table NB.7 of Eurocode 3 part 2 [31].

The damage values for the alternatives is determined and summarized in table 7.10. The values in red indicate a damage value larger than 1.

Table 7.10: Damage value at mid span for traffic category 2

a - t_{dp} - t_{st} [mm]	**Location**	**Damage value**	**Centre distance from 0-point**
300 - 20 - 6	Deck plate - weld root	0	0
	Trough - weld root	0.24	-300
	Trough - weld toe	1.3	200
300 - 20 - 8	Deck plate - weld root	0.15	0
	Trough - weld root	0	-300
	Trough - weld toe	0	300
400 - 20 - 6	Deck plate - weld root	0.52	0
	Trough - weld root	0.24	-300
	Trough - weld toe	1.8	300
400 - 24 - 6	Deck plate -weld root	0	0
	Trough - weld root	0	-200
	Trough - weld toe	0.70	300

Unlike stated in literature, the thickness of the trough web does influence the fatigue performance of the joint at mid span. Because the joint becomes stiffer if the trough thickness increases, stresses in the deck plate slightly increase and the stress in the trough web decreases. The last one will cause a fatigue crack initiation first, and therefore, the increase of the trough thickness can lead to a longer fatigue life for the joint in span.

The fatigue life of the joint in span is longer than the joint at the crossbeam. The joint at the crossbeam is only dependent on the width within the troughs and not in the width between two troughs. Those reasons makes it possible to chose a larger width between the trough webs compared to the width within the trough webs. This may result in extra material reduce.

8

Conclusion and discussion

In this chapter, several conclusions are drawn on the results presented in the report.

8.1. Conclusions

8.1.1. Fatigue analysis

In the first part of the report, results for the stress based fatigue assessment using the nominal, hot spot or effective notch stress and for the local critical plane based method using the swt-parameter are presented. Different FE modelling techniques are used. An answer is found on the following research question:

For which fatigue assessment method, the prediction of the amount of load cycles to failure is most close to experimental results if the rib-to-deck plate joint at the crossbeam is considered?

For the considered fatigue assessment methods, the hot spot stress method gives a most accurate prediction compared to the experimental result. All results are on the safe side if a detail category of 125 MPa is used, which corresponds to a 97.7% failure probability.

- For the hot spot stress approach, a detailed solid element model which includes the weld geometry gives a 44% longer fatigue life compared to the shell element model.
- The hand calculation using a 2D model gives a similar fatigue life prediction as using the hot spot stress approach for a shell element model.
- Fatigue life determined with the effective notch stress method results in a fatigue life less than 10% of the fatigue life determined with the hot spot stress method. Therefore, there can be concluded that this method is conservative if the recommendations for modeling given by the IIW are used.
- A local critical plane based approach using the swt-curve results in an infinite fatigue life if the residual stresses are not considered. Including the residual stress by applying a prescribed stress value in the weld region gives a comparable fatigue life compared to the experimental value.
- Observed is that when a FEM analysis is used for the fatigue assessment of the joint at the crossbeam, stress singularity will always appear at the root of the rib-to-deck plate weld. Therefore, it is not possible to get the stress value directly from the FE model. The stress range determined using the hot spot stress- or effective notch stress method are not affected by this singularity if a good element mesh is chosen. To determine the swt-parameter, the effective notch can also be applied to prevent the appearance of a stress singularity.

8.1.2. Design optimization

In the second part of the report, a parametric study and four alternatives for a case design are described. The results from the first part are used to determine which fatigue assessment method should be used. The results provide an answer on the following research question:

Can there be found a combination of parameters for the OSD which results in a reduced weight of the structure compared to general dimensions with respect to the rib-to-deck plate and crossbeam joint?

When a larger width between the trough webs is chosen, the deck plate thickness should be increased as well. The cross section area and thus the weight of the trough will reduce. However, the weight of the deck plate has most contribution to the total weight of the bridge deck and increasing this deck plate thickness results in a larger bridge deck weight. Therefore, the increased rib spacing will not result in a reduced weight of the bridge deck. For the considered alternatives, the difference in weight is 10% for the lightest and most heaviest option.

Further conclusions about the optimization possibilities of the joint with respect to the fatigue performance are given below. There should be kept in mind that a small increase in stress results in a much larger decrease in fatigue life.

Design:

- The in-plane deformation of the crossbeam influences the stresses in the detail. If deformation of the crossbeam is taken into account, a damage value 2.5 times the damage value for the crossbeam which is fully fixed over the length is found.
- The trough web thickness does not affect the fatigue stress range and the trough shape results in a difference of maximum 5% in stress value.

Loading assumptions:

- The transverse wheel position has only a small influence on the total damage value for the joint at the crossbeam. The transverse wheel position is more important to consider if the width between the trough webs becomes larger. For a width between the troughs of 300 mm, the transverse location gives only 7% of the total damage value. While if the width between the troughs is 400 mm, 17% of the damage value is caused by the transverse position.
- Because the center position contributes most to the total damage value, it is important to take into account that only 50% of the total design load cycles as stated in the Eurocode will pass the center.
- Like for fixed bridges with a thick asphalt layer, for movable bridges with a thin surface layer it is beneficial for the fatigue life to take into account the load dispersal through the surface layer by applying a larger wheel contact area. A damage value which is half of the damage value if the load dispersal is not taken into account can be reached if a shell element model is considered.
- For truck 3 of FLM4, the damage value decreases with 15% if all wheels are placed in the same line instead of if the most unfavourable position of each wheel is chosen. An even more reduced damage value can be reached if the stress range in the deck plate is considered during passing of the truck instead of assuming that the stress range becomes zero after passing of each axle. Considering the truck passing instead of each axle separately, 30% lower damage is found for truck 3 of FLM4. For a final conclusion about the total damage, all trucks from FLM4 should be included in the calculation.

Assessment method:

- For the case alternative with a width between the troughs of 360 mm and a deck plate thickness of 22 mm, the damage value is 1.1 if shell elements are used and 0.63 if a solid sub model is used. A reduced damage value of 35% is reached. Due to using the solid element model, the alternative meets the required damage value smaller than 1, while this requirement is not met if the shell element model is used. Therefore, in some situations, it is beneficial to use a solid element sub model instead of shell elements.
- From the first part of the report, there can be concluded that the hand calculation gives a similar fatigue life prediction as using the hot spot stress approach with a shell element. However, the method has some limitations which results in conservative and non conservative prediction of the fatigue life if it is used for assessment of a real bridge, which are:

  - Shape of the troughs is not considered.
  - In-plane deformation of the crossbeam is not taken into account, while this results in an increase of the stress range.
  - Loading only directly on the crossbeam is considered. Therefore, a conservative stress range is determined.

8.2. Recommendations

Based on the results presented in this report, some new discussion points are appeared. Recommendations for further research are:

- A suitable detail category for the effective notch stress approach can be determined if more experimental data is obtained.
- To take care of the residual stresses in the weld zone, investigation of a prescribed displacement instead of a prescribed stress range can be made. This can result in a more accurate stress and strain range for the unloaded situation.
- According to the Eurocode, the load dispersal can be included by taking a larger wheel contact area. However, the strength reduction due to a surface layer is not only dependent on the load dispersal but also on the composite action of the surface layer and steel deck plate. Therefore, the assumption should be validated to a FE model which includes the surface layer in the design or to experimental results of an OSD which includes the surface layer for a typical movable bridge.
- The effect on the damage value if the epoxy layer is taken into account is large. Therefore, a thicker epoxy layer and thinner steel plate may can be applied which results in an overall reduction of the weight of the bridge. Therefore, the possibilities for the epoxy layer thickness should be investigated.
- The design can be improved further if the width between and within troughs have not the same value. For the rib-to-deck plate joint, the width between the troughs is important, but the width within two troughs does not affect the fatigue life of the joint. In span between the crossbeams, both widths are important. However, the fatigue life is longer for this detail, and therefore, an improvement of the deck segment is possible. If a smaller with between the trough webs is chosen, but the amount of troughs remains the same, a decrease of the deck plate thickness may is possible and therefore, a weight reduction can be reached.
- There can be done more research to the possibility to reduce the stress range in the rib-to-deck plate joint due to the in-plane deformation of the crossbeam is.

Bibliography

[1] Al-Emrani, M. and Aygül, M. (2014). Fatigue design of steel and composite bridges. Technical report, Chalmers University of Technology, Göteborg, Sweden.

[2] Bak, M. (2015). How to account for fatigue data scatter. *CAE Associations Inc.* Retrieved from www.caeai.com/blog/how-account-fatigue-data-scatter.

[3] Connor, R., Fisher, J., Gatti, W., V., G., Kozy, B., Leshko, B., McQuaid, D. L., Medlock, R., Mertz, D., Murphy, T., Paterson, D., Sorensen, O., and Yadlosky, J. (2012). *Manual for Design, Construction and Maintenance of orthotropic steel deck bridges.* US Department of Transportation: Federal Highway Administration. Publication No: FHWA-IF-12-027.

[4] Connor, R. J. and Fisher, J. W. (2006). Consistent approach to calculating stresses for fatigue design of welded rib-to-web connections in steel orthotropic bridge decks. *Journal of Bridge Engineering*, 11(5):517–525. DOI: 10.1061/(ASCE)1084-0702(2006)11:5(517).

[5] de Backer, H. (2016). Orthotropic steel decks. In Pipinato, A., editor, *Innovative Bridge Design Handbook*, pages 597–613. doi.org/10.1016/B978-0-12-800058-8.00022-0.

[6] de Backer, H., Outtier, A., Nagy, W., and Schotte, K. (2017). Innovative fatigue design of orthotropic steel decks. *Bridge Structures*, 13(2-3):69–80. doi.org/10.3233/BRS-170115.

[7] de Jesus, A. M. P., Matos, R., Fontoura, B. F. C., Rebelo, C., Simoes da Silva, L., and Veljkociv, M. (2012). A comparison for the fatigue behavior between s355 and s690 steel grades. *Journal of Constructional Steel Research*, 79:140–150. http://dx.doi.org/10.1016/j.jcsr.2012.07.021.

[8] de Jong, F. B. P. (2004). Overview fatigue phenomenon in orthotropic bridge decks in the netherlands. *Orthotropic Bridge Conference.* Sacramento, California, USA.

[9] de Jong, F. B. P. (2007). *Renovation Techniques for Fatigue Cracked Orthotropic Steel Bridge Decks.* (doctoral dissertation), Delft University of Technology, The Netherlands.

[10] Dung, C. V., Sasaki, E., Tajima, K., and Suzuki, T. (2015). Investigation on the effect of weld penetration on fatigue strength of rib-to-deck welded joints in orthotropic steel decks. *International Journal of Steel Structures*, 15(2):299–310. DOI: 10.1007/s13296-014-1103-4.

[11] Fettahoglu, A. (2016). Optimizing rib width to height and rib spacing to deck plate thickness ratios in orthotropic decks. *Cogent Engineering*, 3. doi.org/10.1080/23311916.2016.1154703.

[12] Hobbacher, A. F. (2016). *Recommendations for Fatigue Design of Welded Joints and components.* International Institute of Welding (IIW), Springer, 2nd edition. IIW document IIW-2259-15exXIII-2460-13/XV-1440-13.

[13] J., L. (2011). Fatigue damage in the orthotropic steel deck with respect to the trough-to-deck plate joint in between crossbeams. (master thesis report), Delft University of Technology, The Netherlands. Retrieved from: http://repository.tudelft.nl.

[14] Kainuma, S., Yang, M., Y.S., J., Inokuchib, S., Kawabata, A., and Uchida, D. (2016). Experiment on fatigue behavior of rib-to-deck weld root in orthotropic steel decks. *Journal of Constructional Steel Research*, 119:113–122. http://dx.doi.org/10.1016/j.jcsr.2012.07.021.

[15] Ke, P., Guo, M., and Xia, L. (2015). The influence of common closed longitudinal rib sections on stress distribution of orthotropic decks. *International Conference on Architectural, Civil and Hydraulics Engineering.* doi:10.2991/icache-15.2015.30.

[16] Kolstein, M. H. (2004). The role of site measurements to improve the knowledge about the fatigue behaviour of steel orthotropic bridges. *Orthotropic Bridge Conference*. Sacramento, California, USA.

[17] Kolstein, M. H. (2007). *Fatigue Classification of Welded Joints in Orthotropic Steel Bridge Decks*. (doctoral dissertation), Delft University of Technology, The Netherlands.

[18] Leendertz, J. S. (2008). *Fatigue Behaviour of Closed Stiffener to Crossbeam Connections in Orthotropic Steel Bridge Decks*. (doctoral dissertation), Delft University of Technology, The Netherlands.

[19] Li, G. and Wu, Y. (2010). A study of the thickness effect in fatigue design using the hot spot stress method. (master thesis report), Chalmers University of Technology, Gotebor, Sweden.

[20] M, A. (2012). Fatigue analysis of welded structures using the finite element method. (master thesis report), Chalmers University of Technology, Gotebor, Sweden.

[21] Majlaars, P., Bonet, E., and Pijpers, R. J. M. (2018). Fatigue resistance of the deck plate in steel orthotropic deckstructures. *Engineering Fracture Mechanics*, 201:214–228. https://doi.org/10.1016/j.engfracmech.2018.06.014.

[22] Mathers, G. (2015). Fatigue testing - part 2. Retrieved from: www.twi-global.com.

[23] Ming, L., Hashimoto, K., and Sufiura, K. (2014). Influence of asphalt surfacing on fatigue evaluation of rib-to-deck joints in orthotropic steel bridge decks. *Journal of Bridge Engineering*, 19(10). DOI: 10.1061/(ASCE)BE.1943-5592.0000610.

[24] Murakoshi, J., Hirano, S., and Harada, H. (n.d.). Effect of deck plate thickness of orthotropic steel deck on fatigue durability. Public Work Research Institute (PWRI). Japan.

[25] Nagy, W., Bogaert, P., and de Backer, H. (2016a). Lefm based fatigue design for welded connections in orthotropic steel bridge decks. *Procedia Engineering*, 133:758–769. doi.org/10.1016/j.proeng.2015.12.658.

[26] Nagy, W., Schotte, K., van Bogaert, P., and de Backer, H. (2016b). Fatigue strength application of fracture mechanics to orthotropic steel decks. *Advances in Structural Engineering*, 19(11):1696–1709. doi.org/10.1177/1369433216649383.

[27] NEN-EN 1991-2 (2011). Eurocode 1: Actions on structures – part 2: Traffic loads on bridges. Brussels: European Standard EN.

[28] NEN-EN 1991-2/NB (2011). Dutch national annex to eurocode 1: Actions on structures – part 2: Traffic loads on bridges. Brussels: European Standard. (in Dutch).

[29] NEN-EN 1993-1-9 (2012). Eurocode 3: Design of steel structures - part 1-9: Fatigue. Brussels: European Standard EN.

[30] NEN-EN 1993-2 (2011). Eurocode 3: Design of steel structures - part 2: Steel bridges. Brussels: European Standard EN.

[31] NEN-EN 1993-2/NB (2011). Dutch national annex to eurocode 3: Design of steel structures – part 2: Steel bridges. Brussels: European Standard. (in Dutch).

[32] Rijkswaterstaat (2017). Richtlijnen ontwerpen kunstwerken (ROK). Document nr: RTD 1001:2017. (in Dutch).

[33] Smith, R., Watson, P., and Topper, T. (1970). A stress-strain parameter for the fatigue of metals. *Journal of Materials*, 5(4):767–778. http://dx.doi.org/10.1016/j.jcsr.2012.07.021.

[34] Spyridoni, K., Xin, H., Hermans, M., and Veljkovic, M. (2019). Calibration of welding simulation parameters of fillet welding joints used in an orthotropic steel deck. *The 14th Nordic Steel Construction Conference, Copenhage, Denmark*. Ernst Sohn: Verlag für Architektur und technische Wissenschaften GmbH Co. KG, Berlin.

[35] Swierstra, E. P. (2017). Fatigue assessment in finite element analysis – a post-processor to fea output for hot spot stress calculation. (master thesis report), Delft University of Technology, The Netherlands. Retrieved from: http://repository.tudelft.nl.

[36] Wang, B. (2017). *A Multiscale Study on Fatigue Mechanism and Life Estimation on Welded Joints of Orthotropic Steel Decks*. (doctoral dissertation), University of Gent, Belgium. Retrieved from: biblio.ugent.be.

[37] Wu, W., Kolstein, H., Veljkovic, M., Pijpers, R., and Vorstenbosch-Krabbe, J. (2017). Fatigue behaviour of the closed rib to deck and crossbeam joint in a newly designed orthotropic bridge deck. *CE/papers*, 1(2-3):2378–2387. doi.org/10.1002/cepa.285.

[38] Yang, M. Y., Liu, R., Ji, B. H., Xu, H. J., Chen, C., and Zhao, D. (2012). Fatigue stress analysis of diaphragm cap hole in orthotropic steel bridge decks. *Applied Mechanics and Materials*, 204-208:3265–3269. doi.org/10.4028/www.scientific.net/AMM.204-208.3265.

A

Strain validation

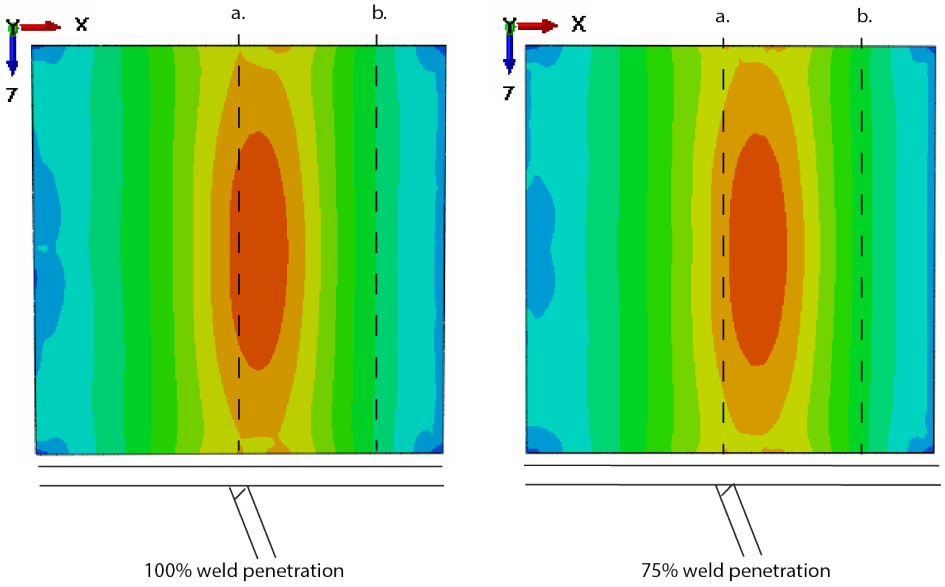

Figure A.1: Strain at top of the deck plate for the reference and 75% weld penetration

B

2D model - bending moment

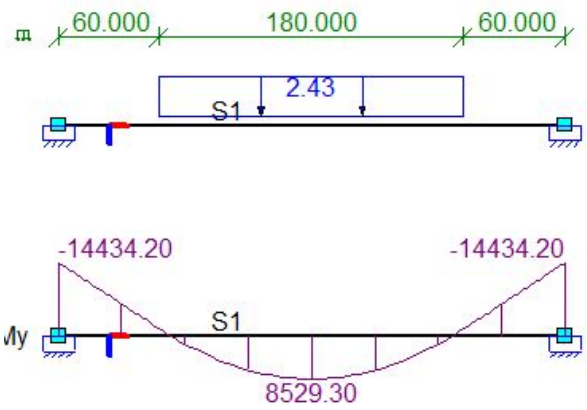

Figure B.1: Input in MatrixFrame (in mm and N/mm^2) and bending moment line (in Nmm)

C

Improved detail category for the effective notch stress method

Strandard deviation:

$$\sigma_n = \sqrt{\frac{\sum_{i=1}^{n}(x_i - \mu)^2}{n}}$$

Where:

- σ_n is standard deviation
- n is amount of specimen
- x_i is value/result of one specimen
- $\mu$is averaged result of all specimens

	Fatigue life
Specimen 1	$4.2*10^6$
Specimen 2	$1.2*10^6$

Table C.1: Result experiment[37]

n = 2
$\mu = 8.0 * 10^5$

$\sigma_n = \sqrt{\frac{\sum_{i=1}^{n}(x_i-\mu)^2}{n}} = 3.75 * 10^5$

Mean:

$$\Delta\sigma = \frac{N_{experiment}}{N_C}^{\frac{1}{3}} * \Delta\sigma_{eff.notch} = \frac{8.0 * 10^5}{2.0 * 10^6}^{\frac{1}{3}} * 1080 = 796MPa$$

C.1. method 1

Design load cycles:
$N_{mean-2sd} = \mu - 2 * \sigma_n = 4.5 * 10^4$

Detail category:

$$\Delta\sigma = \frac{N_{experiment}}{N_C}^{\frac{1}{3}} * \Delta\sigma_{eff.notch} = \frac{4.5 * 10^4}{2.0 * 10^6}^{\frac{1}{3}} * 1080 = 305MPa$$

C.2. method 2

A failure of all test specimen method is assumed because both test specimen has reached the 10% change in strain range, which is assumed as failure criteria. The standard deviation of 0.25 can be used for complex structures at fatigue endurance up to 1 million load cycles. (IIW). The value of factor F is now determined according to table 4.4 from IIW and is equal to 6.86.
Design load cycles:

$$N_d = \frac{N_T}{F} = \frac{8 * 10^5}{6.86} = 1.2 * 10^5$$

Detail category:

$$\Delta\sigma = \frac{N_{experiment}}{N_C} * \Delta\sigma_{eff.notch} = \frac{5.0 * 10^4}{2.0 * 10^6} * 1080 = 316MPa$$

D

Load cycles and damage value

Table D.1: Load cycles per axle from EC1-2 NB.6

Load cycles per wheel type per traffic category					
Wheeltype	**Axle load**	**Traffic category**			
		1	2	3	**4**
		20%	50%	50%	80%
A	70	400000	250000	62500	40000
B	130	400000	250000	62500	40000
		5%	5%	5%	5%
A	70	100000	25000	6250	2500
B	120	100000	25000	6250	2500
B	120	100000	25000	6250	2500
		40%	20%	20%	5%
A	70	800000	100000	25000	2500
B	150	800000	100000	25000	2500
C	90	800000	100000	25000	2500
C	90	800000	100000	25000	2500
C	90	800000	100000	25000	2500
		25%	15%	15%	5%
A	70	500000	75000	18750	2500
B	140	500000	75000	18750	2500
C	90	500000	75000	18750	2500
C	90	500000	75000	18750	2500
		10%	10%	10%	5%
A	70	200000	50000	12500	2500
B	130	200000	50000	12500	2500
C	90	200000	50000	12500	2500
C	80	200000	50000	12500	2500
C	80	200000	50000	12500	2500

Table D.2: Load cycles per wheel (n_i)

Wheel type	Axle load [kN]	Total load cycles	Center position	+/- 100 mm	+/- 200 mm
			50%	18%	7%
A	70	500000	250000	90000	35000
B	120	50000	25000	9000	3500
	130	300000	150000	54000	21000
	140	75000	37500	13500	5250
	150	100000	50000	18000	7000
C	80	100000	50000	18000	7000
	90	500000	250000	90000	35000

Table D.3: Stress value for the detail category and value at the cut-of limit and CAFL for detail category is 125 MPa and partial safety factor is 1.15

Detail category is 125 Mpa

Load cycles	**Stress value**			Ym	1.15
2.0E+06	ds_C =	108.7	N/mm2		
5.0E+06	ds_D =	80.1	N/mm2	m	3
1.0E+08	ds_L =	44.0	N/mm2	m	5

Table D.4: Calculation of damage value. Blue area's is output from the FE model. Other values are automatically calculated in excel.

	s_1.0t	**s_0.4t**	**s_hotspot**	**N**	**D_i,tc2**
A - 70 kN	-24.8	-39.7	49.7	5.44E+07	0.0046
B - 120 kN	-21.1	-33.9	42.5	1.00E+99	0.0000
B - 130 kN	-23.1	-37	46.3	7.73E+07	0.0019
B - 140 kN	-24.3	-39	48.8	5.92E+07	0.0006
B - 150 kN	-26.3	-42.1	52.7	4.06E+07	0.0012
C - 80 kN	-24.3	-40.1	50.7	4.92E+07	0.0010
C - 90 kN	-26.9	-44.4	56.1	2.96E+07	0.0085

Design life	
1	0.02
50	0.89
100	1.79

Damage value is determined for all 5 transverse locations and total damage value is the sum of all locations.

E

Transverse wheel location

Table E.1: Damage value per transverse load position for a=257mm and t=18mm. $\gamma_{Mf} = 1.15$

a=257mm - t=18m					
	Location from center [mm]				
	-200	**-100**	**0**	**100**	**200**
A - 70kN	0	0	0.25	0	0
B - 120 kN	0	0	0	0	0
B - 130 kN	0	0	0.09	0	0
B - 140 kN	0	0	0.03	0	0
B - 150 kN	0	0	0.06	0	0
C - 80 kN	0	0	0.04	0	0
C - 90 kN	0	0.05	0.039	0	0
Total per position	0	0.05	0.88	0	0
				Total damage:	0.93
Percentage of total	0	5	95	0	0

Table E.2: Damage value per transverse load position for a=300mm and t=20mm. $\gamma_{Mf} = 1.15$

a=300mm - t=20m					
	Location from center [mm]				
	-200	**-100**	**0**	**100**	**200**
A - 70kN	0	0	0.23	0	0
B - 120 kN	0	0	0	0	0
B - 130 kN	0	0	0.10	0	0
B - 140 kN	0	0	0.03	0	0
B - 150 kN	0	0.01	0.06	0	0
C - 80 kN	0	0	0.05	0	0
C - 90 kN	0	0.05	0.42	0	0
Total per position	0	0.06	0.89	0	0
				Total damage:	0.96
Percentage of total	0	6	93	0	0

Table E.3: Damage value per transverse load position for a=360mm and t=22mm. $\gamma_{Mf} = 1.15$

a=360mm - t=22m					
	Location from center [mm]				
	-200	**-100**	**0**	**100**	**200**
A - 70kN	0	0	0.23	0	0
B - 120 kN	0	0	0	0	0
B - 130 kN	0	0	0.09	0	0
B - 140 kN	0	0	0.03	0	0
B - 150 kN	0	0.02	0.07	0	0
C - 80 kN	0	0	0.06	0	0
C - 90 kN	0	0.08	0.55	0	0
Total per position	0	0.11	1.03	0	0
				Total damage:	1.14
Percentage of total	0	10	90	0	0

Table E.4: Damage value per transverse load position for a=400mm and t=24mm. $\gamma_{Mf} = 1.15$

a=400mm - t=24m					
	Location from center [mm]				
	-200	**-100**	**0**	**100**	**200**
A - 70kN	0	0	0	0	0
B - 120 kN	0	0	0	0	0
B - 130 kN	0	0	0	0	0
B - 140 kN	0	0	0	0	0
B - 150 kN	0	0	0.02	0	0
C - 80 kN	0	0.01	0.05	0.01	0
C - 90 kN	0	0	0.04	0	0
Total per position	0	0.06	0.31	0	0
				Total damage:	0.49
Percentage of total	0	14	83	3	0

F

Load input for stress range option 3

Load positions for truck 3 to determine the stress range for option 3. Stress range is determined in crossbeam 2 (cb2).

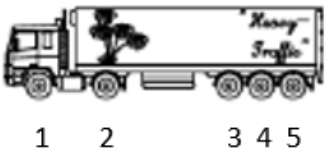

Figure F.1: FLM4 truck 3

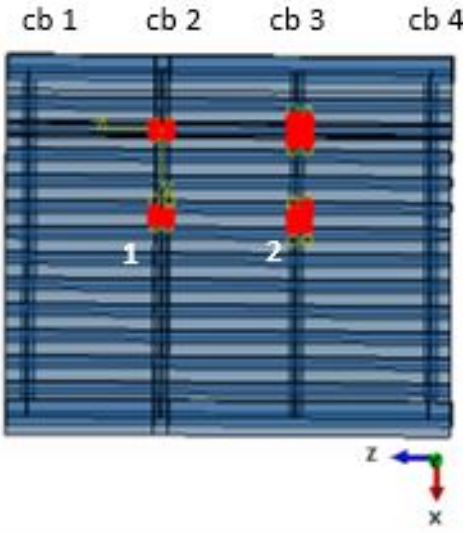

Figure F.2: Position 1

Figure F.3: Position 2

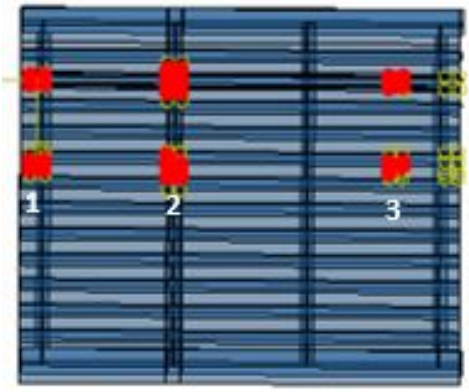

Figure F.4: Position 3

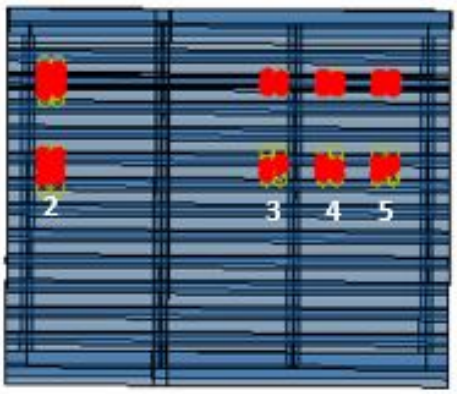

Figure F.5: Position 4

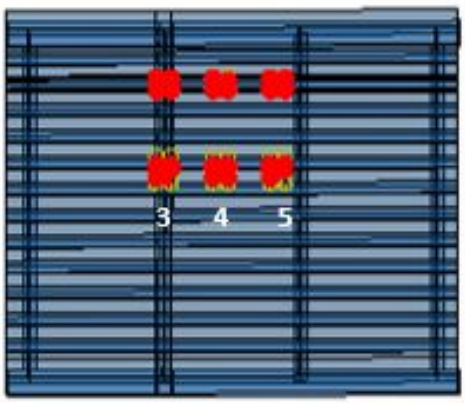

Figure F.6: Position 5

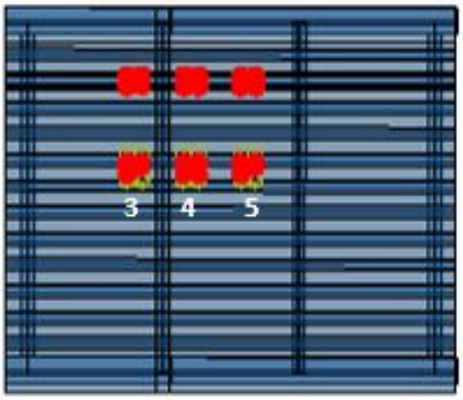

Figure F.7: Position 6

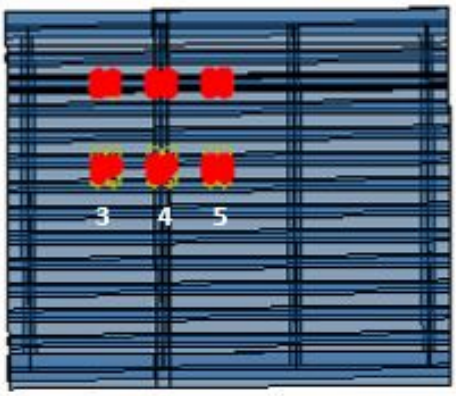

Figure F.8: Position 7

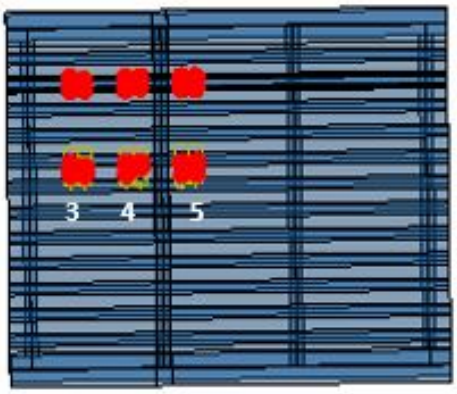

Figure F.9: Position 8

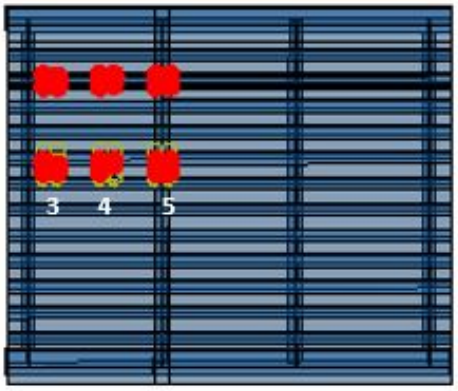

Figure F.10: Position 9